ΠΑΝΕΠΙΣΤΗΜΙΟ ΚΡΗΤΗΣ

ΤΜΗΜΑ ΒΙΟΛΟΓΙΑΣ

ΙΔΡΥΜΑ ΤΕΧΝΟΛΟΓΙΑΣ ΚΑΙ ΕΡΕΥΝΑΣ

ΙΝΣΤΙΤΟΥΤΟ ΜΟΡΙΑΚΗΣ ΒΙΟΛΟΓΙΑΣ ΚΑΙ ΒΙΟΤΕΧΝΟΛΟΓΙΑΣ

ΔΙΔΑΚΤΟΡΙΚΗ ΔΙΑΤΡΙΒΗ

“Ένας μιτοχονδριακός ροοστάτης καθοδηγεί την διαφοροποίηση των γαμετικών βλαστικών κυττάρων στον *Caenorhabditis elegans*”

ΝΙΚΟΛΑΟΣ ΧΑΡΜΠΙΛΑΣ

ΗΡΑΚΛΕΙΟ

ΙΟΥΝΙΟΣ 2018

UNIVERSITY OF CRETE

BIOLOGY DEPARTMENT

FOUNDATION OF RESEARCH AND TECHNOLOGY

INSTITUTE OF MOLECULAR BIOLOGY AND BIOTECHNOLOGY

PhD THESIS

“A mitochondrial rheostat drives germline stem cell differentiation in *Caenorhabditis elegans*”

NIKOLAOS CHARMPILAS

HERAKLION

JUNE 2019

Η παρούσα εργασία υποστηρίχτηκε υλικά και οικονομικά από διδακτορική υποτροφία «Thalis-GEnAge» από το Υπουργείο Παιδείας και Θρησκευμάτων (THALIS MIS380228 GEnAge), το MANNA ERC advanced grant (GA695190- MANNA) και από πόρους του IMBB. Ευχαριστώ ιδιαιτέρως το Ίδρυμα Κρατικών Υποτροφιών (ΙΚΥ) για τη χορήγηση υποτροφίας στο δεύτερο χρόνο των μεταπτυχιακών σπουδών μου και το κληροδότημα Μανασάκη για τη χορήγηση υποτροφίας στον πρώτο χρόνο των διδακτορικών σπουδών μου.

The current work was financially supported by the Thalis-GEnAge PhD fellowship from the Greek Ministry of Education (THALIS MIS380228 GEnAge), as well as from the MANNA ERC advanced grant (GA695190- MANNA) and intramural IMBB funds. I acknowledge the Hellenic State Scholarship Foundation (IKY) for awarding me a fellowship for the second year of my masters and Manassaki foundation for awarding me a fellowship for the first year of my PhD studies.

ΕΠΙΒΛΕΠΩΝ:

Νεκτάριος Ταβερναράκης, Καθηγητής Ιατρικής Σχολής, Πανεπιστήμιο Κρήτης

ΤΡΙΜΕΛΗΣ ΕΠΙΤΡΟΠΗ:

Νεκτάριος Ταβερναράκης, Καθηγητής Ιατρικής Σχολής, Πανεπιστήμιο Κρήτης

Δέσποινα Αλεξανδράκη, Καθηγήτρια Τμήματος Βιολογίας, Πανεπιστήμιο Κρήτης

Γεώργιος Μαυροθαλασσίτης, Καθηγητής Ιατρικής Σχολής, Πανεπιστήμιο Κρήτης

ΕΠΤΑΜΕΛΗΣ ΕΠΙΤΡΟΠΗ:

Νεκτάριος Ταβερναράκης, Καθηγητής Ιατρικής Σχολής, Πανεπιστήμιο Κρήτης

Δέσποινα Αλεξανδράκη, Καθηγήτρια Τμήματος Βιολογίας, Πανεπιστήμιο Κρήτης

Γεώργιος Μαυροθαλασσίτης, Καθηγητής Ιατρικής Σχολής, Πανεπιστήμιο Κρήτης

Χρήστος Δελιδάκης, Καθηγητής Τμήματος Βιολογίας, Πανεπιστήμιο Κρήτης

Κρίτων Καλαντίδης, Καθηγητής Τμήματος Βιολογίας, Πανεπιστήμιο Κρήτης

Ιωάννης Βόντας, Καθηγητής Τμήματος Βιολογίας, Πανεπιστήμιο Κρήτης

Βασιλική Νικολετοπούλου, Ερευνήτρια Ινστιτούτο Μοριακής Βιολογίας και Βιοϊατρικής

Ευχαριστίες

Βλέποντας μια ηλιαχτίδα φωτός και ελπίζοντας πως οδεύω προς την ολοκλήρωση ενός μακρού και επίπονου ταξιδιού, νιώθω την ανάγκη να ευχαριστήσω τους ανθρώπους που έχουν συνεισφέρει ποικιλοτρόπως σε αυτό.

Αρχικά τον καθηγητή κύριο Νεκτάριο Ταβερναράκη για την εμπιστοσύνη που μου έχει δείξει όλα αυτά τα χρόνια που δούλεψα στο εργαστήριο του. Έμαθα πολλά σε ερευνητικό επίπεδο από τις γνώσεις, τις συμβουλές και τις εμπειρίες του. Κατά δεύτερον τα δύο άλλα μέλη της τριμελούς επιτροπής μου, την καθηγήτρια κυρία Δέσποινα Αλεξανδράκη και τον καθηγητή κύριο Γιώργο Μαυροθαλασσίτη, με τους οποίους είχαμε άριστη συνεργασία ήδη από τα χρόνια του μάστερ μου. Τους ευχαριστώ για την συνέπεια και την υποστήριξή τους. Τέλος τα υπόλοιπα μέλη της επταμελούς επιτροπής μου (καθ. Χρήστο Δελιδάκη, καθ. Κρίτωνα Καλαντίδη, καθ. Ιωάννη Βόντα και ερευν. Βασιλική Νικολετοπούλου) για τη προθυμία τους να κρίνουν την διδακτορική μου διατριβή. Τη Βασιλική ιδιαίτερως γιατί υπήρξε η πρώτη μου supervisor μόλις εντάχθηκα στο εργαστήριο Ταβερναράκη και μου δίδαξε πολλά.

Ώρα να περάσω στους συνεργάτες μου στο “wormslab”. Ευχαριστώ ιδιαιτέρως την κυρία Μαίρη Μαρκάκη για την στήριξη σε όλα τα χρόνια παρουσίας μου στο εργαστήριο. Ιδιαιτέρως δε για τη στήριξη σε δύσκολες καταστάσεις (θυμάμαι ουκ ολίγες). Ευχαριστώ την Αγγέλα Πασπαράκη για την ανεκτίμητη συνεισφορά της και γιατί με την παρουσία της κάνει τα πράγματα ευκολότερα για κάθε υποψήφιο διδάκτορα στο “wormslab”. Ευχαριστώ πάρα πολύ τρία μέλη του εργαστηρίου (νυν και πρώην): τον Μάνο Κυριακάκη που τον νιώθω σαν μεγάλο αδερφό, και τους καλούς φίλους Κωνσταντίνο Παληκαρά και την Χριστίνα Πλουμή γιατί με στήριξαν από την αρχή μέχρι το τέλος και γιατί μου έχουν μάθει πολλά πράγματα σε επαγγελματικό και κυρίως προσωπικό επίπεδο. Ευχαριστώ ιδιαιτέρως το Μάνο γιατί μου έδωσε τη δυνατότητα να συνεργαστώ μαζί του και να βοηθήσω στην ολοκλήρωση του project του. Να εξάρω επίσης τη συνεισφορά της κυρίας Μαίρης, του Κωνσταντίνου και του Μάνου στη βελτίωση του manuscript που συνοψίζει την εργασία μου. Επιπρόσθετα όλα τα υπόλοιπα μέλη του εργαστηρίου για τη εποικοδομητική συνεργασία όλα αυτά τα χρόνια: Ιωάννα Δασκαλάκη, Ειρήνη Λιονάκη, Μαργαρίτα Παπανδρέου, Διονυσία Πετράτου, Andrea Princz, Κων/νο Κουνάκη, Θάνο Μεταξάκη, Ηλία Γκίκα, Ευρυδίκη Ασημάκη και Μάνο Χανιωτάκη. Τέλος τους δύο φοιτητές τους οποίους επέβλεψα: Γιάννη Ευαγγελάκο και Ουρανία Γαλανοπούλου.

Ευχαριστώ από καρδιάς τους φίλους που απέκτησα αυτά τα χρόνια εντός και εκτός του εργασιακού χώρου. Ιδιαιτέρως δύο άτομα που αισθάνομαι σαν αδέρφια: Ηλία Καλαφατάκη, Γεράσιμο Αναγνωστόπουλο. Τίποτα δεν θα ήταν ίδιο χωρίς άτομα σαν τη Λίντα, τη Κέλλυ, τη Μαίρη γύρω μου. Όλους μου τους συμπαίκτες και συμπαίκτριες στις πανεπιστημιακές ομάδες μπάσκετ και βόλλευ (είναι πολλοί) γιατί μου χάρισαν όμορφες και δυνατές στιγμές εκτός εργαστηρίου.

Ευχαριστώ τη Γεωργία Τσικαλά γιατί χωρίς τη αέναη και έμπρακτη της στήριξη μπορεί να μην έγραφα τώρα αυτά τα λόγια. Την ευχαριστώ για την ενθάρρυνση, την εμπιστοσύνη και την αγάπη που μου δείχνει καθημερινά, χρόνια τώρα. Ελπίζω να είμαι άξιος της αγάπης της.

Τέλος, ένα μεγάλο ευχαριστώ στην οικογένεια μου, τη μητέρα μου Αγγελική και τον αδερφό μου Αντρέα γιατί χωρίς αυτούς τίποτα απ’ όλα αυτά δεν θα είχε νόημα. Εσάς θα σκέφτομαι πάντα στα δύσκολα και για σας θα συνεχίζω να παλεύω. Τέλος, θα ήθελα να ευχαριστήσω τον πατέρα μου που δυστυχώς δε θα είναι εκεί για να με ακούσει να παρουσιάζω. Ξέρω ότι θα ένιωθε πολύ περήφανος και χαρούμενος για μένα. Μπαμπά όσα έχω μάθει από σένα έχουν διαμορφώσει τον χαρακτήρα και την προσωπικότητά μου. Στην οικογένεια μου αφιερώνω το σύγγραμμα αυτό.

“Even if you cut all the flowers, you cannot keep spring from coming”

P. Neruda

Περίληψη

Η γαμετική σειρά του *C. elegans* προσομοιάζει τους βλαστικούς θύλακες των θηλαστικών και έχει αποδειχτεί ανεκτίμητης αξίας για την κατανόηση βασικών πτυχών της βιολογίας των βλαστικών κυττάρων. Παρόλα αυτά, πολλά από τα μοριακά και φυσιολογικά προαπαιτούμενα για τη διατήρηση της ομοιόστασης των γαμετικών βλαστικών κυττάρων παραμένουν άγνωστα. Ερευνήσαμε το ρόλο της μιτοχονδριακής βιογένεσης και λειτουργίας στην διατήρηση της ταυτότητας των γαμετικών βλαστικών κυττάρων. Η δουλειά μας καταδεικνύει πως η μιτοχονδριακή μεταγραφή στα γαμετικά μιτοχόνδρια είναι διαμερισματοποιημένη και έρχεται παράλληλα με την μιτοχονδριακή ωρίμανση. Η έκφραση της RPOM-1, της μιτοχονδριακής RNA πολυμεράσης, αυξάνεται καθώς οι γαμετικοί πυρήνες μεταβαίνουν από τον άπω στον εγγύς βραχίονα της γονάδας και σχηματίζουν ωοκύτταρα. Η έκφραση της RPOM-1 ρυθμίζεται από τον IFET-1, ένα μεταφραστικό καταστολέα και συστατικό των P granules. Τα μιτοχόνδρια αυτά καθ' αυτά μεταβαίνουν από μια σφαιρική σε μια επιμήκη μορφολογία και πολώνονται καθώς πλησιάζουν τον εγγύς βραχίονα της γονάδας και η παραγωγή ATP και ROS αυξάνεται. Μια αντίστοιχη μετάβαση και αλλαγή στην έκφραση της μιτοχονδριακής RNA πολυμεράσης χαρακτηρίζει και την διαφοροποίηση των βλαστικών κυττάρων των θηλαστικών. Διατάραξη της διαδικασίας αυτής προκαλεί υπερπλασία στο συγκύτιο της γονάδας λόγω αλλαγής στην ισορροπία μεταξύ μίτωσης και διαφοροποίησης σε ωοκύτταρα και ακολουθείται από μείωση της γονιμότητας. Ως αποτέλεσμα, η απόπτωση ενεργοποιείται για να αντισταθμίσει την υπερπλασία. Σήματα σπερματικής προέλευσης (MSP) προάγουν την μιτοχονδριακή ωρίμανση και διαφοροποίηση των γαμετικών κυττάρων μέσω του MEK/ERK μονοπατιού κινασών. Η μοίρα των γαμετικών κυττάρων καθορίζεται από την αλληλεπίδραση των μοναπατιών Insulin/IGF-1, TGF-β, των ρυθμών πρωτεϊνοσύνθεσης και των μιτοχονδρίων. Τα ευρήματα μας εμπλέκουν αλλαγές στη μιτοχονδριακή ενεργότητα στην διαφοροποίηση των βλαστικών κυττάρων και τη μιτοχονδριακή μεταγραφή στη διαφοροποίηση των γαμετικών κυττάρων και την υπερπλασία.

Abstract

The *C. elegans* germline recapitulates mammalian stem cell niches, and has proven instrumental in understanding key aspects of stem cell biology. However, the molecular and physiological requirements for germline stem cell homeostasis remain largely elusive. We investigated the role of mitochondrial biogenesis and function in the preservation of germline stem cell identity. Here, we show that general transcription activity in germline mitochondria is highly compartmentalized and parallels mitochondrial maturation. Expression of RPOM-1, the mitochondrial RNA polymerase, increases as germ nuclei progress from the distal to the proximal gonadal arm to form oocytes, and is directly regulated by IFET-1, a translational repressor required for normal P granule formation. Mitochondria transition from globular to tubular morphology and become polarized, as they approach the proximal gonad arm. Notably, we find that a similar transition and temporal mitochondrial RNA polymerase expression profile characterizes differentiation of mammalian stem cells. This shift is accompanied by increased ATP and ROS production. Perturbation of mitochondrial bioenergetics causes gonad syncytium hyperplasia by disrupting the balance between mitosis and differentiation to oocytes, resulting in a marked reduction of fecundity. Consequently, compensatory apoptosis is induced in the germline. Sperm-derived signals promote mitochondrial maturation and germ cell differentiation via the MEK/ERK kinase pathway. Germ cell fate decisions are determined by a crosstalk between Insulin/IGF-1 and TGF-β signaling, mitochondria and protein synthesis. Our findings demonstrate that a shift in mitochondrial bioenergetics guides germline stem cell differentiation, and implicate mitochondrial transcription in germ cell differentiation and germline tumor development.

Contents

1. INTRODUCTION

Mitochondria: Ubiquitous organelles with prokaryotic origin

Mitochondria are the main energy producing centers of eukaryotic cells. They are thought to have arisen from endosymbiotic cells of ancestral eukaryotic cells with once free-living proteobacteria (Archibald, 2015). They principally rely on proteins which are encoded by the nuclear genome to execute their functions. The vast majority (more than 99%) of mitochondria-residing proteins is encoded by the nuclear genome (figure IA). These proteins are translated by cytosolic ribosomes and are then imported in the double-membrane enclosed organelles through the TOM and TIM translocator complexes. Upon entry into mitochondria they are sorted into their final destination, which can be the mitochondrial matrix, the outer or inner mitochondrial membrane or the intermembrane space (Neupert and Herrmann, 2007; Schmidt et al., 2010). Extensive proteomic analyses have identified approximately 900 mitochondrial proteins encoded by the yeast genome (Reinders et al., 2006; Sickmann et al., 2003) and 1100 mouse mitochondrial proteins (Pagliarini et al., 2008). For their entry in mitochondria, most of these proteins possess a cleavable, positively charged mitochondrial targeting signal residing in the N-terminus of their polypeptide chain. However, non-cleavable, internal targeting signals have been also characterized, required especially for those proteins which are destined for integration in mitochondrial membranes or the intermembrane space (figure IB) (Chacinska et al., 2009).

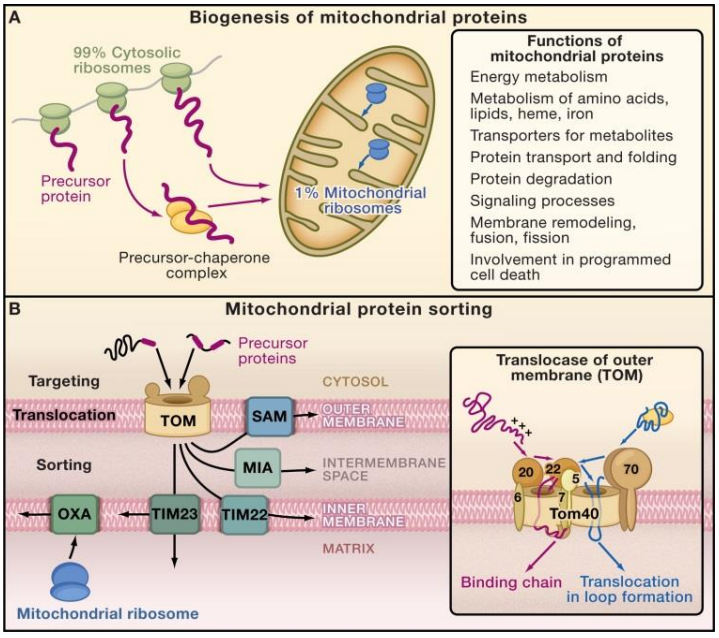

Figure I: Mitochondria are semi-autonomous organelles. A) The majority of mitochondrial proteins are encoded by the nuclear genome. B) TOM and TIM importers with the aid of additional partners import proteins in mitochondria. The final destination of each protein is dictated by the type of targeting signal it harbors. Figure adapted from *Chacinska et al. Cell, 2009.*

Mitochondrial DNA and its transcription

Despite their strong dependence on nuclear genome-encoded products, mitochondria still retain their own genome (mtDNA), a remnant of the ancestral prokaryotic genome. The mitochondrial genome is polyploid (hundreds of copies within each cell) and is maternally inherited. mtDNA in humans is a relatively small (around 16kb), gene dense, circular DNA molecule. Almost 93% of its sequence is transcribed, with the exception of the so called D-loop, a regulatory region where the protein factors involved in the replication and transcription of mtDNA are recruited. It encodes for thirteen electron transport chain (ETC) components, two rRNA (12S and 16S) molecules which are structural constituents of the mitochondrial 55S ribosome, as well as the full repertoire of twenty two tRNAs required for protein translation inside mitochondria (Taanman, 1999). The 55S mitochondrial ribosome which forms from the two mtDNA-encoded rRNAs and with exclusively nuclear genome-encoded ribosomal proteins is distinct from the cytoplasmic one and its crystal structure was recently solved (Amunts et al., 2015; Greber et al., 2015; Yakubovskaya et al., 2014). Mitochondrial genome integrity is crucial, since point mutations or rearrangements in mtDNA have been associated with a wide spectrum of human diseases, including Leigh syndrome, Kearns-Sayre syndrome, several forms of myopathies and cancer (Tuppen et al., 2010). An extensive analysis of conplastic mouse strains, which differ only in their mitochondrial haplotype, albeit the nuclear genome is identical, revealed profound differences in numerous health span parameters (Latorre-Pellicer et al., 2016). Moreover, a causative relationship between mtDNA and ageing has been established, since a large 5kb deletion has been detected in post-mitotic cells of aged individuals (Cortopassi and Arnheim, 1990) and mouse models for defective mitochondrial DNA polymerase (polymerase gamma, POLG) exhibit hallmarks of progeria (Kujoth et al., 2005; Trifunovic et al., 2004).

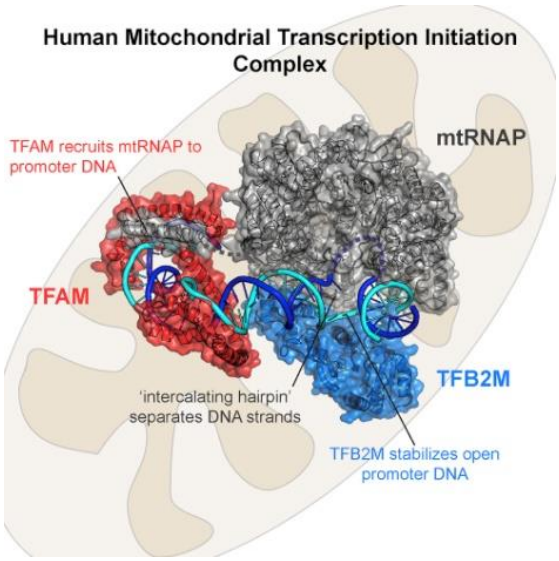

Figure II: Structure of human mtTIC. A dedicated RNA polymerase with the aid of two auxiliary factors transcribes the mitochondrial genome. Figure adapted from Hillen et al., Cell, 2017.

A tripartite complex consisting of a dedicated RNA polymerase (POLRMT) as well as two auxiliary transcription factors (TFAM and TFB2M) constitute the mitochondrial transcription initiation complex (mtTIC), which is involved in the transcription of the mitochondrial genome (figure II) (Hillen et al., 2017). POLRMT is homologous to bacteriophage T3 and T7 polymerases. Its crystal structure revealed the presence of a C-terminal catalytic domain, an N-terminal domain important for promoter recognition and an N-terminal extension (Ringel et al., 2011). Interestingly, POLRMT can have additional roles apart from transcription, in the regulation of mitochondrial translation, since POLRMT directly interacts with TFB1M (a human homologue of TFB2M with 12S-methytransferase activity), increasing its activity and promoting the stable formation of 55S mitochondrial ribosomes (Surovtseva and Shadel, 2013). Mitochondrial transcription factor A (TFAM), a high mobility group (HMG) protein, has numerous functions inside the organelle, since it also participates in the replication of mtDNA as well as its packaging into nucleoids (Kukat and Larsson, 2013). The prevailing theory is that TFAM is responsible for recruiting POLRMT and TFB2M at the site of transcription initiation by bending DNA and directly associating with them (Shi et al., 2012). Mitochondrial transcription factor B2 (TFB2M) is orthologous to TFB1M, both of

them sharing high homology with bacterial enzymes possessing 12S rRNA-methyltransferase activity (Shutt and Gray, 2006). Initially thought to be redundant (McCulloch and Shadel, 2003), it is now presumed that the two orthologues have distinct functions. Specifically, it is thought that TFB2M accompanies POLRMT aiding the transcription of mtDNA (Sologub et al., 2009), whereas TFB1M methylates 12S rRNA to promote small ribosomal subunit biogenesis and stability of the mitochondrial ribosome (Cotney et al., 2009; Metodiev et al., 2009).

The mtDNA of the nematode *C. elegans* is a bit smaller, since it lacks the ATP8 gene of its human counterpart (figure III) (Okimoto et al., 1992). All of the dozen proteins encoded by the mtDNA are subunits of the mitochondrial respiratory chain (figure IV). The uaDf5 3.1kb deletion spanning ctb-1, ND2, ATP6 and ND1 genes has been described as a selfish DNA element and its maintenance and propagation to the next generations depends on mitochondrial unfolded protein response (UPR^{mt}) activation (Gitschlag et al., 2016; Lin et al., 2016). RPOM-1 is the mammalian POLRMT homologue. HMG-5 is reported as a putative TFAM homologue in *C. elegans* (Sumitani et al., 2011). Nematodes have a TFB1M homologue A (gene name: *tfbm-1*), nevertheless a TFB2M homologue has not yet been identified.

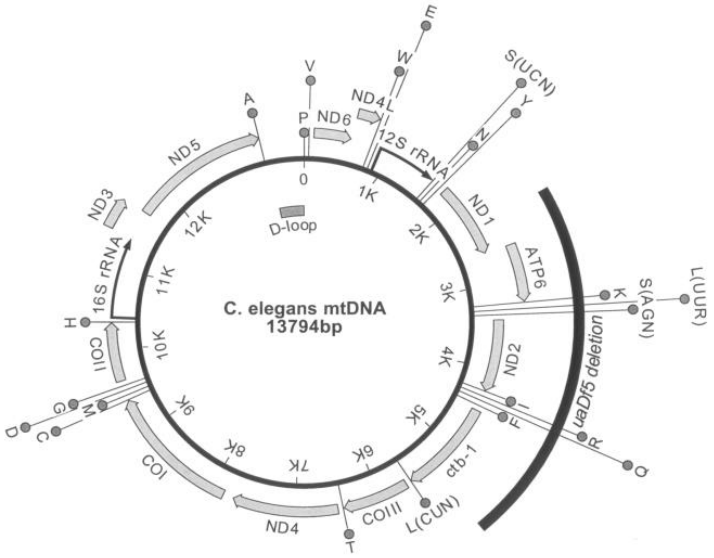

Figure III: Structure of the C. elegans mtDNA. mtDNA is 13,794 nucleotides in length and encodes 36 genes: 2 ribosomal RNAs, 22 transfer RNAs, and 12 ETC components. Figure adapted from Wormbook.

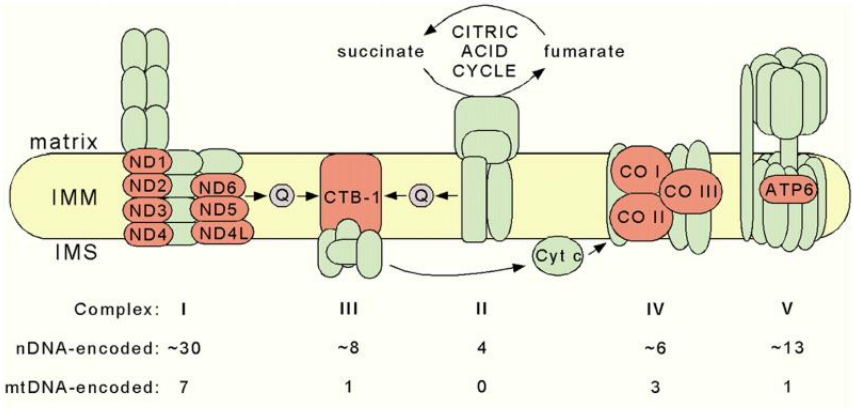

Figure IV: Schematic representation of the ETC. The components shown in red are derived from the mitochondrial genome (mtDNA). Only complex II does not contain any mtDNA-derived protein. Figure adapted from Wormbook.

Mitochondria in the regulation of lifespan

Apart from ATP production, mitochondria are implicated in several other processes, such as regulation of programmed cell death (apoptosis), nucleotide and amino acid biosynthesis, calcium buffering, β-fatty acid oxidation and reactive oxygen species (ROS) generation, among others. Taking into consideration the pleiad of cellular functions where mitochondria are involved, it is not surprising that mitochondrial dysfunction has been associated with severe human pathologies, ranging from neurodegeneration to metabolic disorders (Nunnari and Suomalainen, 2012). Pioneer research performed in several model organisms has linked impaired mitochondrial function with decline in stem cell function and the onset of cellular senescence, key aspects of the ageing process (Sun et al., 2016). In *C. elegans* particularly, RNAi inhibition of several ETC components during development significantly extends lifespan (Dillin et al., 2002). Furthermore, missense mutations in isp-1 (the “Rieske” iron sulfur protein), or *nuo-6* (which encodes the NDUFB4 subunit of the ETC complex I) profoundly increase lifespan (Feng et al., 2001; Yang and Hekimi, 2010). The extension of lifespan in these two genetic backgrounds depends on ROS generation by mitochondria and is strongly suppressed by mutations in the intrinsic apoptotic pathway (Yee et al., 2014). On the contrary, mutations in *gas-1*, which is also a subunit of ETC complex I, shorten the lifespan of worms (Kayser et al., 2001; Pujol et al., 2013). Similarly,

mutations in *mev-1*, which encodes the succinate dehydrogenase cytochrome b enzyme, shorten the lifespan by affecting the superoxide levels, hence the organismal response to oxidative stress (Ishii et al., 1998). Collectively, a moderate reduction in ETC function can be beneficial in regard to lifespan, whereas severe mitochondrial dysfunction can prove detrimental (Rea et al., 2007). Similarly, RNAi inhibition of five ETC components in Drosophila is sufficient to extend the lifespan of flies (Copeland et al., 2009). In mice, disruption in SURF1, a complex IV assembly factor, prolongs lifespan protects from chemical-induced neurotoxicity (Dell'agnello et al., 2007). Moreover, Ames dwarf mice exhibit altered ETC function in specific tissues (such as kidney) which may account for their extended lifespan (Choksi et al., 2011). Intriguingly, ageing affects mitochondrial membrane structure both in Drosophilae and mice, highlighting the reciprocal relationship between mitochondria and the ageing process (Brandt et al., 2017).

Caenorhabditis elegans **as a model for biological studies**

Caenorhabditis elegans is a tiny (maximum 1mM in length), hermaphrodite nematode, which normally inhabits the soil and feeds with rotting vegetables, using bacteria as its main food source. Its development is quite rapid, as eggs develop into adult animals within only three days at 20^{o}C and each adult animal gives rise to approximately 300 genetically identical descendants. Its transparency, relatively short lifespan (median lifespan of around 15 days), well-characterized neuronal system (consisting of around 300 neurons), simple anatomy and sequenced genome render *C. elegans* as an invaluable model for biological studies (Corsi et al., 2015). Males arise spontaneously under normal rearing conditions or upon heat stress-induced meiotic nondisjunction, enabling crosses between different genetic backgrounds. Four distinct larval stages (L1, L2, L3, L4) precede the reproductive maturation of the animal (figure V). Under non-favorable conditions (such as food scarcity or overcrowding), L2-L3 larvae can enter into a distinct developmental program, called dauer diapause (Fielenbach and Antebi, 2008).

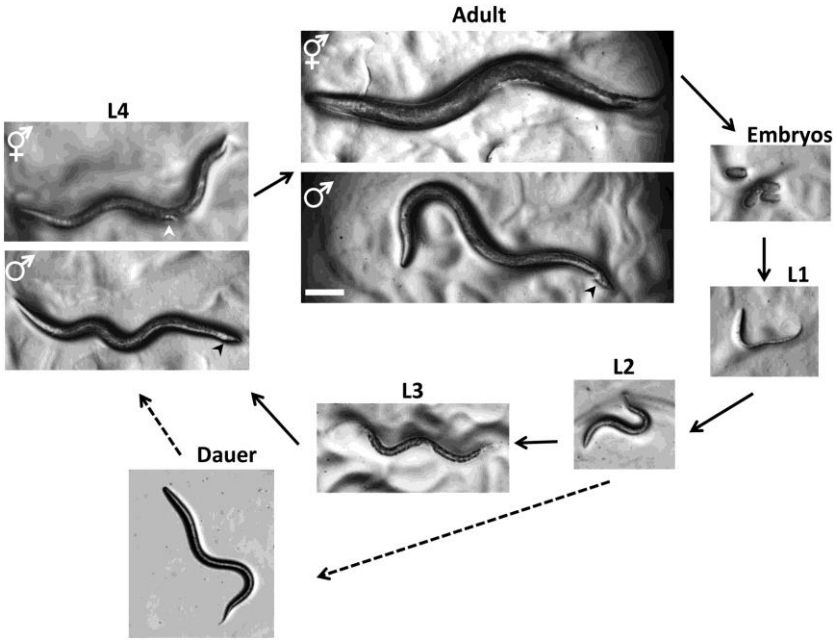

FigV: Representation of the *C. elegans* development. Eggs develop to reproductively mature nematodes within only three days at 20°C, which is the standard rearing temperature of the organism in the laboratory. Dauer diapause represents a mode of developmental plasticity for the nematodes to adjust to variable environmental conditions. Figure adapted from Corsi et al., 2015.

A synopsis of *C. elegans* germline development

Each adult nematode contains a total of 959 somatic cells. Those cells arise from coordinated, tightly regulated divisions occurring during embryogenesis and larval stages and are post-mitotic or terminally differentiated. The germline, consisting of around 1000 germ cells in each of the two gonad arms, is generated from the clonal expansion of two embryonic germline stem cells (GSCs) (Kimble and Hirsh, 1979). Each first instar larva (L1) which hatches possesses four germline precursors (Z1, Z2, Z3, Z4). Z1 and Z4 give rise to the somatic gonad (distal tip cell, gonad sheath, spermatheca, spermatheca-uterine valve and uterus), whereas Z2 and Z3 give rise to the germ cells. When the germline precursor cells (Z2 and Z3) are laser ablated at hatching the animals live approximately 60% longer than their wild-type counterparts (Hsin and Kenyon, 1999). Similarly, worm mutants in whom the germ cell pool is exhausted exhibit an extended lifespan (Arantes-Oliveira et al., 2002; Berman and Kenyon, 2006). Interestingly, this

seems to be a conserved phenomenon across species, since removing flowers is known to increase the lifespan of plants (Leopold et al., 1959) and the loss of germ cells is sufficient to extend lifespan in flies (Flatt et al., 2008). Transplantation of young ovaries to old mice increases life span of ovariectomized recipients (Mason et al., 2009) and castration increases longevity in men (Min et al., 2012), highlighting that signals from reproductive tissues influence lifespan.

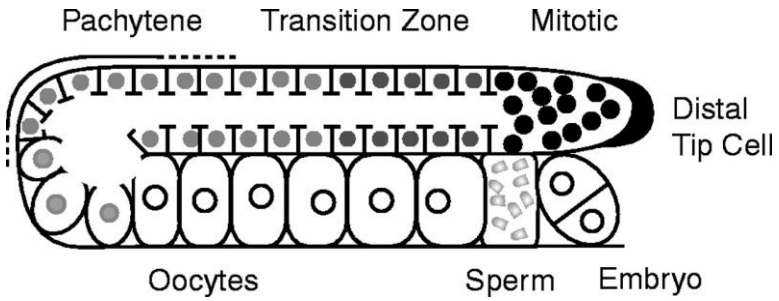

FigVI: Schematic representation of the *C. elegans* germ cell development. Mitotically-dividing germline nuclei in the distal arm transition to meiosis as they progress towards the proximal arm. Meiosis I arrests at the diakinesis stage of prophase I and is completed upon fertilization. Figure adapted from (Boag et al., 2005).

The two U-shaped gonads of each hermaphrodite are the only compartments which harbor mitotically-dividing nuclei during adulthood. The germ stem cell pool is located at the distal tip of each gonad arm and maintained via a spatially-defined mechanism through GLP-1/Notch signaling (Crittenden et al., 2006). The distal tip cell (DTC), a somatic cell of mesenchymal origin forms a LAG-2/Delta-positive membrane plexus which surrounds approximately 30-70 germ nuclei in its proximity, preserving their mitotic potential (Byrd et al., 2014). This is considered as the only stem cell niche paradigm in *C. elegans* (Kimble and Seidel, 2013). The majority of germline nuclei complete a single mitotic division before entering meiosis (Fox and Schedl, 2015). When the germ nuclei escape the DTC's vicinity they invariably progress towards differentiation (Cinquin et al., 2010). Those nuclei "switch off" their mitotic program and enter meiotic prophase I (pathytene, diplotene, diakinesis), become enclosed by cell membranes and finally form oocytes

which are finally fertilized in the spermatheca prior to egg laying in the proximal gonad arm (summarized in figure VI). Spermatogenesis in the hermaphrodites gonads is a distinct developmental process which begins prior to oogenesis (Ellis and Stanfield, 2014). The *C. elegans* germ stem cell niche is considered a faithful analogue of mammalian stem cell niches and has been employed for studying how different factors affect cell fate decisions (Albert Hubbard, 2007; Joshi et al., 2010).

The mitotic potential of germline stem cell nuclei downstream of GLP-1/Notch signaling is preserved by its immediate target genes, encoding “stemness” proteins, such as LST-1, SYGL-1 which act redundantly to promote GSCs self-renewal (Kershner et al., 2014). Regulation at the post-transcriptional level through the coordinated function of several RNA-binding proteins is also pivotal (Nousch and Eckmann, 2013). Specifically, members of the PUF (Pumilio and FBF) protein family are indispensable for mitotic division and their depletion is sufficient to drive meiotic entry and differentiation (Lamont et al., 2004). PUF proteins are predominantly translational repressors, since they bind at conserved motifs found in the 3’ UTR of their mRNA targets and repress their translation (Bernstein et al., 2005). Upon binding of PUFs, target mRNAs can be either de-adenylated through CCR4/Not complex or bind to an Argonaute-eIF1A repressor complex (Friend et al., 2012). In both cases the translation of the target mRNAs is inhibited and the respective transcripts can be also destabilized. FBFs are broad translational repressors and genome-wide studies have revealed that they can bind up to 7% of the total mRNA molecules transcribed by the *C. elegans* genome (Kershner and Kimble, 2010). Targets of FBF include genes which are required for differentiation into multiple somatic cell lineages (such as LIN-3, MPK-1 etc), sperm cell fate determinants (such as FOGs), as well as regulators (GLD-1, GLD-2 and GLD-3) and executors (proteins required for recombination) of meiotic entry (summarized in figure VII). Acting in an antagonistic mode with PUFs, GLD-1, a KH motif RNA binding protein, is required for germ nuclei differentiation and meiotic entry (Francis et al., 1995). GLD-1, itself directly repressed by FBFs, recognizes several features of its target transcripts (such as the mitotic *cyclin E* mRNA) and represses their translation (Doh et al., 2013) Similar to FBFs, GLD-1 binds to hundreds of germline transcripts (Scheckel et al., 2012; Wright et al., 2011). GLD-1 safe-

guards totipotency by repressing the precocious translation of transcripts destined for expression in early embryonic differentiation (Ciosk et al., 2006). Hence, reciprocal genetic interactions, where RNA-binding proteins play a crucial role, dictate GSCs fate decisions in the *C. elegans* germline (Hansen and Schedl, 2013).

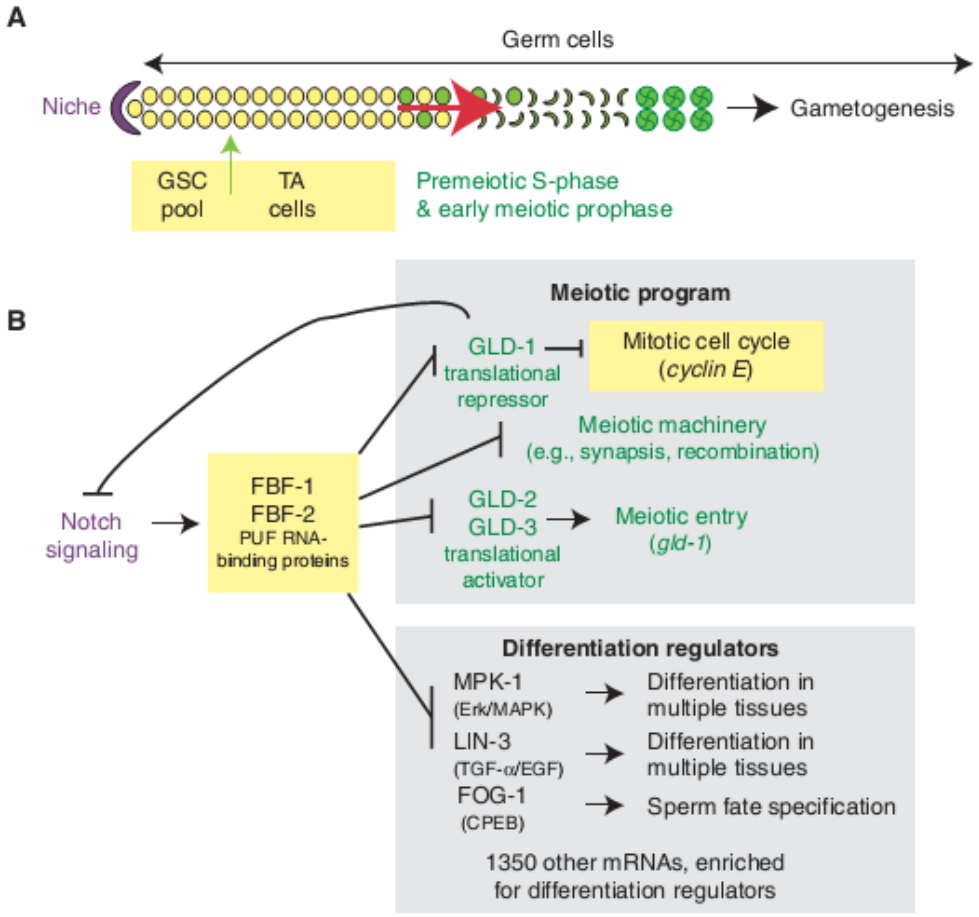

FigVII: The balance between FBFs and GLDs determines GSCs fate decisions in *C. elegans* germline. A) Germline nuclei transition from mitosis to meiosis as they escape the DTC's vicinity. B) PUFs repress the translation of differentiation factors, preserving the mitotic potential of germline nuclei in the proliferative zone, whereas GLDs are required for meiotic entry. Figure adapted from (Kimble, 2011).

Secreted sperm-derived signals (the so called major sperm proteins, MSPs) are essential for oocyte meiotic maturation and sheath cell contraction (collectively referred to as ovulation) to occur (McCarter et al., 1999). MSPs are perceived by the gonad sheath cells and act through the

Gα s-adenylate cyclase-protein kinase A pathway and specifically GSA-1, the worm Gs alpha subunit of heterotrimeric G proteins, to promote meiotic maturation in the presence of sperm. In the same pathway, GOA-1, the Go/i alpha subunit, is a negative regulator of meiotic maturation when the sperm is absent (Govindan et al., 2006; Govindan et al., 2009). Thus, the antagonistic interaction between Ga o/i and Ga s couples sperm availability with the rate of meiotic maturation in the proximal gonad arm. A prominent role for MSP signaling is to activate the MPK-1/MAPK kinase (Miller et al., 2001). The MPK-1/MAPK kinase has pleiotropic functions in the germline, including the specification of the male germline fate in males and hermaphrodites, progression through pachytene, the negative regulation of physiological apoptosis in the germline, and the control of oocyte growth and meiotic maturation (Lee et al., 2007). Overall, a unifying scheme is emerging, where two major signaling centers, one localized in the distal gonad arm (DTC) and the other in the proximal gonad arm (sperm), coordinate several spatially and temporally defined processes for GSCs' differentiation into functional oocytes in the *C. elegans* germline (figure VIII) (Nadarajan et al., 2009).

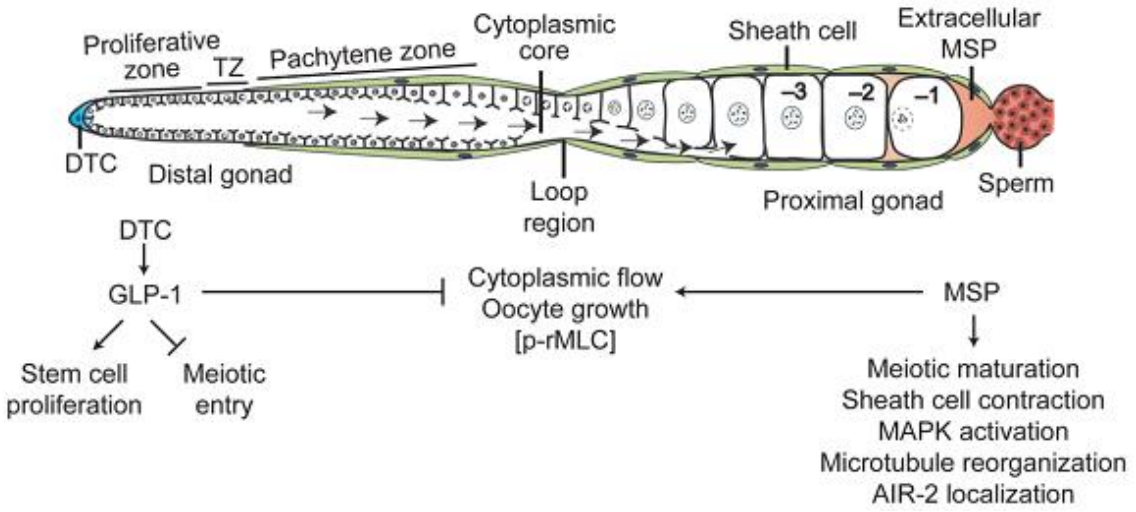

FigVIII: Two separate signaling centers regulate germline morphogenesis in *C. elegans*. GLP-1/Notch signaling from the DTC (blue color) safe-guards the mitotic identity of GSCs and prevents meiotic entry, while MSP signaling (red color) regulates several aspects associated with meiotic maturation and ovulation. Figure adapted from (Kim et al., 2013).

Key findings

The key findings of our study are the following (summarized in Fig8):

- We show that mitochondria are an inseparable component of the *C. elegans* germline. Specifically, abrogation of the transcription of the mitochondrial genome (via knockdown of the mitochondrial RNA polymerase RPOM-1) leads to an arrest of germ cell differentiation at the pachytene stage of meiosis I and concomitant hyperplasia of the gonad syncytium. This in turn causes an up to 50% reduction of the brood size of adult hermaphrodites (Fig1). Moreover, the germline of *rpom-1(RNAi)*-treated hermaphrodites is quite sensitive, since a mild temperature elevation causes severe defects in fecundity and the appearance of dead corpses.
- Compensatory apoptosis is induced following inhibition of mitochondrial biogenesis. Apoptosis acts protectively to restrict the extent of hyperplasia (Fig2).
- Mitochondrial bioenergetics in circuit with extrinsic signaling pathways (such as Insulin/IGF-1 and TGF-β) and internal gonad parameters shape the balance between mitosis and differentiation. While RPOM-1 depletion causes germline hyperplasia in wild-type animals, it produces atrophic gonads when nutrition signals (Insulin/IGF-1 and TGF-β) are also deprived. In contrast, attenuation of protein synthesis is beneficial and confers protection under conditions of compromised mitochondrial function (Fig3).
- RPOM-1 expression is compartmentalized. It firstly becomes evident as the germ nuclei reach the pachytene stage of meiotic prophase I and is even higher close to the gonad turn and at the proximal arm, where the oocytes are produced (Fig4).
- We suggest that a mitochondrial maturation process underlies germ cell differentiation. En route to oocyte production, mitochondria transition from a globular to a tubular shape (Fig5) and acquire several hallmarks of functional maturation, such as increased electrochemical potential as well as elevated ROS and ATP production (Fig6).
- We find that mitochondrial maturation is under the control of major sperm protein (MSP) and MAPK/ERK signaling. Genetic inhibition of the aforementioned pathways is sufficient

to block mitochondrial elongation (FigS8) and efficient polarization in the proximal arm (FigS9).

- Mitochondrial network elongation and elevation of POLRMT (mammalian RPOM-1 homologue) are conserved in mammalian stem cell differentiation. Increased cytoplasmic versus nuclear abundance of OCT-4 pluripotency transcription factor is associated with elevated POLRMT expression (Fig7 and FigS10).

2. RESULTS

Results

Intact mitochondrial function is indispensable for fecundity in *C. elegans*

The mitochondrial genome of *C. elegans* encodes twelve ETC protein-coding genes, lacking the ATP8 gene of its human counterpart (Okimoto et al., 1992). HMG-5, a high mobility group protein which regulates mitochondrial DNA content, is considered a putative nematode TFAM homologue, with important roles in replication, transcription and packaging of mtDNA into nucleoids (Kukat and Larsson, 2013; Sumitani et al., 2011), while a TFB2M homologue has not been yet identified. However, *C. elegans* possesses a TFB1M homologue, a protein with 16S rRNA methyltransferase activity, which shares some similar properties, but has distinct functions from TFB2M (Cotney et al., 2009). *Rpom-1* gene encodes the mammalian POLRMT homologue. CLUSTALW alignment of the catalytic domain of RPOM-1 and its putative homologues revealed extensive conservation from yeast to mammals (Fig. S1). We created RNAi constructs to specifically target *hmg-5*, *rpom-1* and *tfbm-1* transcripts, since mutants for the respective genes are lethal and sterile. We verified that our RNAi constructs knocked down the expression of the three mRNAs using real-time PCR (data not shown). RNAi-mediated knockdown of *hmg-5*, *rpom-1* and *tfbm-1* compromised mitochondrial function, as quantitatively assayed by TMRE (Tetramethylrhodamine, Ethyl Ester, Perchlorate) and MitoTracker Red CM-H2XROS stainings as well as ATP measurement in worm extracts (Fig. S2A-C). Importantly, we found that RPOM-1 depletion dramatically reduced mitochondrial DNA content, at levels comparable to HMG-5 depletion. This can be attributed to the fact that POLRMTs, apart from their role in mtDNA transcription, also provide RNA primers for the initiation of mtDNA replication by the mitochondrial-specific DNA polymerase (POLG-1 in *C. elegans*). In contrast, the mitochondrial copy number remained unaffected in animals subjected to *tfbm-1(RNAi)*, proving the specificity of our measurements (Fig. S2D). The aforementioned highlight the importance of intact transcription machinery residing in mitochondria for preserving full organelle function.

We noticed that RNAi-mediated knockdown of *rpom-1* dramatically reduced the brood size of wild-type nematodes (Fig. 1A, B). The defect was even more pronounced in elevated

temperatures and subsequent generations, indicating the existence of a maternal-effect phenotype (data not shown). Intriguingly, we detected hyperplasia in the meiotic prophase I pachytene syncytium region in the gonads of animals fed with bacteria expressing *rpom-1(RNAi)* (Fig. 1C). We reasoned that hyperplasia in RPOM-1 depleted nematodes could be a consequence of elevated mitotic activity in the proliferative region of the gonad. To check this hypothesis, we stained extruded gonads from control and *rpom-1(RNAi)*-treated animals with an antibody specific to phosphorylated serine 10 of histone H3 (anti-pH3), a widely-used marker for mitotic-phase nuclei (Goto et al., 1999; Van Hooser et al., 1998). RPOM-1 depletion didn't cause any significant defect on the proliferative capacity of the mitotic region (Fig. 1D, E). We then investigated whether germ nuclei accumulate in the pachytene region due to their inability to properly differentiate and produce oocytes in the proximal gonad arm. By utilizing a fluorescent reporter strain for EGG-1, a protein which normally localizes to oocyte membranes, we detected three times less EGG-1::GFP positive cells (i.e oocytes) in *rpom-1(RNAi)*-treated animals compared to their control counterparts (Fig. 1F, G). Furthermore, we didn't observe any gross morphological defect in somatic tissues that support the gonads, such as the gonad sheath (Fig. S3A) and the distal tip cell (Fig. S3B). Hence, impaired differentiation of germ cells to oocytes leads to germline hyperplasia in *rpom-1(RNAi)*-treated animals.

Germline apoptosis counterbalances hyperplasia

We surveyed for cellular responses triggered by aberrant mitochondrial biogenesis. RPOM-1 depletion resulted in accumulation of apoptotic corpses in the gonad syncytium, which were clearly evident using differential interference contrast (Nomarski) microscopy and a CED-1::GFP reporter strain (Fig. 2A). CED-1 is a transmembrane receptor which normally clusters around apoptotic corpses before they are engulfed and removed by gonad sheath cells (Li et al., 2012; Zhou et al., 2001). Furthermore, both HMG-5 and TFBM-1 depletion efficiently induced apoptosis, although to a lesser extent than *rpom-1(RNAi)* (Fig. 2B), indicating that distinct signals emanating from dysfunctional mitochondria may trigger programmed cell death. Inhibition of

apoptosis in homozygous *ced-3*/caspase mutants can lead to the accumulation of germ cell corpses that cannot be removed (Gumienny et al., 1999). Notably, *rpom-1* knockdown in *ced-3(n717)* homozygous mutants enhanced the germline hyperplasia observed in wild type nematodes. By contrast, loss of function mutants for *ced-9(n2814)*/BCL-2, where apoptosis is induced, exhibit no signs of hyperplasia upon *rpom-1* downregulation (Fig. 2C). Hence, induction of apoptosis compensates for the hyperplasia phenotype caused by the inhibition of mitochondrial transcription.

Mitochondrial transcription acts in parallel with signaling pathways converging on the germline

We investigated the impact of RPOM-1 depletion in mutants with reported defects in germline homeostasis. Insulin/IGF-1 signaling is proposed to promote proliferation of germline stem cells (Michaelson et al., 2010). While *rpom-1* downregulation caused hyperplasia in the germline syncytium of wild type animals (Fig. 3A, B), it differentially affected *daf-2(e1370)*/IGFR mutants by producing dwarf gonads at 20^{o}C and aggravating the proliferative defect caused by Insulin/IGF-1 signaling inhibition (Fig. 3C, D). TGF-β signaling is also reported to affect the balance between mitosis and differentiation in *C. elegans* germline, in response to environmental cues. ASI neurons sense food abundance and population density in the environment and send a TGF-β signal which is perceived by the DTC to dictate the rate of proliferation in the germline stem cell niche (Dalfó et al., 2012). RPOM-1 depletion in *daf-1(m40)*/TGFR mutants behaved similarly to *daf-2(e1370)*/IGFR mutants, since it produced gonads with further compromised proliferative potential compared to their respective controls (Fig. 3E, F). In sharp contrast, *rsks-1(ok1255)*/ S6K mutants, which exhibit attenuated protein synthesis, were insensitive to *rpom-1(RNAi)* and their gonads were identical to those of control animals (Fig. 3G, H). Importantly, *ife-5(ok1934)*/eIF4E mutants, similarly to *rsks-1(ok1255)* mutant animals, remained unaffected by RPOM-1 depletion (Fig. 3I, J). Furthermore, the egg laying defect caused by RPOM-1 deficiency was completely absent in protein synthesis-defective nematodes, as evident by the brood size of

individual animals, as well as the number of germ cell nuclei reaching diakinesis (Fig. 3M, N). This can be attributed to the lower energy expenditure of *rsks-1* and *ife-5* mutants and indicates that reduced protein synthesis provides a selective advantage in preserving germline homeostasis under conditions of impaired mitochondrial ATP production. Finally, *rpom-1(RNAi)*-treated *glp-1(e2141)*/Notch loss of function mutants were indistinguishable from controls under restrictive temperatures, producing germline-less hermaphrodites (Fig. 3K, L). Numerous nematode strains bearing mutations for germline components, such as P-granules, are fully fertile at standard nematode growth conditions (20^{o}C), but become sterile following a switch to a higher temperature (25^{o}C) (Spike et al., 2008). The defects accompanying RPOM-1 depletion became even more prominent when the animals were raised at 25^{o}C. The gonads at that temperature virtually collapse, barely produce a few diplotene and diakinesis-staged germ nuclei and accumulate dead corpses (Fig. S4), indicating that external stress insults aggravate the phenotypes caused by RPOM-1 deficiency. The aforementioned results suggest that the precise coordination of signaling pathways (Insulin/IGF-1, TGF-β, Notch/Delta) and internal gonad processes (mitochondrial transcription, protein synthesis) finally shapes the balance between mitosis and progression to meiosis in the *C. elegans* germline stem cell niche.

RPOM-1 expression is compartmentalized

To monitor endogenous RPOM-1 expression *in vivo*, we generated a translational reporter by fusing GFP to the carboxyl terminus of full-length *rpom-1* cDNA regulated by its endogenous operon promoter. RPOM-1 is expressed in several somatic tissues including muscles along the body, the intestine, vulva and numerous neuronal cells in the nerve ring region and the tail, in a pattern reminiscent of proteins localizing in the mitochondrial matrix (Fig. S5). RPOM-1 is also strongly expressed in the germline of hermaphrodite animals in a punctuate pattern. In the gonads, mitochondria surround and enwrap germ cell nuclei in the syncytium region (Fig. S6). We crossed RPOM-1::GFP transgenic animals with p$_{lag-2}$MYR::tdTomato animals, to visualize RPOM-1 expression in regard to the position of the distal tip cell. We noticed

that RPOM-1 expression is relatively low in the mitotic region distally, but increases profoundly as germ cell nuclei mature, are enclosed by cell membranes and form oocytes (Fig. 4A, Fig. S7A). Interestingly, RPOM-1 levels increase at the onset of pachytene, the exact same region where germ nuclei arrest in wild type animals upon RPOM-1 depletion. To achieve a faithful reconstitution of the endogenous RPOM-1 expression pattern, we also generated a reporter strain that expresses a transgene carrying the endogenous *rpom-1* 3'UTR cloned downstream of the full length *rpom-1* cDNA under the control of its operon promoter. On a similar note, RPOM-1 expression was elevated in the oocytes of the proximal arm, while it was weaker in the syncytium region in the distal arm (Fig. 4B). The expression of the operon's promoter *per se* gradually increases in a distal to proximal manner (Fig. S7B). IFET-1, which localizes to P-granules and is required for normal gonad development, is a general translational repressor that resides in the germline (Sengupta et al., 2013). Treatment of our reporter animals with *ifet-1(RNAi)* de-repressed RPOM-1 expression more distally (Fig. S7C). Hence, RPOM-1 expression in the germline is compartmentalized and increases as germ nuclei progress to the proximal arm and form oocytes.

Transition to tubular mitochondria is a hallmark of differentiation

Mitochondrial shape is malleable and alters to fulfill physiological demands, in response to stress and other intracellular or environmental signals. Specialized dynamin GTPase family members FZO-1/Mitofusin and EAT-3/OPA-1 mediate fusion, while DRP-1 is required for fission (Youle and van der Bliek, 2012). Whilst *fzo-1(tm1133)* and *drp-1(tm1108)* mutants are viable and fertile at 20^{o}C, they became sterile even from the first generation when the rearing temperature was shifted to 25^{o}C. The defect was less severe, nonetheless evident, in *eat-3(ad465)* mutants (Fig. S8A). We noticed that mitochondrial morphology alters during the course of germ cell differentiation to oocytes. Whilst the distal arm was abundant with globular mitochondria, we could mainly visualize elongated organelles in the proximal gonad arm (Fig. 5A, Fig. S8B). By thoroughly monitoring mitochondrial morphology, we observed that both globular and tubular

mitochondria coexist in the gonad turn region (Fig. 5B). Close to the turn, an actin-dependent cytoplasmic streaming is known to deposit cytoplasmic material and mitochondria to the oocytes (Wolke et al., 2007). Accumulating evidence suggests that a reciprocal relationship between mitochondrial morphology and metabolic activity occurs, since elongated mitochondria are associated with elevated electron transport chain activity and vice versa (Liesa and Shirihai, 2013; Mishra and Chan, 2016). Interestingly, *fzo-1(tm1133)* mutant animals possess significantly less germ nuclei in diplotene as well as oocytes in diakinesis stages of meiosis I, producing fewer offspring compared to wild-type nematodes (Fig. 5C, D). We propose that tubular mitochondria in the proximal arm represent the outcome of a maturation process, which is essential for oocytes to cope with their high-energy demands.

To shed light on the molecular mechanism that governs the alteration of mitochondrial morphology, we focused on well characterized pathways associated with germ cell differentiation in *C. elegans*. Spatial activation of MPK-1/MAPK signaling is crucial for germ cell exit from pachytene and oocyte production. *Mpk-1* deficient mutants exhibit pachytene arrest, phenocopying RPOM-1 depletion (Lee et al., 2007). Interestingly, we could not observe transition to tubular organelles upon knockdown of *mek-2* or *mpk-1*, the homologues of mammalian MEK and ERK kinases respectively (Fig. S8C, E, F, I). GLD-1 is an RNA-binding protein which binds to the 3'UTR of target mRNAs, repressing their translation. GLD-1 function is required for germ nuclei to enter the meiotic phase, since germ nuclei of *gld-1* loss of function mutants exit meiosis and return to mitosis, forming germline tumors (Francis et al., 1995). Similarly to MPK-1/MAPK signaling inhibition, *gld-1(RNAi)*-treated animals contain exclusively globular in the proximal gonad arm (Fig. S8C, G, I). Gonadal sheath cells are known to respond to sperm-derived signals (major sperm proteins, MSPs) and promote oocyte maturation through activation of the $G\alpha_s$-adenylate cyclase-protein kinase A pathway (Kim et al., 2013). Inhibition of *gsa-1*, which encodes the worm Gs alpha subunit of heterotrimeric G proteins, prevents the maturation of oocytes, even when sperm signaling is present (Govindan et al., 2006). Interestingly, mitochondria could not elongate in the proximal arm of *gsa-1(RNAi)*-treated animals (Fig. S8C, H, I) and the existing organelles were not efficiently polarized (Fig. S9A, C, D). Conversely, inhibition of GOA-1, a

negative regulator of oocyte maturation and GSA-1 antagonist boosted mitochondrial potential in the proximal arm (Fig. S9A, B, D). Altogether, these findings suggest that germ nuclei maturation is intertwined with mitochondrial maturation and the latter appears to rely on two important signaling pathways, namely MPK-1/MAPK and MSP.

Mitochondria functionally mature en route to germ cell differentiation

The already established interplay between mitochondrial morphology and metabolic activity prompted us to test whether mitochondria functionally mature in a progressive manner in the *C. elegans* gonad. We utilized Perceval, a fluorescent reporter for adenylate nucleotides constructed by combining a circularly permuted GFP version with GlnK1, a bacterial regulatory protein from a *Methanococcus* species (Berg et al., 2009). We cloned Perceval downstream of the *pie-1* promoter, to uniformly express it in the germline. We also fused the *tbb-2* 3'UTR, which is unresponsive to inhibition by GLD-1 RNA-binding protein, with the C-terminus of Perceval to avoid undesired silencing of our transgene (Merritt et al., 2008). Interestingly, we managed to detect expression in the oocytes of the proximal arm, but not in the syncytium region of the gonads (Fig. 6A). This indicates that ATP accumulates proximally, in the area which is abundant with tubular mitochondria. To further verify this finding, we stained whole animals with mitochondrial dyes which stain according to membrane potential, such as TMRE (Tetramethylrhodamine, Ethyl Ester, Perchlorate), DIOC6(3) (3,3'-Dihexyloxacarbocyanine Iodide) and MitoTracker Red CM-H2XROS. In congruence with the Perceval findings, mitochondrial membrane potential and ROS levels were elevated in developing oocytes, while staining in the distal arm was relatively weaker. (Fig. 6B, C, D). We postulate that mitochondrial elongation is a primitive step in a maturation process which results in enhanced polarization of mitochondrial membranes and concomitant ATP and ROS production in oocytes, just before their fertilization in the spermatheca.

Elevated POLRMT expression and switch to tubular mitochondria are conserved during evolution

We next wondered whether a similar mechanism controls mouse stem cell differentiation. We employed J1 cells, which have derived from the inner cell mass of mouse blastocysts and grow on spherical colonies in the presence of LIF cytokine. We removed LIF from our culture medium and let the cells differentiate in an unbiased manner towards various cell lineages. We stained with antibodies for POLRMT and MTCO1, the cytochrome c oxidase subunit I, which is encoded by the mitochondrial genome. The staining was much weaker at the core of the stem cell colonies and progressively increased as cells differentiated and extended membrane projections typical of differentiated cells (Fig. S10). Furthermore, 48 hours after LIF removal, we managed to observe POLRMT-positive mitochondria with tubular shape (Fig. S10, red panel). We also simultaneously stained with POLRMT and OCT-4 antibodies. OCT-4 is a key pluripotency transcription factor (Joshi et al., 2010). OCT-4 is known to shuttle between the nucleus and the cytoplasm and its nuclear retention enhances reprogramming efficiency and is associated with pluripotency (Oka et al., 2013). Notably, the cytoplasmic abundance of OCT-4 was increased along with POLRMT expression. By contrast, retention of OCT-4 in the nucleus coincided with reduced POLRMT expression (Fig. 7). In summary, in agreement with the *C. elegans* findings, mouse stem cells exhibit low POLRMT expression and globular mitochondria, while differentiation is accompanied by an increase in POLRMT expression and the appearance of elongated mitochondria.

3. DISCUSSION

Discussion

The term *stem cell niche* refers to the specific microenvironment which ensures that stem cells are protected from harmful agents, divide and differentiate to constantly replenish organs (Morrison and Spradling, 2008). The *C. elegans* gonad hosts the sole stem cell niche in an otherwise post-mitotic organism (Joshi et al., 2010). Moreover, it is considered as the main tissue where mitochondrial DNA replication occurs (Bratic et al., 2009). A previous study showed that perturbation of a germline-specific mitochondrial ATPase subunit impairs fecundity (Kawasaki et al., 2007). We find that mitochondria are an integral and inseparable component of this niche and that perturbation of their biogenesis, energy production and dynamics, collectively referred to as bioenergetics, can profoundly affect germ cell differentiation. We describe a maturation process, whereby globular, immature mitochondria are gradually converted to elongated, functional organelles to support increased oocyte energy demands (Fig. 8A). This switch is tightly regulated by two core signaling pathways associated with oocyte production and maturation, namely MAPK/ERK and MSP signaling. The MAPK/ERK pathway has pleiotropic functions in the *C. elegans* germline (Lee et al., 2007); however information concerning its downstream effectors remains limited. The DDX-19 helicase and GSK-3 kinase have been shown to be direct MPK-1 targets *in vivo* (Arur et al., 2009). Additionally, MPK-1 phosphorylates NOS-3, promoting degradation of TRA-1 by the FEM-CUL2 complex, to facilitate oocyte membrane organization (Arur et al., 2011). The MAPK/ERK pathway itself lies downstream, and is positively regulated, by MSP signaling (Miller et al., 2001). Thus, mitochondrial bioenergetics is likely a nodal point modulated by these cascades, in stem cells.

Our findings indicate that expression of mitochondrial RNA polymerase progressively increases during germ cell differentiation. This increase is accompanied by a transition of mitochondria to an elongated shape and the manifestation of several metabolic activity hallmarks, such as increased electron potential, ATP and ROS production. *Rpom-1* mRNA is one of the numerous targets of FBF-1, a Pumilio family, RNA-binding protein which acts in the mitotic region

to negatively regulate the expression of mRNAs implicated in meiotic entry (Crittenden et al., 2002; Kershner and Kimble, 2010). In addition, localized transcription and mRNA translation likely contribute to the subcellular compartmentalization of RPOM-1. Taken together, our observations indicate that upon perturbation of germ cell bioenergetics, germ nuclei stall in the pachytene stage and fail to differentiate, generating less functional oocytes and progeny. Consistent with this notion, mitochondrial ATP synthase function is required for the maturation of mitochondrial cristae and consequently, germ cell differentiation, in *Drosophila* ovaries (Teixeira et al., 2015). Similarly, the pluripotent state of mammalian stem cells has been linked to decreased mitochondrial respiration, in favor of anaerobic glycolysis (Xu et al., 2013). Previous studies have demonstrated that mitochondrial mass, mtDNA copy number and oxygen consumption increase during stem cell differentiation (Cho et al., 2006; Varum et al., 2011; Zhang et al., 2013). By contrast, successful induction of pluripotent stem cell (iPSCs) lines is marked by reduction of ETC function (Armstrong et al., 2010). Hence, a switch to enhanced ETC activity for efficient mitochondrial respiration and ATP production is a prerequisite for stem cell differentiation across species.

Recent work has shown that conserved signaling pathways implicated in lifespan regulation and dauer formation, also influence germline homeostasis. For example, mutants for DAF-2, the worm homologue of Insulin/IGF-1 receptor display decreased germ cell proliferation, while DAF-16/FOXO activity is beneficial for stem cell pool maintenance during ageing (Michaelson et al., 2010; Qin and Hubbard, 2015). Furthermore, TORC1 and RSKS-1/S6K is autonomously required for efficient proliferation of germ cell progenitors, implicating TOR activity and protein synthesis in germline maintenance (Korta et al., 2012). In addition, external cues determine the balance between mitosis and differentiation, via soma to germline communication. Under favorable conditions (low dauer pheromone, low population density), a TGF-β signal arising from the ASI neuron is received by the DAF-1/ TGF-β receptor in the DTC. Activation of SMAD-mediated transcription, together with GLP-1/ LAG-2 signaling, which is indispensable for maintaining stem cell pool, ultimately shape the balance of mitosis versus differentiation in the *C. elegans* gonad (Dalfó et al., 2012). Attenuation of Insulin/IGF-1 and TGF-β signaling, combined

with perturbation of mitochondrial transcription generates an atrophic germline, and exacerbates proliferation defects, indicating that mitochondrial function acts in parallel with extrinsic growth stimuli to dictate mitosis versus differentiation decisions (Fig. 8B). Similarly, energy is diverted to stress resistance and maintenance mechanisms in mutants with reduced protein synthesis that also display extended lifespan (Hansen et al., 2007; Syntichaki et al., 2007). In this context, as the disposable soma concept postulates, damage repair takes precedence over protein synthesis for germline maintenance and reproduction.

The precise balance between mitosis and differentiation is of utmost importance for tissue and organismal homeostasis. Our work provides novel insights on how mitochondrial bioenergetics participates in cell fate decisions and integrates mitochondria at the core of the developmental modules that shape the *C. elegans* germline. Perturbation of mitochondrial function obstructs germ nuclei differentiation and causes cancer-like phenotypes (Fig. 8C). One of the main challenges for future research is to delineate the molecular underpinnings of the germline mitochondrial metabolic switch as well as its temporal and spatial regulation.

4. FIGURES

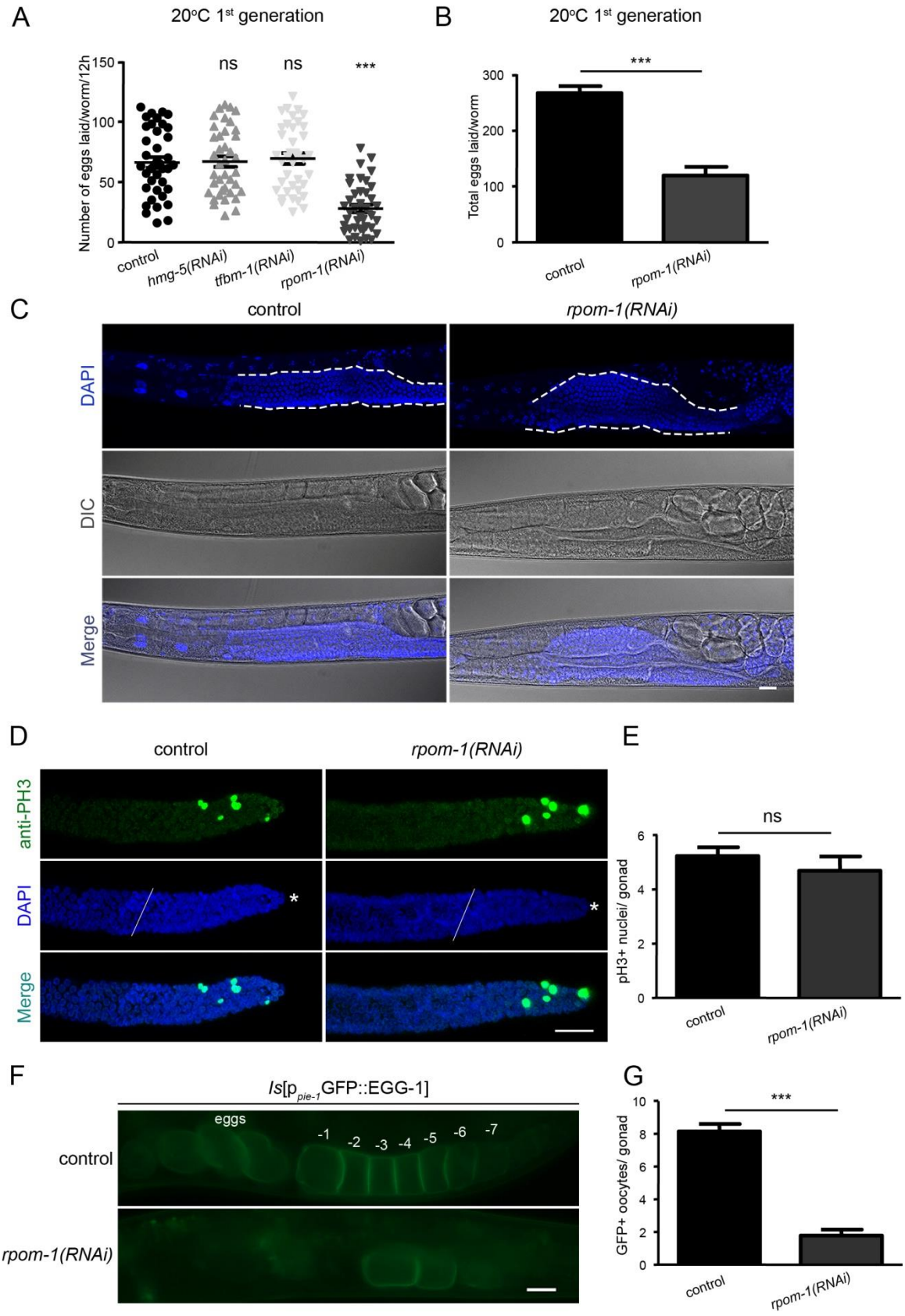
A
20°C 1st generation
Number of eggs laid/worm/12h
150
100
50
0
ns
ns
***
control
hmg-5(RNAi)
tfbm-1(RNAi)
rpom-1(RNAi)
B
20°C 1st generation
Total eggs laid/worm
300
200
100
0
***
control
rpom-1(RNAi)
C
control
rpom-1(RNAi)
DAPI
DIC
Merge
D
control
rpom-1(RNAi)
anti-PH3
DAPI
Merge
*
*
E
ns
pH3+ nuclei/ gonad
6
4
2
0
control
rpom-1(RNAi)
F
Is[p pie-1 GFP::EGG-1]
eggs
-1
-2
-3
-4
-5
-6
-7
control
rpom-1(RNAi)
G
***
GFP+ oocytes/ gonad
10
8
6
4
2
0
control
rpom-1(RNAi)

Figure 1: RPOM-1 depletion causes germline hyperplasia in *C. elegans*. A, B,) The brood size of *rpom-1(RNAi)*-treated hermaphrodites is significantly reduced (up to 50%) compared to their control counterparts. Unpaired *t*-test was used for the estimation of statistical significance (n>40; ***$P < 0.001$). D) Inhibition of mitochondrial transcription results in hyperplasia phenotype and germ nuclei arrest in the pachytene region of prophase I in the germline syncytium of elsewhere wild-type animals. The dashed lines surround the germline syncytium. E) Phosphorylated histone H3 antibody staining of extruded gonads for the detection of mitotic nuclei in the distal gonad arm. The dashed lines highlight the border between the mitotic region and the transition zone, marked by the appearance of crescent-shape nuclei, while the asterisk marks the tip of the distal gonad arm. F) Quantification of phosphorylated histone 3 positive germ nuclei in control and *rpom-1(RNAi)*-treated hermaphrodites. G) RPOM-1-depleted nematodes produce three times less EGG-1 positive oocytes compared to their control counterparts. H) Quantification of EGG-1 positive oocytes in control and *rpom-1(RNAi)*-treated hermaphrodites. Unpaired *t*-test was used for the estimation of statistical significance (n>40; ***$P < 0.001$). Error bars, s.e.m. Images were acquired using a X40 objective lens. Scale bars, 20μm.

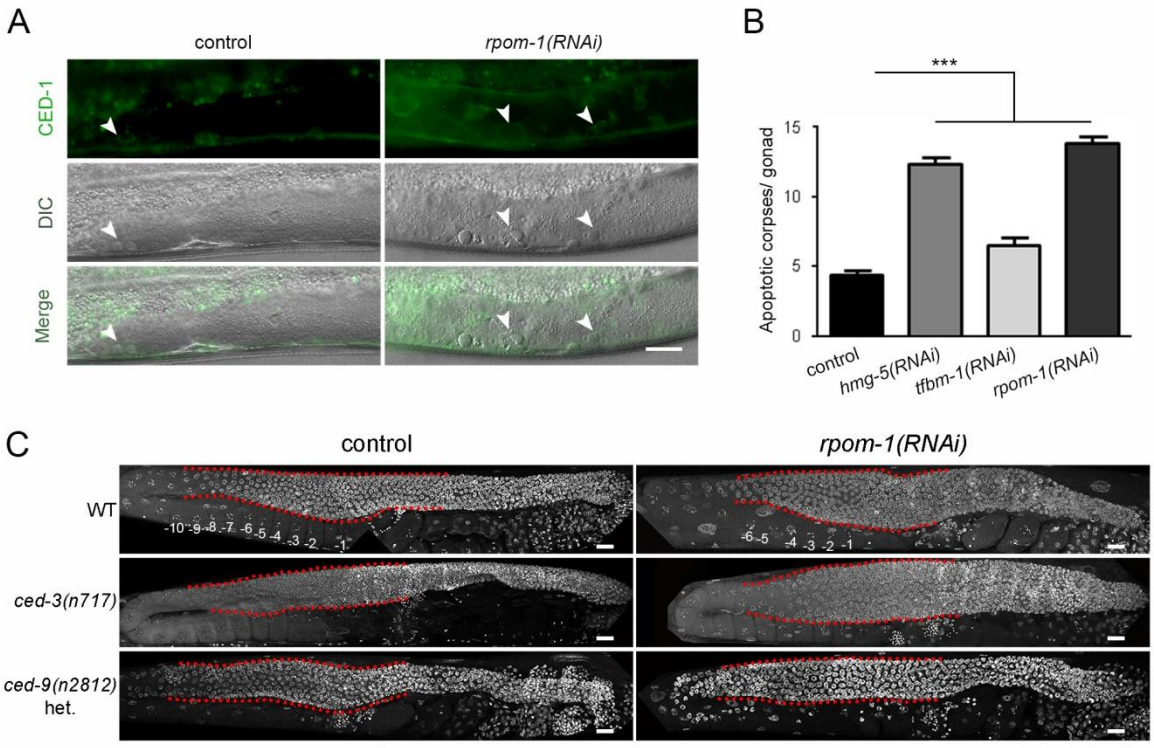

Figure 2: Induction of apoptosis prevents excessive hyperplasia. A) Apoptosis induction following *rpom-1* downregulation, as monitored using the CED-1::GFP reporter in combination with Nomarski optics. B) A two-fold induction in the number of early apoptotic corpses can be detected upon RPOM-1 depletion. *Hmg-5* and *tfbm-1* downregulation also trigger apoptosis (n=40; ****P* < 0.001, one-way ANOVA was used for multiple comparisons). C) RPOM-1 depletion in *ced-3(n717)*/caspase-deficient animals causes pronounced hyperplasia, even more severe than in wild-type worms. Heterozygous *ced-9(n2812)* animals exhibit no sign of hyperplasia. Images were acquired using a X40 objective lens. Error bars, s.e.m. Scale bars, 20µm.

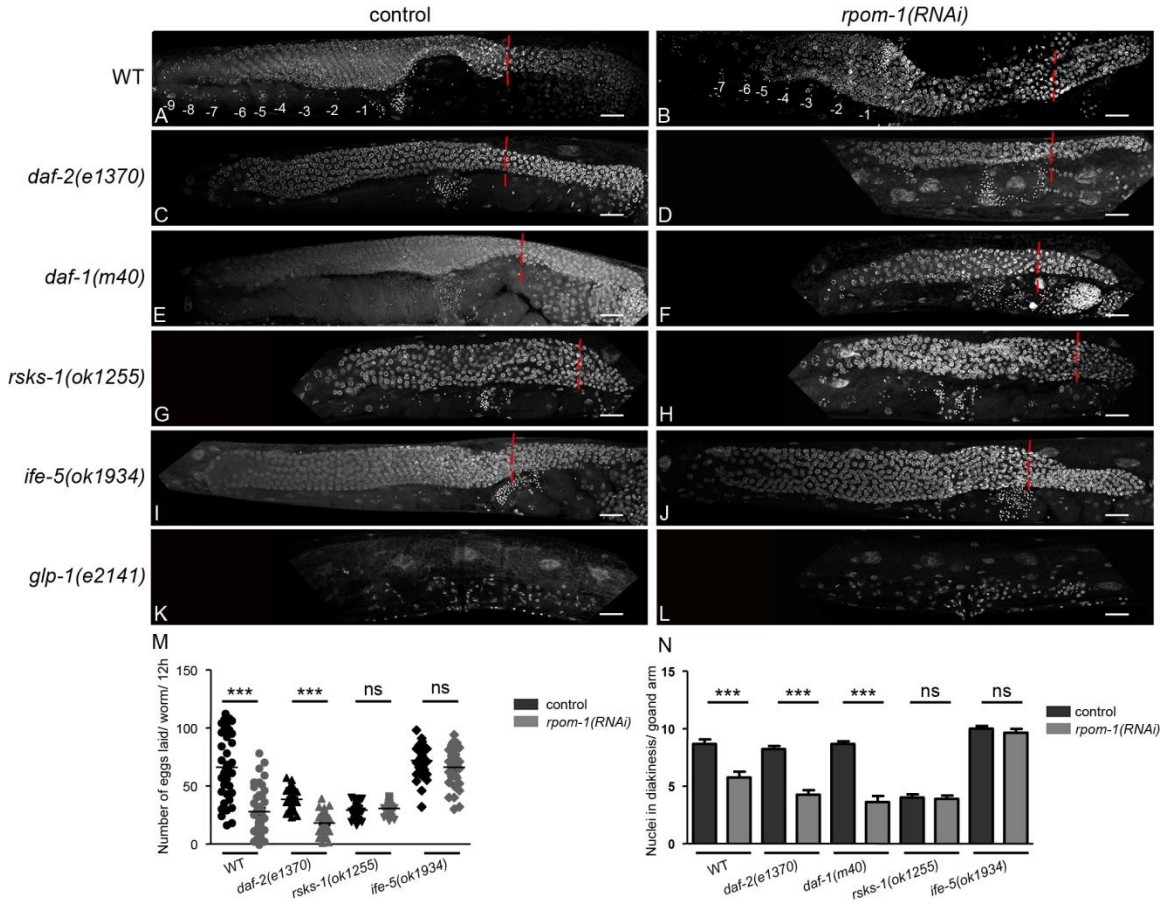

Figure 3: Mitochondrial transcription acts in parallel with signaling pathways converging on the germline. A, B) Inhibition of mitochondrial transcription causes germline hyperplasia in otherwise wild type animals. In contrast, treatment of *daf-2*/ IGFR (C, D) and *daf-1*/ TGFR (E, F) homozygous mutants with *rpom-1(RNAi)* at 20ºC produces dwarf gonads and augments their mitotic defects. Mutants with attenuated protein synthesis rates, such as *rsks-1*/ S6K (G, H) and *ife-5*/eIF4E (I, J) are indistinguishable from their control counterparts upon treatment with rpom-1(RNAi). (K, L) *Glp-1*/Notch loss of function produces germline-less animals at restrictive temperatures. The red dashed lines indicate the border between the mitotic region and the transition zone. M) Egg laying measurements in wild-type and *daf-2(e1370)*, *rsks-1(ok1255)* and *ife-5(ok1934)* mutants. N) Quantification of the number of germ nuclei reaching diakinesis in wild type, *daf-2(e1370)*, *daf-1(m40)*, *rsks-1(ok1255)* and *ife-5(ok1934)* genetic backgrounds. (n>40; ***$P < 0.001$, unpaired *t*-test). Error bars, s.e.m. Images were acquired using a X40 objective lens. Scale bars 20μm.

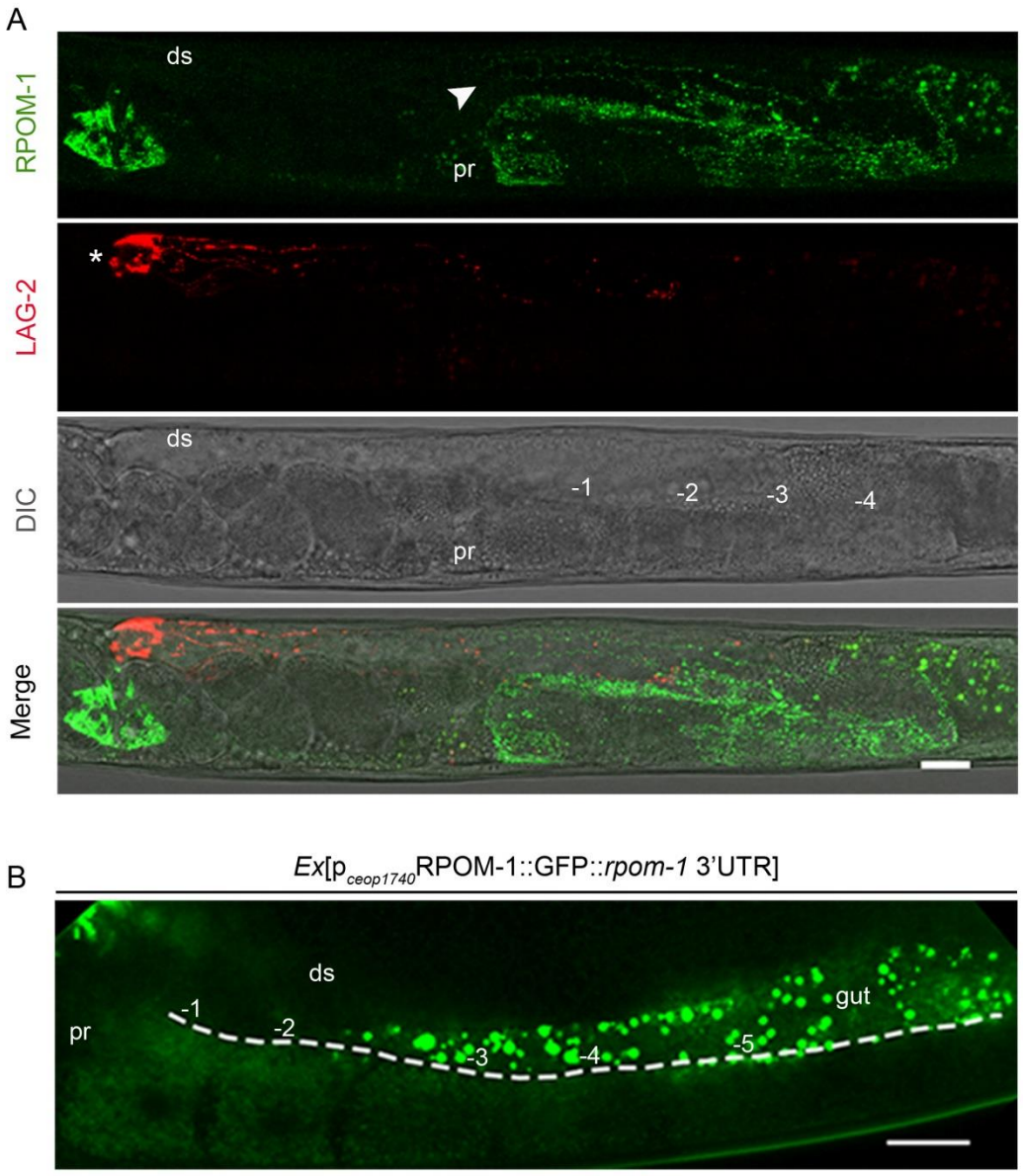

Figure 4: RPOM-1 expression is compartmentalized. A) RPOM-1 expression (in green) is low in the distal arm and the mitotic region of the gonads, becomes evident at the onset of the pachytene region (arrowhead) and substantially increases close to the turn and in the proximal arm, where the oocytes mature. LAG-2 (in red) is the Delta homologue which is expressed by the distal tip cell (white star). B) A reporter strain overexpressing RPOM-1 under the control of its endogenous promoter and 3'UTR reveals higher expression in the oocytes and lower in the syncytium. Ds; distal, pr; proximal, -1 denotes the proximal-most oocyte. Images were acquired using X40 and X63 objective lenses. Scale bars, 20µm.

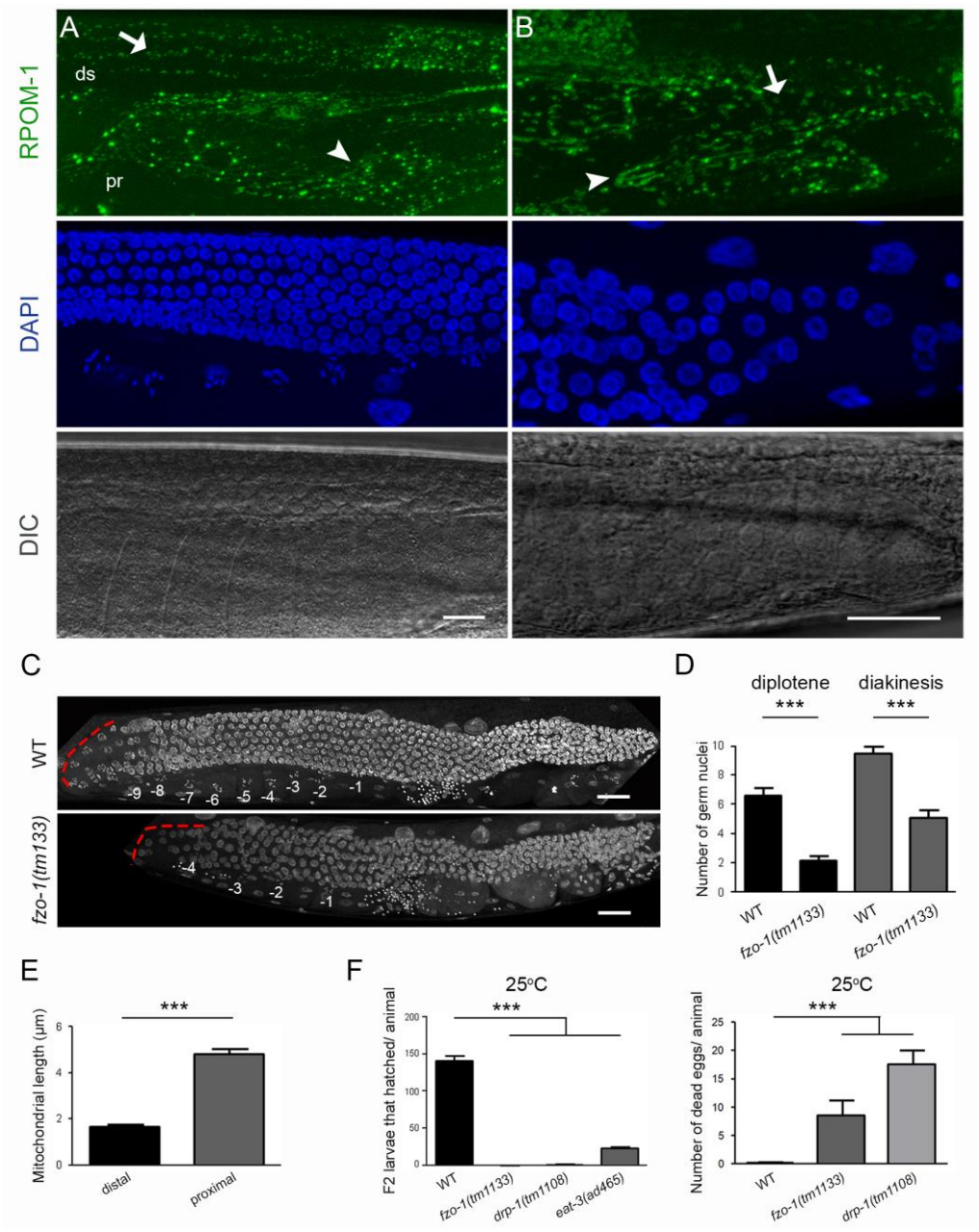

Figure 5: Transition from globular to tubular mitochondria is a prerequisite for germline homeostasis. A) Confocal image of an adult *C. elegans* gonad. In the distal arm, mitochondria have a globular shape (arrow), which gradually switches to a more elongated/ tubular one in the oocytes of the proximal arm (arrowhead). B) The turn of the gonad, shown in magnification, is the site where the shape alteration occurs. There, both globular (arrow) and tubular (arrowhead) mitochondria can be observed. C) DAPI staining of wild-type and *fzo-1(tm1133)*/Mitofusin

homozygous mutants. The red dashed line marks the gonad turn. D) Day 1 adult *fzo-1(tm1133)*/Mitofusin mutant animals, bearing defects in mitochondrial fusion, produce significantly fewer germ nuclei in diplotene as well as nuclei in diakinesis compared to their control counterparts. (n>40; ***$P < 0.001$, unpaired *t*-test). E) Quantification of mitochondrial length in the proximal and distal arm of the gonads. F) Animals with perturbed mitochondrial dynamics (fusion-fission), such as *fzo-1*, *drp-1* and *eat-3* mutants become sterile when exposed to a mild heat stress (25^{o}C). One-way ANOVA was used for the estimation of statistical significance (n>40; ***$P < 0.001$). Error bars, s.e.m. Images were acquired using X40 and X63 objective lenses. Ds; distal, pr; proximal, -1 denotes the proximal-most oocyte. Scale bars, 20μm.

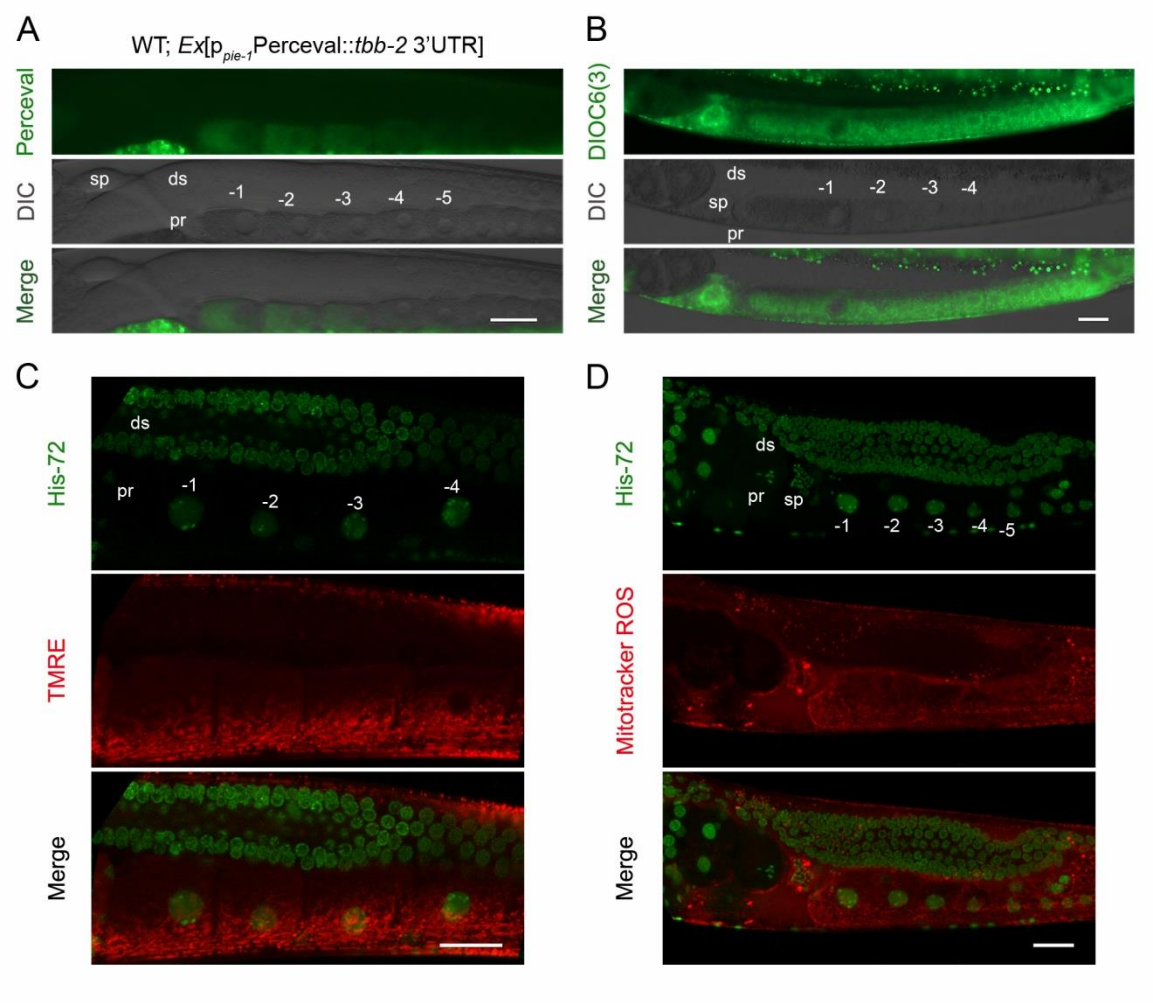

Figure 6: Mitochondria mature during germ nuclei differentiation. A) The ATP/ADP sensor Perceval was overexpressed in *C. elegans* germline under the regulation of *pie-1* promoter, to achieve germline-specific expression. Perceval emission increases upon ATP binding. Fluorescence could be mainly detected in the oocytes, indicating increased ATP production in the proximal arm. B) DIOC6(3) mitochondrial dye preferentially stains energized mitochondria in the proximal gonad arm. C) TMRE staining reveals increased electrochemical potential in the oocytes of the proximal arm. C) ROS production increases as the germ nuclei mature and give rise to oocytes. Sp; spermatheca, ds; distal, pr; proximal, -1 denotes the proximal-most oocyte. Images were acquired using X40 and X63 objective lenses. Scale bars, 20μm.

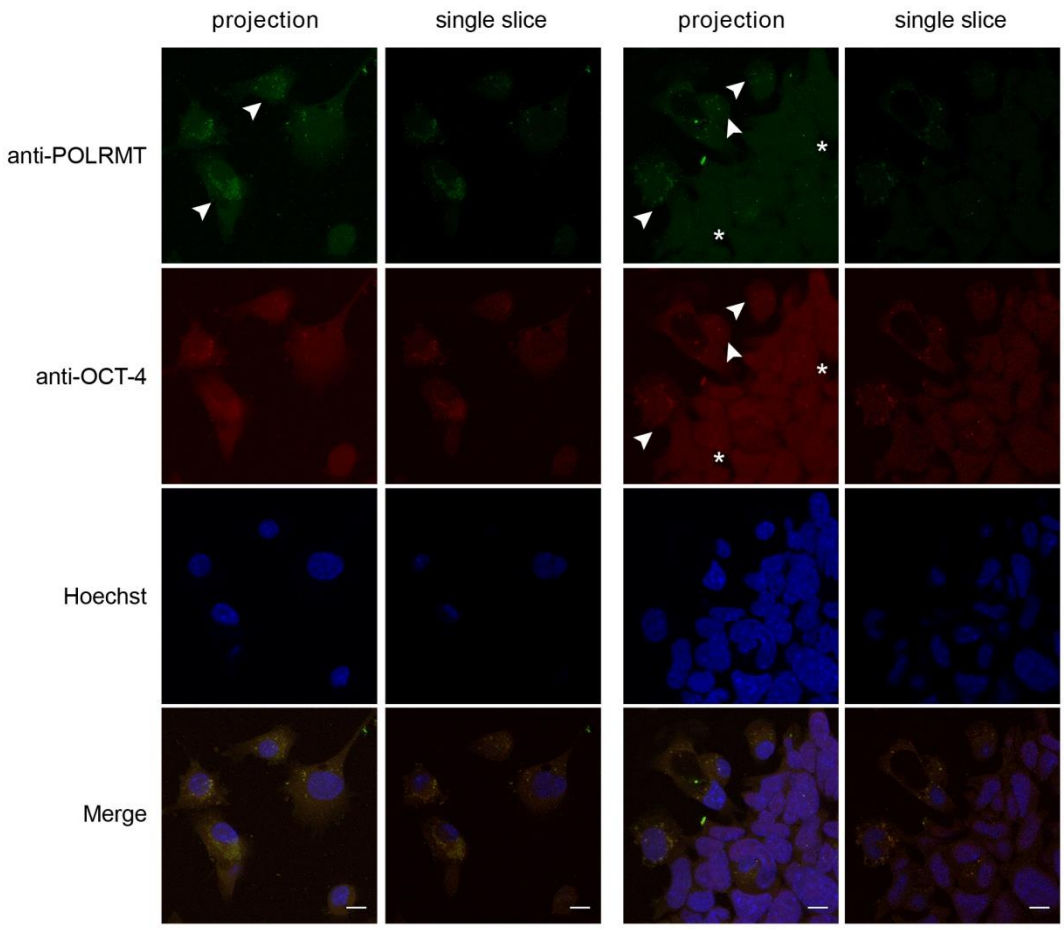

Figure 7: Mammalian stem cell differentiation upon LIF removal is accompanied by an increase in POLRMT expression. Elevated POLRMT expression is observed in cells with increased cytoplasmic OCT-4 abundance (arrowheads). In contrast, areas with increased nuclear OCT-4 abundance (stars) display lower POLRMT expression. Images were acquired using a X40 objective lens. Scale bars, 20μm.

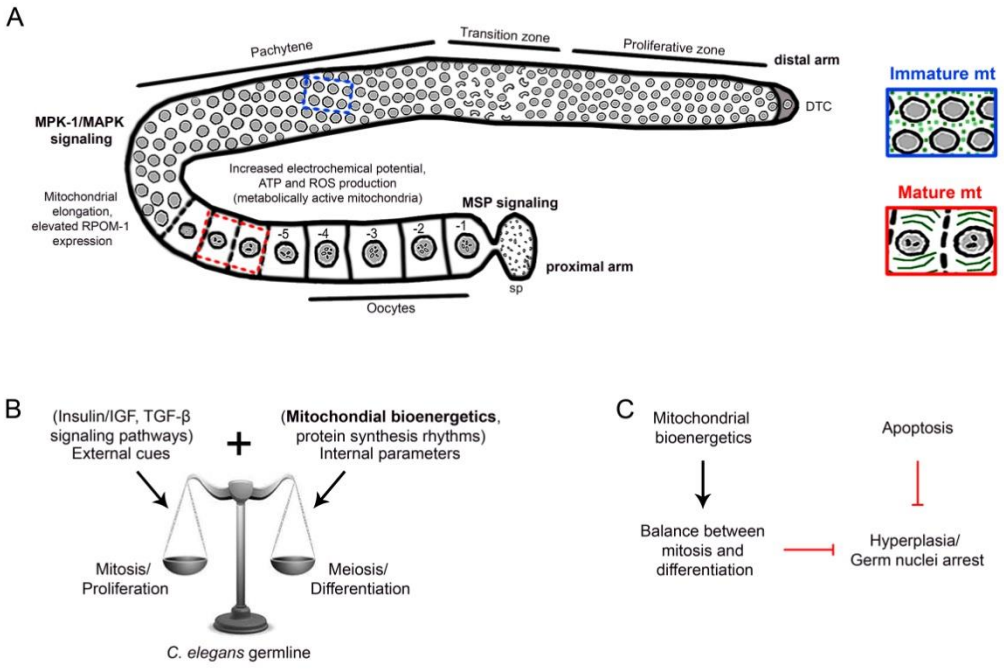

Figure 8: Intact mitochondrial bioenergetics safeguards germline homeostasis. A) Expression of RPOM-1 (the nematode homologue of POLRMT) increases progressively as the germ nuclei mature and mitochondria acquire an elongated, tubular shape. The boost in mitochondrial metabolic activity is manifested by enhanced ATP and ROS production, as well as increased electrochemical potential in the proximal gonad arm. Interestingly, some of the features characterizing the *C. elegans* gonad paradigm are conserved during evolution, since differentiation of mouse stem cells following LIF removal is accompanied by an increase in POLRMT expression and the appearance of tubular mitochondria. B) Mitochondrial bioenergetics cooperates with signaling pathways (Insulin/IGF and TGF-β) to dictate the balance between mitosis and differentiation in the *C. elegans* gonad. C) Intact mitochondrial biogenesis, energy production and dynamics are crucial for fine-tuning the balance of mitosis versus differentiation in the nematode gonads. Abrogation of mitochondrial transcription leads to the manifestation of severe gonad defects, such as hyperplasia, impaired oogenesis and gonad collapse upon a mild heat stress. Induction of apoptosis acts as a compensatory mechanism to ameliorate the defects and protect germline integrity.

	Identities	Positives
ScRPO41	39%	56%
DmMTRNAPOL	53%	65%
MmPOLRMT	48%	63%
HsPOLRMT	47%	62%

Figure S1: The catalytic domain of mitochondrial RNA polymerases is highly conserved. CLUSTALW alignment of the catalytic domains from five model organisms (*S. cerevisiae*, *D. melanogaster*, *M. musculus*, *H. sapiens*) reveals high conservation of POLRMTs in evolutionarily diverse species. The table displays the percentage of identical residues as well as positive substitutions in pair-wise comparisons of *C. elegans* mitochondrial RNA polymerase (RPOM-1) and its identified homologues.

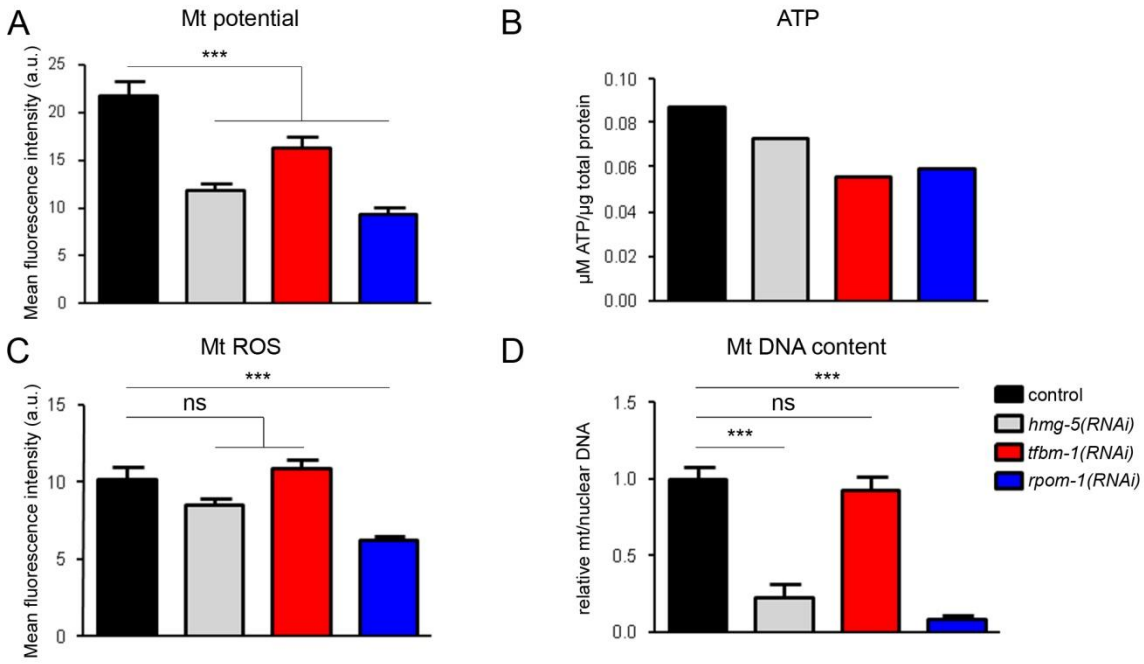

Figure S2: Reduction of mitochondrial transcription compromises mitochondrial activity. Mitochondrial function following genetic inhibition of HMG-5/TFAM, RPOM-1/POLRMT and TFBM-1/TFB1M was assayed by staining with potential-based dyes, such as TMRE (A), Mitotracker ROS (C) and by measuring ATP production (B). D) RPOM-1 depletion dramatically reduces mitochondrial DNA content, at levels comparable to HMG-5 depletion. One-way ANOVA was used for multiple comparisons (n=40; ***P < 0.001). Unpaired *t*-test was used for pairwise comparisons (n=40; ***P < 0.001). Error bars, s.e.m.

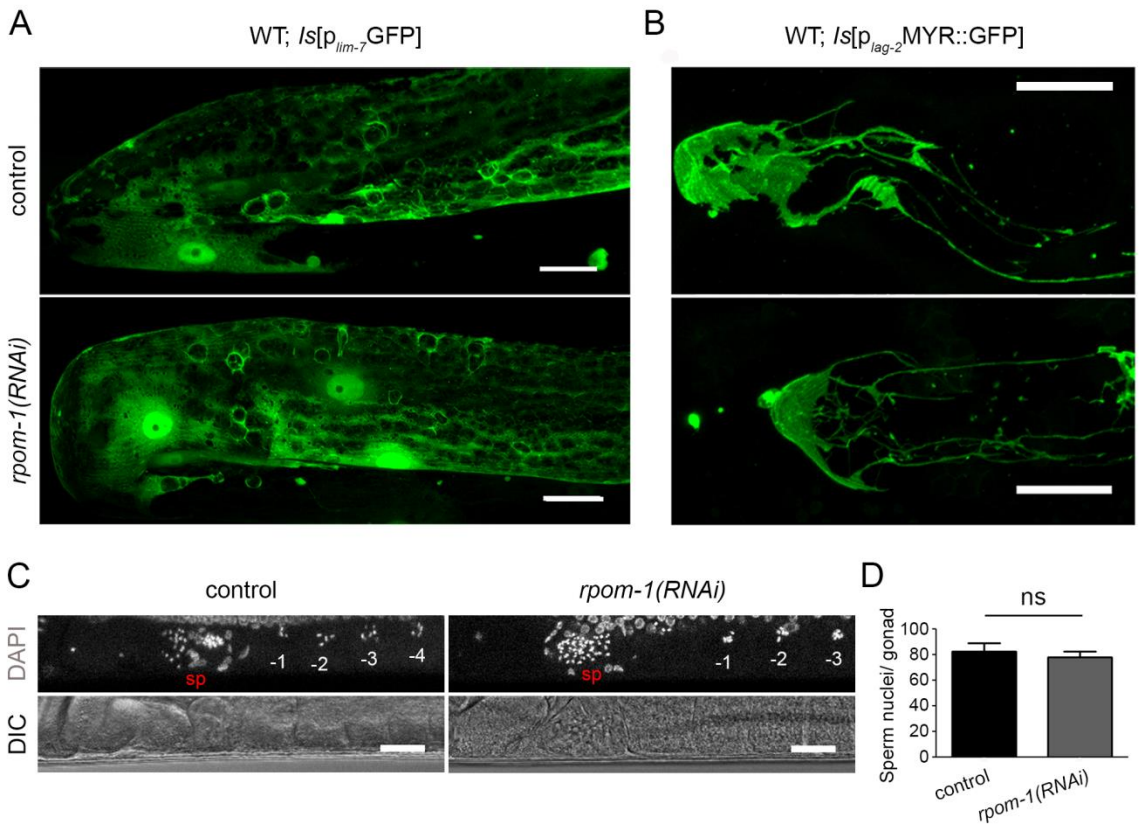

Figure S3: The somatic gonad and sperm number are not affected by RPOM-1 depletion. The gonad sheath and the distal tip cell do not display any observable morphological defect following RPOM-1 depletion, as indicated by the p*lim-7*GFP (A) and p*lag-2*MYR::GFP (B) transcriptional reporters, respectively. C) Confocal images of the proximal gonad arm upon treatment with control and *rpom-1(RNAi)*. sp stands for sperm and -1 denotes the most proximal oocyte. D) Quantification of sperm nuclei per gonad in day 2 adult animals upon treatment with control and *rpom-1(RNAi)*. Images were acquired using a X40 objective lens. Scale bars, 20µm.

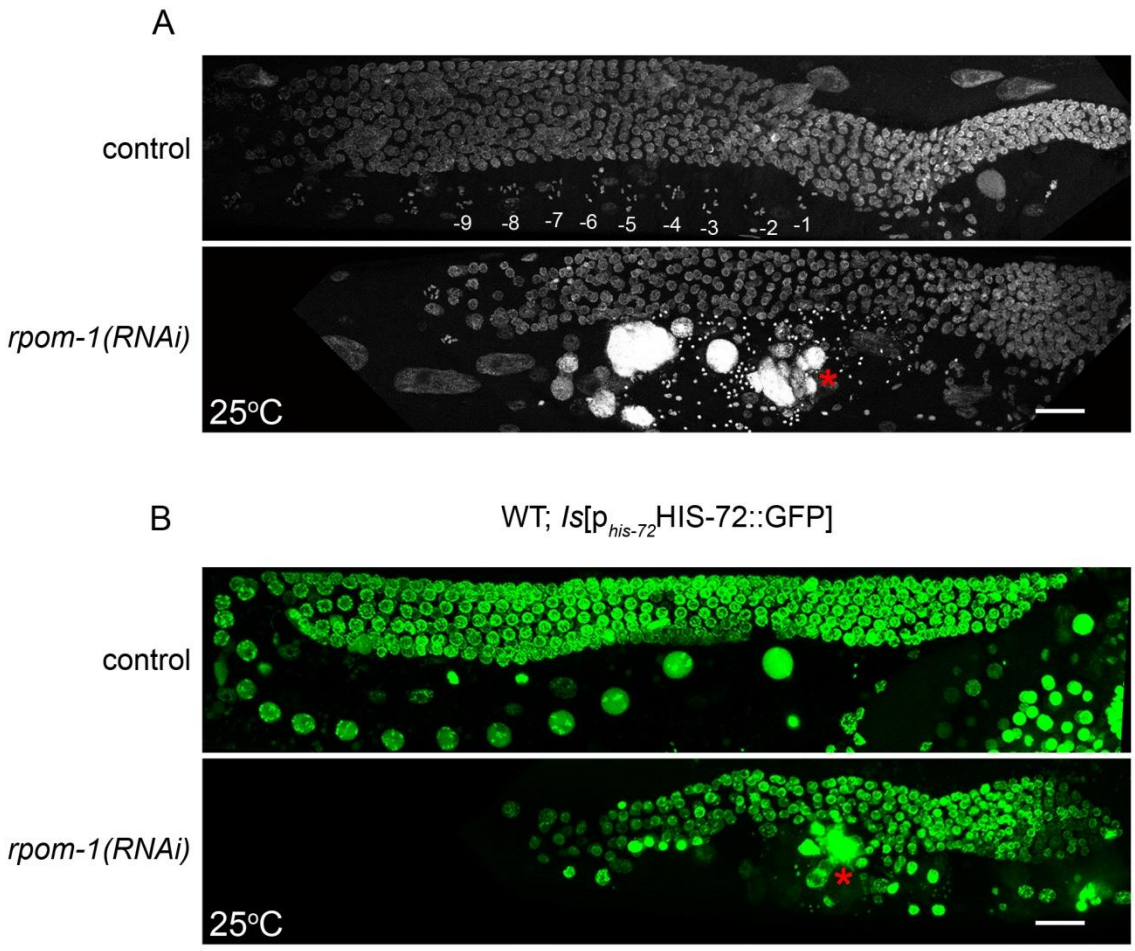

Figure S4: RPOM-1-depleted gonads are sensitive to mild heat stress. Mild heat stress (25°C) upon *rpom-1* downregulation is detrimental for gonads, as monitored with DAPI staining in fixed animals (A) and with a HIS-72::GFP nuclear reporter *in vivo* (B). The red stars highlight dead corpses in the proximal gonad arm. Images were acquired using a X40 objective lens. Scale bars, 20µm.

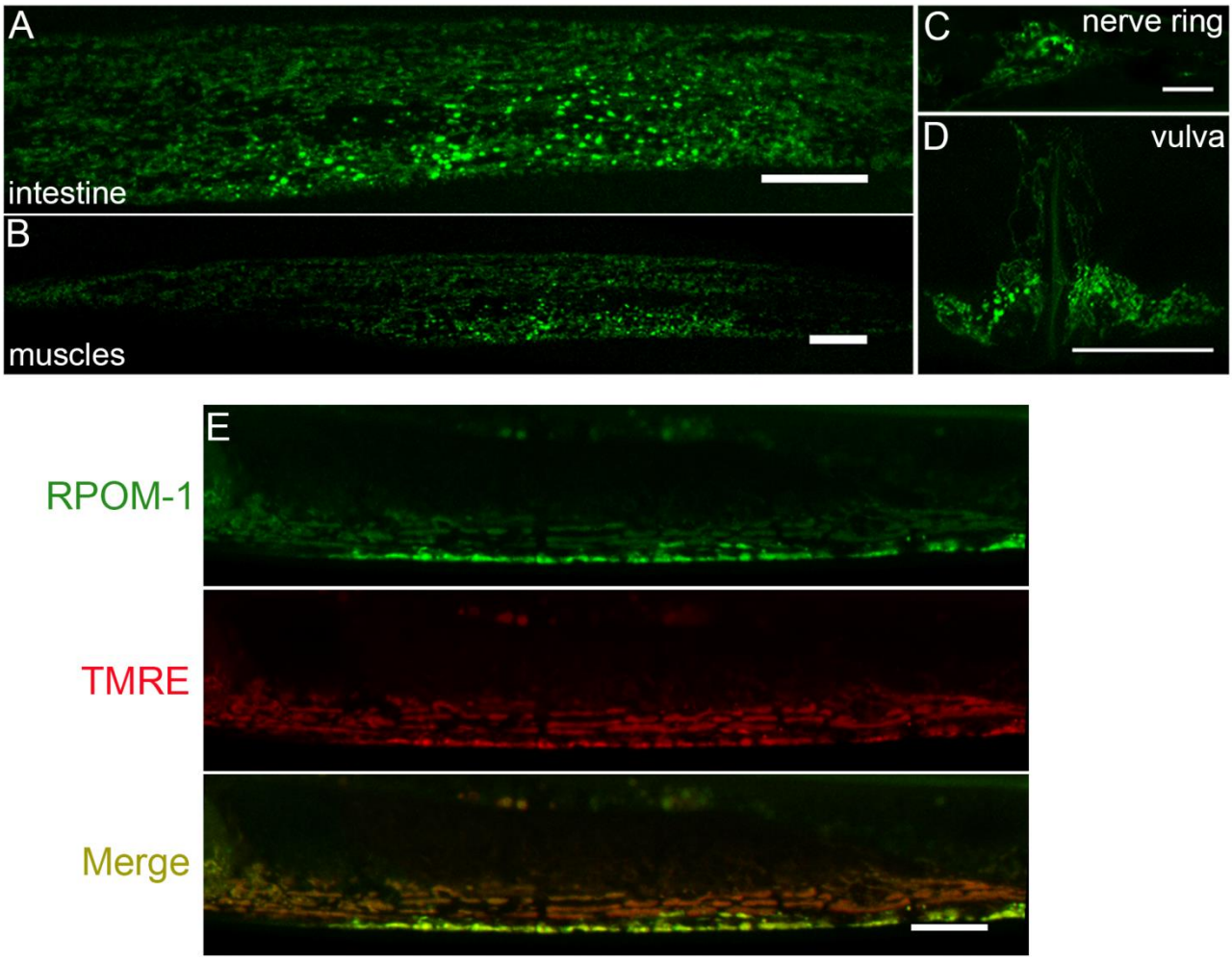

Figure S5: RPOM-1 is broadly expressed in *C. elegans* somatic tissues and localizes in mitochondria. RPOM-1 is expressed in various somatic tissues, such as the intestine (A), muscles (B), in neurons of the nerve ring (C), as well as the vulva (D). E) Confocal image of RPOM-1::GFP translational reporter animals stained with TMRE (Tetramethylrhodamine, ethyl ester, perchlorate). The expression pattern is reminiscent of proteins localized in the mitochondrial matrix. Images were acquired using a X40 objective lens. Scale bars, 20μm.

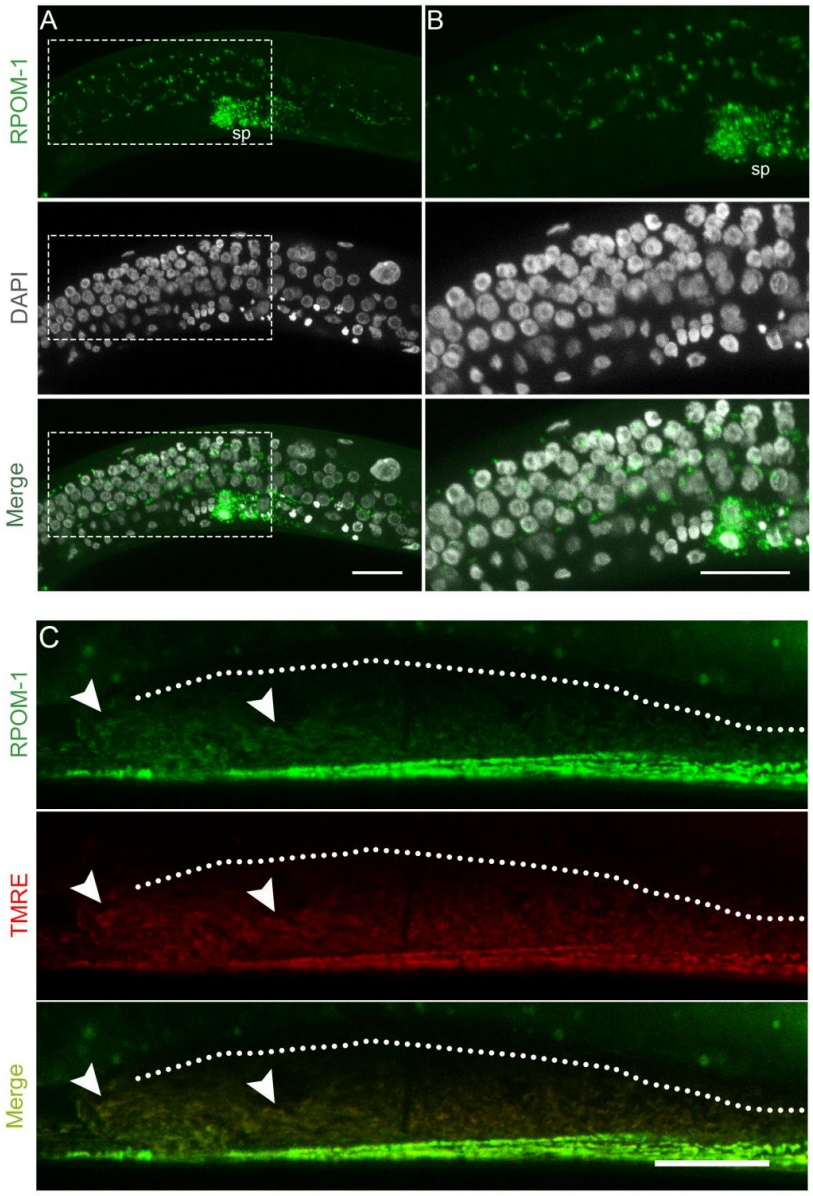

Figure S6: RPOM-1 expression in the germline. A) DAPI staining of transgenic animals harboring an RPOM-1 translational reporter, at late L4 stage, reveals syncytium mitochondria which enwrap germline nuclei. B) Zoom-in of the highlighted area shows high RPOM-1 expression in the spermatheca. C) Staining of RPOM-1::GFP translational reporter animals with TMRE. Arrowheads indicate tubular mitochondria in the proximal gonad arm, where the two signals co-localize. Images were acquired using X40 and X63 objective lenses. Scale bars, 20µm.

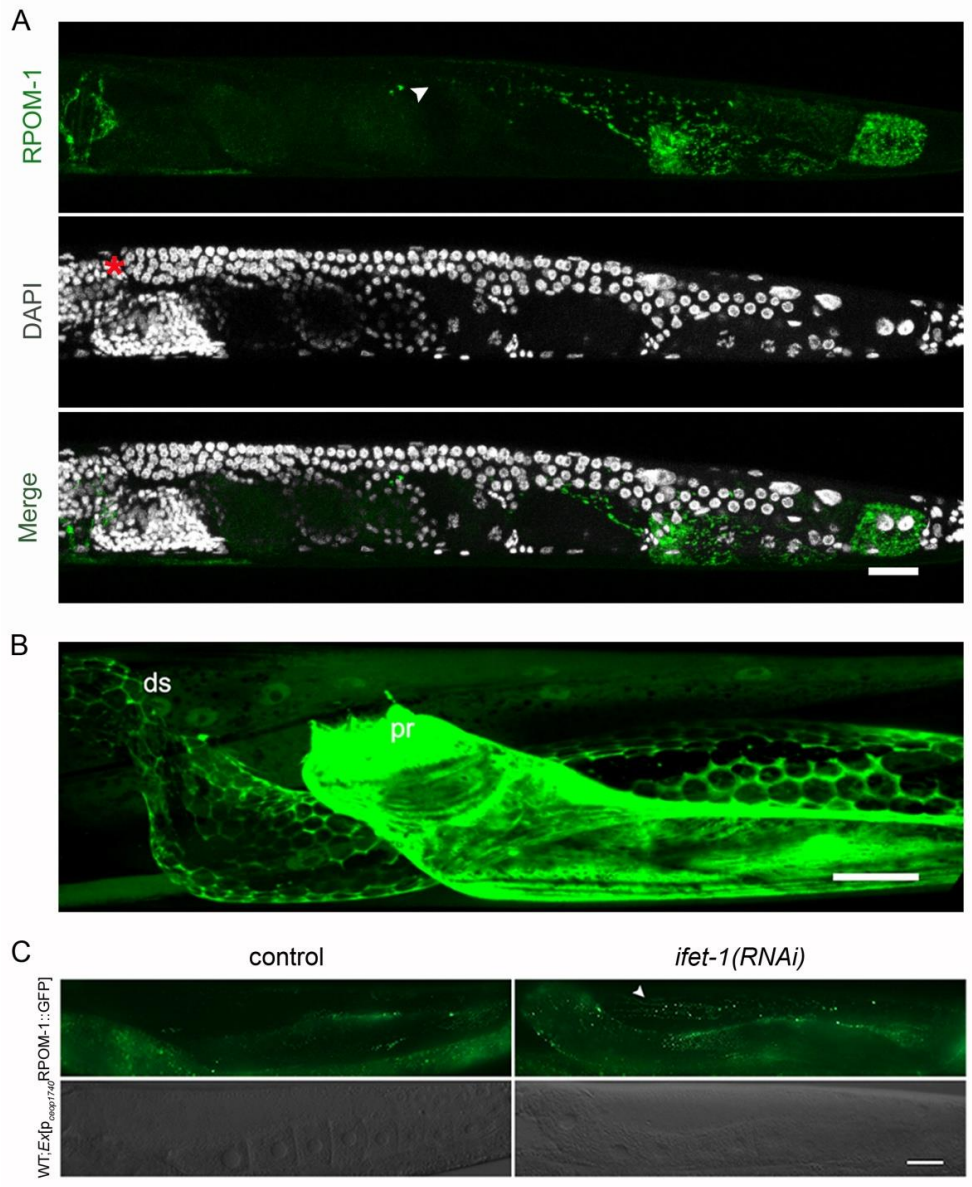

Figure S7: RPOM-1 accumulates in differentiated germ cells and oocytes. A) Image of a full gonad from a D1 adult RPOM-1::GFP transgenic worms stained with DAPI. The arrowheads point to the distal-most expression observed, while the red asterisk marks the relative position of the distal tip cell. B) Gonadal expression of $p_{ceop1740}$GFP transcriptional reporter animals. C) Knockdown of *ifet-1* derepresses RPOM-1 expression in more distal regions of the gonad syncytium. Images were acquired using a X40 objective lens. Ds; distal, pr; proximal. Scale bars, 20µm.

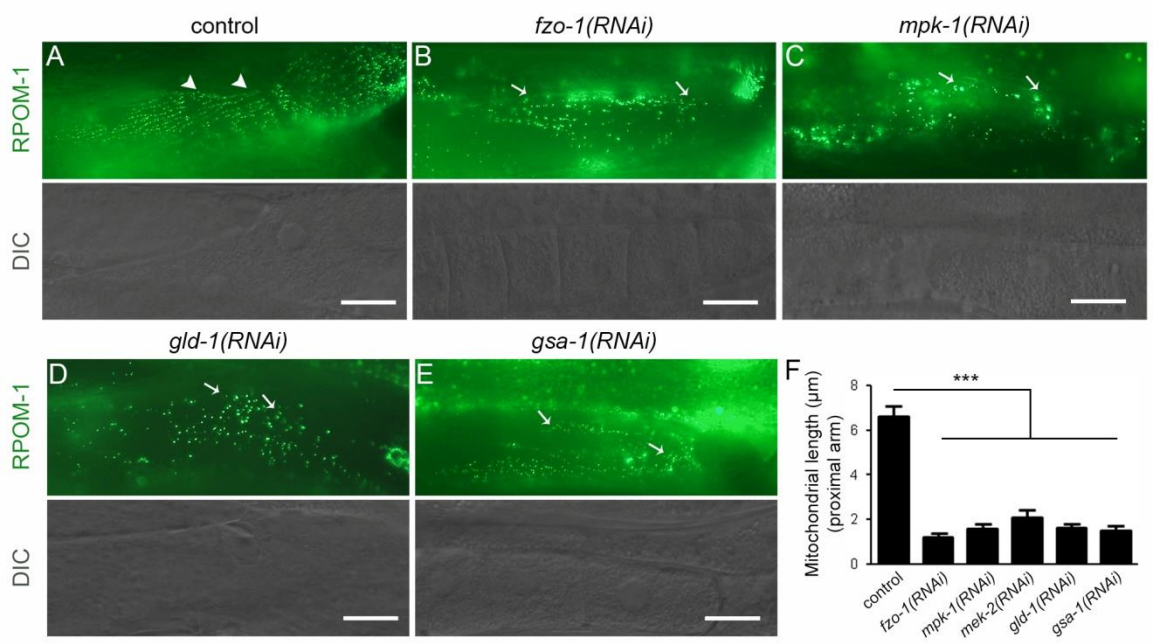

Figure S8: Mitochondrial elongation is coupled with germ cell differentiation. A) Mitochondria in the proximal gonad arm are tubular under control conditions (arrowheads). B) Knockdown of *fzo-1* leads to mitochondrial network fragmentation and globular mitochondria in the proximal gonad arm (arrows). C) Inhibition of MPK-1/MAPK signaling via *mpk-1(RNAi)* results in a failure of mitochondria to elongate proximally (arrows). D) Mitochondria are exclusively globular in the proximal arm of *gld-1(RNAi)*-treated animals (arrows). E) GSA-1 inhibition results in failure of oocyte maturation as well as mitochondrial elongation. F) Quantification of mitochondrial length in proximal gonad arm oocytes upon the respective RNAi treatments (n=40; ***P < 0.001, one-way ANOVA was used for multiple comparisons). Error bars, s.e.m. Images were acquired using a X40 objective lens. Scale bar, 20µm.

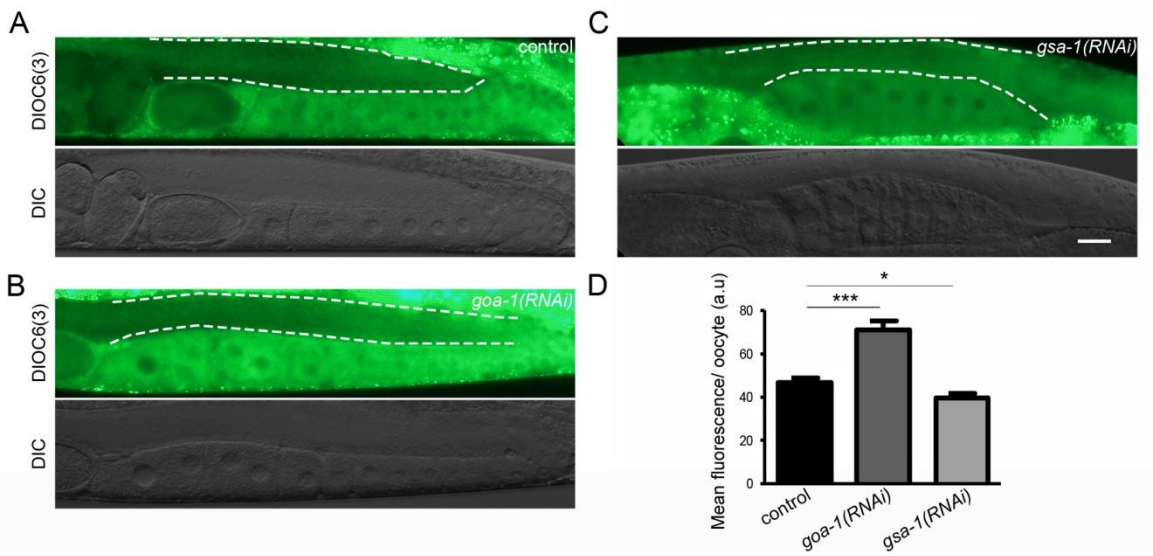

Figure S9: Sperm signaling promotes mitochondrial polarization. A) DIOC6(3) staining reveals that mitochondria polarize in the course of germ cell differentiation. B) Inhibition of GOA-1, a negative regulator of sperm signaling, boosts mitochondrial potential in the proximal gonad arm. C) Treatment with *gsa-1(RNAi)* results in a failure of mitochondria to polarize proximally. D) Quantification of DIOC6(3) fluorescence in proximal gonad oocytes upon the respective RNAi treatments. The dashed lines surround the germline syncytium. (n=40; ***$P < 0.001$, unpaired *t*-test). Error bars, s.e.m. Images were acquired using the X40 objective lens. Scale bar, 20µm.

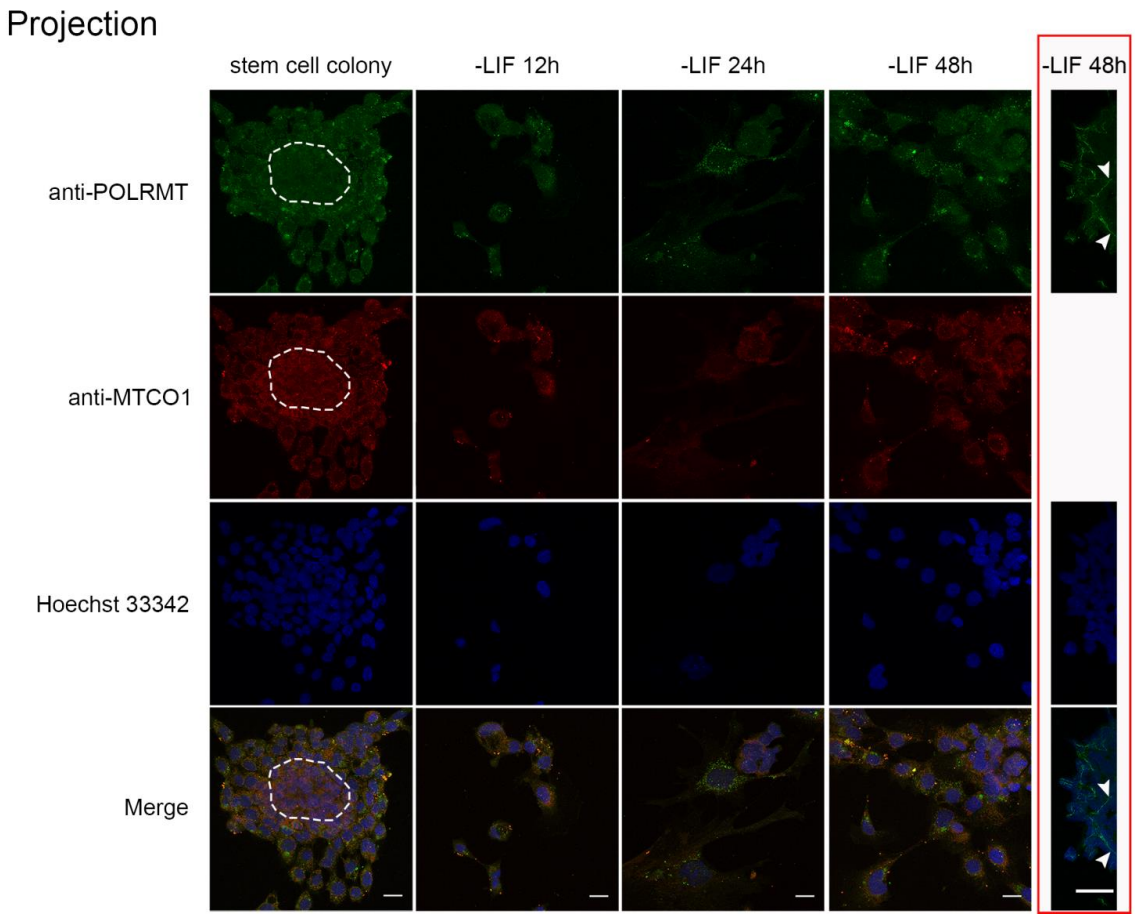

Figure S10: POLRMT and MTCO1 expression increases during mammalian stem cell differentiation. Staining of J1 cultured cells with antibodies against POLRMT and MTCO1. Low expression of both proteins can be detected at the core of the stem cell colony (white circle) and higher in the periphery. Upon LIF removal, as the cells progress towards differentiation, an elevation of the expression of both proteins can be observed. In parallel, mitochondria with elongated shape (red panel, arrowheads) can be visualized. Images were acquired using a X40 objective lens. Scale bars, 20μm.

5. MATERIALS AND METHODS

Strains and genetics

We followed standard procedures for maintaining *C. elegans* strains. Rearing temperature was set at 20^{o}C for most of our experiments unless noted otherwise, but was raised at 25^{o}C when germline expression was assessed to avoid transgene silencing which occurs at 20^{o}C. The following nematode strains were utilized in this study: N2: wild-type Bristol isolate, CU5991: *fzo-1(tm1133) II*, CU6372: *drp-1(1108) IV*, DA631: *eat-3(ad426) II; him-8(e1489) IV*, MT7686: *ced-9(n2812)*/qC1 [*dpy-19(e1259) glp-1(q339)*] III, MT1522: *ced-3(n717) IV*, CB1370: *daf-2(e1370) III*, DR40: *daf-1(m40) IV*, RB1206: *rsks-1(ok1255) III*, KX80: *ife-5(ok1934) II*, CB4037: *glp-1(e2141) III*. We used the JJ1850: *unc-119(ed3) III*; *Is*[his-72(1kb 5' UTR)::his-72::SRPVAT::GFP::his-72 (1KB 3' UTR)] strain (Ooi et al., 2006) for monitoring germline nuclei *in vivo* and the AD189: *unc-119(ed3) III*; *Is*[unc-119(+) + ppie-1::GFP::egg-1] for monitoring oocyte membranes *in vivo*. JK4472: N2; *Is*[lag-2p::MYR::tdTomato + ttx-3p::GFP] and JK4475: N2; *Is*[lag-2p::MYR::GFP + ttx-3p::DsRed] were used for monitoring the DTC's membrane plexus, while DG1575: N2; *Is* [lim-7::GFP + rol-6(su1006)] was used for monitoring gonad sheath morphology.

Molecular cloning

The following primers were used for generation of RNAi constructs. For *rpom-1(RNAi)*: 5'-ATGAGAAGACTGGAACGAATTGTC-3' and 5'-TAGTGTTCAATCCCTCACCAATC-3', for *hmg-5(RNAi)*: 5'-GGATCCAATGTTGGGAACAATTTC-3' and 5'-ACCGGTGGTTGATCTGCATTTTC-3', for *tfbm-1(RNAi)*: 5'-ATGGCTTCTGCTTCACGTCTCC-3' and 5'-CATCTTAGGCTCTGCCACGTATTG-3', for *gld-1(RNAi)*: 5'-CACTCCAACTTACGGTGTTTCG-3' and 5'-TCTACCGACGAAGTTATACTGAAATG-3', for *mpk-1(RNAi)*: FW: 5'-GTTCATGGGCAACTTTTTGAG-3' and 5'-GATTACTGAGCATTTCTGCGAG-3', for *mek-2(RNAi)*: 5'-CGTAATCCGTTGGGACTCAG-3' and 5'-CGAGAATCCTGCGAGAACTG-3', for *goa-1(RNAi)*: 5'-CCACATACAGTGAGTGAGTAGAG-3' and 5'-CTCTCTGTCAGCCGAACC-3' and for *gsa-1(RNAi)*: 5'-AGCAAAAAAGAACGAGCAAC-3' and 5'-TGTCCTCCCAGAGTACAAGA-3'. For the generation of RNAi constructs, the respective genomic

fragments corresponding to the gene of interest were inserted in the pL4440 vector backbone and positive clones were transformed in HT115 bacteria to allow knockdown through feeding (Fire et al., 1998).

For cloning the minimal 2.1kb operon promoter upstream of CEOP1740 operon, which contains the *rpom-1* gene, we used the 5'-CCATGAAATTGAGGATTCTGAAAC-3' and 5'-ATTTCCGTTTAGTAGCGATTTTTAACAG-3' primer pair. The corresponding product was inserted in TOPO and then in pPD95.77 linearized with PstI-BamHI digestion. For cloning the 3.5 kb *rpom-1* full length cDNA, we utilized *C. elegans* total RNA as a template to synthesize the *rpom-1* single-strand cDNA with the PrimeScript™ Reverse Transcriptase kit (Taqara) and the 5'-ACCGGTGGACTAAAAAAATAAACAGAATCCTTGAC-3' gene-specific reverse primer. Then, the previous primer was used in the same reaction with the 5'-GGATCCATGAGAAGACTGGAACGAATTGTC-3' forward primer to synthesize the full length *rpom-1* cDNA. Expand high fidelity DNA polymerase (Roche) was used in the PCR reaction to minimize errors. The amplified fragment was inserted upstream of GFP in the pPD95.77 expression vector linearized with BamHI-AgeI restriction digestion. For amplifying the 0.1kb *rpom-1* 3'UTR fragment we used the 5'-GAATTCAGTTAGAAGTGTTTTTTTTGTTG-3' and 5'-GGGCCCCATTTTCTGATTCCAGCG-3' pair of primers. Upon ligation into TOPO vector, we isolated the corresponding fragment using EcoRI-ApaI restriction digestion. This was then inserted in pPD95.77 linearized with EcoRI-ApaI digestion downstream of the *rpom-1* cDNA::GFP cassette to replace the *unc-54* 3'UTR fragment. For creating the *pie-1* promoter Perceval::tbb-2 3'UTR plasmid, we extracted the Perceval from the pRsetB-his7-Perceval plasmid (catalogue number 20336, Addgene) using XbaI-XhoI digestion (Berg et al., 2009). In parallel, we amplified the tbb-2 3'UTR using the 5'-CTCGAGCAATAAATGCAAGATCCTTTCAAGC-3' and 5'-GAATTCTTTCCTCTTTTTGTTGGGTCACTC-3' pair of primers. We digested pPD95.77 with XbaI-EcoRI digestion to remove GFP and we simultaneously ligated the two inserts with the linearized vector in a single reaction. An extended *pie-1* promoter was amplified using the 5'-GTCGACTCGTATTTCTCAGTCATTTTTGTG-3' and 5'-CCATGGATCGTTTTGTATTCTGTGTGCTGG-3' primer pair and was inserted upstream of the

Perceval::tbb-2 cassette using SalI-NcoI restriction sites. All the primers used in the current study are listed in table 1.

Nematode strain generation

We used both microinjection into *C. elegans* gonads and bombardment with gold nanoparticles to generate transgenic strains. To avoid undesired transgene in the germline, in our microinjection setup we used low micromolar concentrations (5ng/µL) of both the reporter plasmid and the co-transformation marker and an excess of PvuII-digested *E. coli* genomic fragments (50ng/µL), as previously described (Kelly et al., 1997).

Mitochondrial DNA quantification

mtDNA was quantified using quantitative real time PCR-based method as previously described (Cristina et al., 2009). Briefly, the 5'-GTTTATGCTGCTGTAGCGTG-3' and 5'-CTGTTAAAGCAAGTGGACGAG-3' primer pair was used for measuring mtDNA levels. The results were normalized to genomic DNA amplified with the 5'-TGGAACTCTGGAGTCACACC-3' and 5'-CATCCTCCTTCATTGAACGG-3' primer pair, which hybridizes to the genomic region of *ama-1* gene. Quantitative PCR was performed using a Bio-Rad CFX96 Real-Time PCR system, and was repeated three times.

Egg laying assays

For assessing egg laying, we placed single, precisely synchronized gravid adult nematodes (at D1-D2 of adulthood) in individual 33mm NGM plates seeded with a standard OP50 bacterial lawn. The number of eggs that each adult worm produced in the next twelve hours was measured. At least twenty individual measurements were acquired per experimental condition. The egg laying assays were performed at 20^{o}C.

Nuclear staining of nematodes

We synchronized adult worms of the genotypes of interest at the first day of adulthood (D1). We stained with Hoechst 33342 to monitor germline nuclei at this stage. First we washed NGM plates with M9 buffer and collected the animals in a 1.5mL Eppendorf tube. We let the worms pellet with gravity and we washed once with PBS-Tween20® 0.01%. We centrifuged at 3000rpm for one minute to pellet the animals and we removed the supernatant. Fixation was performed with cold methanol 100% for maximum five minutes at -20ºC. The Eppendorf tubes were spinned and the fixative was removed. Upon fixation, cell membranes were permeated by washing once with PBS-Tween20® 0.1%. Upon centrifugation at 3000rpm for one minute, the worm pellet was stained by adding 300μL of diluted Hoechst33342 solution (final concentration 1μg/mL) for five minutes in the dark. The Eppendorf tubes were centrifuged, the supernatant was removed and the pellet was washed for a final time with PBS-Tween20® 0.1% to remove excessive Hoechst stain. The supernatant was aspirated; 20μL 80% glycerol was added in each Eppendorf tube and the samples were mounted in microscopic slides prior to observation. The transition zone nuclei were distinguished due to the polarized localization of chromosomes in germ nuclei.

Immunofluorescence of *C. elegans* gonads

A large number of synchronized D1 adult worms grown on NGM plates were washed two repetitive times with M9 buffer and 20μL of 20mM levamisole was added on the worm pellet to anaesthetize the animals. About 7-8μL of the mix were placed on top of polylysine-treated slides and the animals were dissected using a 8mm insulin syringe, until the gonads were released from the animals due to mechanical pressure. The extracted tissue was fixed with 4% paraformaldehyde in PBS for twenty minutes at room temperature. The fixative was removed by washing the specimen twice with PBS. Then, the gonads were permeabilized with 0.2% Triton X-100 in PBS 1X for five minutes and rinsed twice with PBS. Next, the tissue was incubated in blocking solution (1% BSA in PBS-Tween 0.02%) for one hour at room temperature. The incubation with the rabbit anti-PH3 (Millipore) antibody (diluted 1:300 in blocking solution) was performed overnight in the dark at 4ºC and the slides were sealed to avoid evaporation. The

sample was washed thrice with PBS-Tween 0.02% to remove the primary antibody excess. Finally, the gonads were incubated for one hour with the anti-rabbit IgG AlexaFluor ® 488 (Catalogue Number ab150077, Abcam) secondary antibody (diluted 1:500 in PBS-Tween 0.02%) and DAPI (final concentration 2μg/mL) to stain germline nuclei, rinsed three times with PBS and mounted with glycerol prior to observation.

Staining germline mitochondria in live animals

To stain germline mitochondria, mitochondrial dyes were added on top of standard NGM plates containing OP50 *E. coli* bacterial food. The plates were previously placed in a UV-crosslinker for 15min to avoid undesired catabolism of the compounds by bacteria. TMRE (Tetramethylrhodamine, ethyl ester, perchlorate, catalogue number T-669; Molecular Probes, Invitrogen), Mitotracker Red CM-H2X ROS (catalogue number M-7513; Molecular Probes, Invitrogen) were administered by food in a final concentration of 1μM per plate and DIOC6(3) (3,3'-Dihexyloxacarbocyanine Iodide, CAS Number 53213-82-4, Sigma-Aldrich) in a final concentration of 2μM per plate. The plates were allowed to dry, constantly protected from light, and then wild-type eggs harvested from hypochlorite-treated, well-fed adult animals were placed on top of the bacterial lawn. The larvae which hatched were fed with the dyes for three consecutive days at 25^{o}C (when His-72::GFP transgenic animals were used) or for four consecutive days at 20^{o}C (when wild-type animals were used), until they produced D1-2 gravid adult nematodes. Adult animals were anaesthetized with 20mM levamisole and were microscopically examined using a ZEISS LSM 710 confocal microscope.

Mammalian cell culture and immunofluorescence

Standard cell culture procedures were followed. J1 embryonic stem cells were initially cultured for four passages on top of Mitomycin C-treated mouse fibroblasts and then on gelatin in LIF cytokine-containing ES medium to preserve their pluripotent identity. Large globular ES colonies were acquired. LIF was removed and the ES medium was replaced with EB medium to favor unbiased differentiation towards multiple cell lineages. Cells were grown for up to 48 hours

on EB medium on 12-well plates on top of cover slips. For immunofluorescence experiments, cells were washed three times with PBS before they were fixed with 4% paraformaldehyde in RT. The cover slips were washed again three times with PBS. The blocking was performed with 0.2% Triton X, 10% FBS for one hour. Mouse monoclonal anti-MTCO1 (Catalogue Number ab14705, Abcam), rabbit polyclonal anti-POLRMT (Catalogue Number PA5-28196, Thermo Scientific) and mouse monoclonal anti-OCT4 (Catalogue Number sc-5279, Santa Cruz Biotechnology) were used as primary antibodies according to the manufacturer's instructions. The appropriate primary antibody combination was added in blocking solution and was incubated overnight with the specimen at 4ºC. Next day, the specimen was rinsed thrice with PBS and was incubated with anti-rabbit IgG AlexaFluor ® 488 (Catalogue Number ab150077, Abcam), anti-mouse IgG AlexaFluor ® 594 (Catalogue Number ab150116, Abcam) fluorescent secondary antibodies and Hoechst 33342 diluted in PBS for an hour in RT. Finally the slides were mounted with prolong ® gold antifade reagent (Catalogue number 9071, Cell Signaling) and stored, protected from light at 4ºC prior to microscopic observation.

List of primers		
RNAi constructs	**FW primer (5'-3')**	**REV primer (5'-3')**
rpom-1(RNAi)	ATGAGAAGACTGGAACGAATTGTC	TAGTGTTCAATCCCTCACCAATC
hmg-5(RNAi)	GGATCCAATGTTGGGAACAATTTC	ACCGGTGGTTGATCTGCATTTTC
tfbm-1(RNAi)	ATGGCTTCTGCTTCACGTCTCC	CATCTTAGGCTCTGCCACGTATTG
gld-1(RNAi)	CACTCCAACTTACGGTGTTTCG	TCTACCGACGAAGTTATACTGAAATG
mpk-1(RNAi)	GTTCATGGGCAACTTTTTGAG	GATTACTGAGCATTTCTGCGAG
mek-2(RNAi)	CGTAATCCGTTGGGACTCAG	CGAGAATCCTGCGAGAACTG
goa-1(RNAi)	CCACATACAGTGAGTGAGTAGAG	CTCTCTGTCAGCCGAACC
gsa-1(RNAi)	AGCAAAAAAGAACGAGCAAC	TGTCCTCCCAGAGTACAAGA
RPOM-1 reporter		
CEOP1740 promoter	CCATGAAATTGAGGATTCTGAAAC	ATTTCCGTTTAGTAGCGATTTTTAACAG
rpom-1 cDNA	GGATCCATGAGAAGACTGGAACGAATTGTC	ACCGGTGGACTAAAAAAATAAACAGAATCCTTGAC
rpom-1 3'UTR	GAATTCAGTTAGAAGTGTTTTTTTTGTTG	GGGCCCCATTTTCTGATTCCAGCG

Table 1: List of primers used in the current study.

6. References

Albert Hubbard, E.J. (2007). Caenorhabditis elegans germ line: A model for stem cell biology. Developmental Dynamics *236*, 3343-3357.

Amunts, A., Brown, A., Toots, J., Scheres, S.H.W., and Ramakrishnan, V. (2015). The structure of the human mitochondrial ribosome. Science *348*, 95-98.

Arantes-Oliveira, N., Apfeld, J., Dillin, A., and Kenyon, C. (2002). Regulation of life-span by germ-line stem cells in Caenorhabditis elegans. Science *295*, 502-505.

Archibald, John M. (2015). Endosymbiosis and Eukaryotic Cell Evolution. Current Biology *25*, R911-R921.

Armstrong, L., Tilgner, K., Saretzki, G., Atkinson, S.P., Stojkovic, M., Moreno, R., Przyborski, S., and Lako, M. (2010). Human Induced Pluripotent Stem Cell Lines Show Stress Defense Mechanisms and Mitochondrial Regulation Similar to Those of Human Embryonic Stem Cells. STEM CELLS *28*, 661-673.

Arur, S., Ohmachi, M., Berkseth, M., Nayak, S., Hansen, D., Zarkower, D., and Schedl, T. (2011). MPK-1 ERK controls membrane organization in C. elegans oogenesis via a sex determination module. Developmental cell *20*, 677-688.

Arur, S., Ohmachi, M., Nayak, S., Hayes, M., Miranda, A., Hay, A., Golden, A., and Schedl, T. (2009). Multiple ERK substrates execute single biological processes in Caenorhabditis elegans germ-line development. Proceedings of the National Academy of Sciences of the United States of America *106*, 4776-4781.

Berg, J., Hung, Y.P., and Yellen, G. (2009). A genetically encoded fluorescent reporter of ATP:ADP ratio. Nat Meth *6*, 161-166.

Berman, J.R., and Kenyon, C. (2006). Germ-Cell Loss Extends C. elegans Life Span through Regulation of DAF-16 by kri-1 and Lipophilic-Hormone Signaling. Cell *124*, 1055-1068.

Bernstein, D., Hook, B., Hajarnavis, A., Opperman, L., and Wickens, M. (2005). Binding specificity and mRNA targets of a C. elegans PUF protein, FBF-1. Rna *11*, 447-458.

Boag, P.R., Nakamura, A., and Blackwell, T.K. (2005). A conserved RNA-protein complex component involved in physiological germline apoptosis regulation in C. elegans. Development *132*, 4975-4986.

Brandt, T., Mourier, A., Tain, L.S., Partridge, L., Larsson, N.-G., and Kühlbrandt, W. (2017). Changes of mitochondrial ultrastructure and function during ageing in mice and Drosophila. eLife *6*, e24662.

Bratic, I., Hench, J., Henriksson, J., Antebi, A., Bürglin, T.R., and Trifunovic, A. (2009). Mitochondrial DNA level, but not active replicase, is essential for Caenorhabditis elegans development. Nucleic Acids Research *37*, 1817-1828.

Byrd, D.T., Knobel, K., Affeldt, K., Crittenden, S.L., and Kimble, J. (2014). A DTC Niche Plexus Surrounds the Germline Stem Cell Pool in Caenorhabditis elegans. PLoS ONE *9*, e88372.

Chacinska, A., Koehler, C.M., Milenkovic, D., Lithgow, T., and Pfanner, N. (2009). Importing Mitochondrial Proteins: Machineries and Mechanisms. Cell *138*, 628-644.

Cho, Y.M., Kwon, S., Pak, Y.K., Seol, H.W., Choi, Y.M., Park, D.J., Park, K.S., and Lee, H.K. (2006). Dynamic changes in mitochondrial biogenesis and antioxidant enzymes during the spontaneous differentiation of human embryonic stem cells. Biochemical and Biophysical Research Communications *348*, 1472-1478.

Choksi, K.B., Nuss, J.E., DeFord, J.H., and Papaconstantinou, J. (2011). Mitochondrial electron transport chain functions in long-lived Ames dwarf mice. Aging (Albany NY) *3*, 754-767.

Cinquin, O., Crittenden, S.L., Morgan, D.E., and Kimble, J. (2010). Progression from a stem cell–like state to early differentiation in the C. elegans germ line. Proceedings of the National Academy of Sciences *107*, 2048.
Ciosk, R., DePalma, M., and Priess, J.R. (2006). Translational regulators maintain totipotency in the Caenorhabditis elegans germline. Science *311*, 851-853.
Copeland, J.M., Cho, J., Lo, T., Jr., Hur, J.H., Bahadorani, S., Arabyan, T., Rabie, J., Soh, J., and Walker, D.W. (2009). Extension of Drosophila life span by RNAi of the mitochondrial respiratory chain. Curr Biol *19*, 1591-1598.
Corsi, A.K., Wightman, B., and Chalfie, M. (2015). A transparent window into biology: A primer on Caenorhabditis elegans. Genetics *200*, 387-407.
Cortopassi, G.A., and Arnheim, N. (1990). Detection of a specific mitochondrial DNA deletion in tissues of older humans. Nucleic Acids Research *18*, 6927-6933.
Cotney, J., McKay, S.E., and Shadel, G.S. (2009). Elucidation of separate, but collaborative functions of the rRNA methyltransferase-related human mitochondrial transcription factors B1 and B2 in mitochondrial biogenesis reveals new insight into maternally inherited deafness. Human Molecular Genetics *18*, 2670-2682.
Cristina, D., Cary, M., Lunceford, A., Clarke, C., and Kenyon, C. (2009). A Regulated Response to Impaired Respiration Slows Behavioral Rates and Increases Lifespan in Caenorhabditis elegans. PLoS Genet *5*, e1000450.
Crittenden, S.L., Bernstein, D.S., Bachorik, J.L., Thompson, B.E., Gallegos, M., Petcherski, A.G., Moulder, G., Barstead, R., Wickens, M., and Kimble, J. (2002). A conserved RNA-binding protein controls germline stem cells in Caenorhabditis elegans. Nature *417*, 660-663.
Crittenden, S.L., Leonhard, K.A., Byrd, D.T., and Kimble, J. (2006). Cellular Analyses of the Mitotic Region in the Caenorhabditis elegans Adult Germ Line. Molecular Biology of the Cell *17*, 3051-3061.
Dalfó, D., Michaelson, D., and Hubbard, E.J.A. (2012). Sensory regulation of reproduction via TGFβ signaling through the stem cell niche. Current biology : CB *22*, 712-719.
Dell'agnello, C., Leo, S., Agostino, A., Szabadkai, G., Tiveron, C., Zulian, A., Prelle, A., Roubertoux, P., Rizzuto, R., and Zeviani, M. (2007). Increased longevity and refractoriness to Ca(2+)-dependent neurodegeneration in Surf1 knockout mice. Hum Mol Genet *16*, 431-444.
Dillin, A., Hsu, A.-L., Arantes-Oliveira, N., Lehrer-Graiwer, J., Hsin, H., Fraser, A.G., Kamath, R.S., Ahringer, J., and Kenyon, C. (2002). Rates of Behavior and Aging Specified by Mitochondrial Function During Development. Science *298*, 2398.
Doh, J.H., Jung, Y., Reinke, V., and Lee, M.-H. (2013). C. elegans RNA-binding protein GLD-1 recognizes its multiple targets using sequence, context, and structural information to repress translation. Worm *2*, e26548.
Ellis, R.E., and Stanfield, G.M. (2014). The regulation of spermatogenesis and sperm function in nematodes. Seminars in cell & developmental biology *29*, 17-30.
Feng, J., Bussière, F., and Hekimi, S. (2001). Mitochondrial Electron Transport Is a Key Determinant of Life Span in Caenorhabditis elegans. Developmental Cell *1*, 633-644.
Fielenbach, N., and Antebi, A. (2008). C. elegans dauer formation and the molecular basis of plasticity. Genes & Development *22*, 2149-2165.
Fire, A., Xu, S., Montgomery, M.K., Kostas, S.A., Driver, S.E., and Mello, C.C. (1998). Potent and specific genetic interference by double-stranded RNA in Caenorhabditis elegans. Nature *391*, 806-811.
Flatt, T., Min, K.-J., Alterio, C., Villa-Cuesta, E., Cumbers, J., Lehmann, R., Jones, D.L., and Tatar, M. (2008). Drosophila germ-line modulation of insulin signaling and lifespan. Proceedings of the National Academy of Sciences *105*, 6368.

Fox, P.M., and Schedl, T. (2015). Analysis of Germline Stem Cell Differentiation Following Loss of GLP-1 Notch Activity in Caenorhabditis elegans. Genetics *201*, 167-184.
Francis, R., Barton, M.K., Kimble, J., and Schedl, T. (1995). gld-1, a tumor suppressor gene required for oocyte development in Caenorhabditis elegans. Genetics *139*, 579.
Friend, K., Campbell, Z.T., Cooke, A., Kroll-Conner, P., Wickens, M.P., and Kimble, J. (2012). A conserved PUF/Ago/eEF1A complex attenuates translation elongation. Nature structural & molecular biology *19*, 176-183.
Gitschlag, B.L., Kirby, C.S., Samuels, D.C., Gangula, R.D., Mallal, S.A., and Patel, M.R. (2016). Homeostatic responses regulate selfish mitochondrial genome dynamics in C. elegans. Cell metabolism *24*, 91-103.
Goto, H., Tomono, Y., Ajiro, K., Kosako, H., Fujita, M., Sakurai, M., Okawa, K., Iwamatsu, A., Okigaki, T., Takahashi, T*., et al.* (1999). Identification of a Novel Phosphorylation Site on Histone H3 Coupled with Mitotic Chromosome Condensation. Journal of Biological Chemistry *274*, 25543-25549.
Govindan, J.A., Cheng, H., Harris, J.E., and Greenstein, D. (2006). Gαo/i and Gαs Signaling Function in Parallel with the MSP/Eph Receptor to Control Meiotic Diapause in C. elegans. Current Biology *16*, 1257-1268.
Govindan, J.A., Nadarajan, S., Kim, S., Starich, T.A., and Greenstein, D. (2009). Somatic cAMP signaling regulates MSP-dependent oocyte growth and meiotic maturation in C. elegans. Development *136*, 2211-2221.
Greber, B.J., Bieri, P., Leibundgut, M., Leitner, A., Aebersold, R., Boehringer, D., and Ban, N. (2015). The complete structure of the 55S mammalian mitochondrial ribosome. Science *348*, 303.
Gumienny, T.L., Lambie, E., Hartwieg, E., Horvitz, H.R., and Hengartner, M.O. (1999). Genetic control of programmed cell death in the Caenorhabditis elegans hermaphrodite germline. Development *126*, 1011-1022.
Hansen, D., and Schedl, T. (2013). Chapter 4. Stem cell proliferation versus meiotic fate decision in C. elegans. Advances in experimental medicine and biology *757*, 71-99.
Hansen, M., Taubert, S., Crawford, D., Libina, N., Lee, S.-J., and Kenyon, C. (2007). Lifespan extension by conditions that inhibit translation in Caenorhabditis elegans. Aging Cell *6*, 95-110.
Hillen, H.S., Morozov, Y.I., Sarfallah, A., Temiakov, D., and Cramer, P. (2017). Structural Basis of Mitochondrial Transcription Initiation. Cell *171*, 1072-1081.e1010.
Hsin, H., and Kenyon, C. (1999). Signals from the reproductive system regulate the lifespan of C. elegans. Nature *399*, 362-366.
Ishii, N., Fujii, M., Hartman, P.S., Tsuda, M., Yasuda, K., Senoo-Matsuda, N., Yanase, S., Ayusawa, D., and Suzuki, K. (1998). A mutation in succinate dehydrogenase cytochrome b causes oxidative stress and ageing in nematodes. Nature *394*, 694-697.
Joshi, P.M., Riddle, M.R., Djabrayan, N.J.V., and Rothman, J.H. (2010). C. elegans as a model for stem cell biology. Developmental dynamics : an official publication of the American Association of Anatomists *239*, 1539-1554.
Kawasaki, I., Hanazawa, M., Gengyo-Ando, K., Mitani, S., Maruyama, I., and Iino, Y. (2007). ASB-1, a germline-specific isoform of mitochondrial ATP synthase b subunit, is required to maintain the rate of germline development in Caenorhabditis elegans. Mechanisms of Development *124*, 237-251.
Kayser, E.-B., Morgan, P.G., Hoppel, C.L., and Sedensky, M.M. (2001). Mitochondrial Expression and Function of GAS-1 in Caenorhabditis elegans. Journal of Biological Chemistry *276*, 20551-20558.

Kelly, W.G., Xu, S., Montgomery, M.K., and Fire, A. (1997). Distinct Requirements for Somatic and Germline Expression of a Generally Expressed Caernorhabditis Elegans Gene. Genetics *146*, 227-238.
Kershner, A.M., and Kimble, J. (2010). Genome-wide analysis of mRNA targets for Caenorhabditis elegans FBF, a conserved stem cell regulator. Proceedings of the National Academy of Sciences of the United States of America *107*, 3936-3941.
Kershner, A.M., Shin, H., Hansen, T.J., and Kimble, J. (2014). Discovery of two GLP-1/Notch target genes that account for the role of GLP-1/Notch signaling in stem cell maintenance. Proc Natl Acad Sci U S A *111*, 3739-3744.
Kim, S., Spike, C., and Greenstein, D. (2013). Control of Oocyte Growth and Meiotic Maturation in C. elegans. Advances in experimental medicine and biology *757*, 10.1007/1978-1001-4614-4015-1004_1010.
Kimble, J. (2011). Molecular Regulation of the Mitosis/Meiosis Decision in Multicellular Organisms. Cold Spring Harbor Perspectives in Biology *3*, a002683.
Kimble, J., and Hirsh, D. (1979). The postembryonic cell lineages of the hermaphrodite and male gonads in Caenorhabditis elegans. Dev Biol *70*, 396-417.
Kimble, J., and Seidel, H. (2013). C. elegans germline stem cells and their niche. StemBook.
Korta, D.Z., Tuck, S., and Hubbard, E.J.A. (2012). S6K links cell fate, cell cycle and nutrient response in C. elegans germline stem/progenitor cells. Development *139*, 859-870.
Kujoth, G.C., Hiona, A., Pugh, T.D., Someya, S., Panzer, K., Wohlgemuth, S.E., Hofer, T., Seo, A.Y., Sullivan, R., Jobling, W.A*., et al.* (2005). Mitochondrial DNA mutations, oxidative stress, and apoptosis in mammalian aging. Science *309*, 481-484.
Kukat, C., and Larsson, N.-G. (2013). mtDNA makes a U-turn for the mitochondrial nucleoid. Trends in Cell Biology *23*, 457-463.
Lamont, L.B., Crittenden, S.L., Bernstein, D., Wickens, M., and Kimble, J. (2004). FBF-1 and FBF-2 Regulate the Size of the Mitotic Region in the C. elegans Germline. Developmental Cell *7*, 697-707.
Latorre-Pellicer, A., Moreno-Loshuertos, R., Lechuga-Vieco, A.V., Sánchez-Cabo, F., Torroja, C., Acín-Pérez, R., Calvo, E., Aix, E., González-Guerra, A., Logan, A*., et al.* (2016). Mitochondrial and nuclear DNA matching shapes metabolism and healthy ageing. Nature *535*, 561.
Lee, M.-H., Ohmachi, M., Arur, S., Nayak, S., Francis, R., Church, D., Lambie, E., and Schedl, T. (2007). Multiple Functions and Dynamic Activation of MPK-1 Extracellular Signal-Regulated Kinase Signaling in Caenorhabditis elegans Germline Development. Genetics *177*, 2039-2062.
Leopold, A.C., Niedergang-Kamien, E., and Janick, J. (1959). Experimental Modification of Plant Senescence. Plant Physiology *34*, 570.
Li, X., Johnson, R.W., Park, D., Chin-Sang, I., and Chamberlin, H.M. (2012). Somatic gonad sheath cells and Eph receptor signaling promote germ-cell death in C. elegans. Cell Death Differ *19*, 1080-1089.
Liesa, M., and Shirihai, Orian S. (2013). Mitochondrial Dynamics in the Regulation of Nutrient Utilization and Energy Expenditure. Cell Metabolism *17*, 491-506.
Lin, Y.-F., Schulz, A.M., Pellegrino, M.W., Lu, Y., Shaham, S., and Haynes, C.M. (2016). Maintenance and propagation of a deleterious mitochondrial genome by the mitochondrial unfolded protein response. Nature *533*, 416.
Mason, J.B., Cargill, S.L., Anderson, G.B., and Carey, J.R. (2009). Transplantation of Young Ovaries to Old Mice Increased Life Span in Transplant Recipients. The Journals of Gerontology Series A: Biological Sciences and Medical Sciences *64A*, 1207-1211.
McCarter, J., Bartlett, B., Dang, T., and Schedl, T. (1999). On the control of oocyte meiotic maturation and ovulation in Caenorhabditis elegans. Dev Biol *205*, 111-128.

McCulloch, V., and Shadel, G.S. (2003). Human Mitochondrial Transcription Factor B1 Interacts with the C-Terminal Activation Region of h-mtTFA and Stimulates Transcription Independently of Its RNA Methyltransferase Activity. Molecular and Cellular Biology *23*, 5816-5824.
Merritt, C., Rasoloson, D., Ko, D., and Seydoux, G. (2008). 3' UTRs are the primary regulators of gene expression in the C. elegans germline. Current biology : CB *18*, 1476-1482.
Metodiev, M.D., Lesko, N., Park, C.B., Camara, Y., Shi, Y., Wibom, R., Hultenby, K., Gustafsson, C.M., and Larsson, N.G. (2009). Methylation of 12S rRNA is necessary for in vivo stability of the small subunit of the mammalian mitochondrial ribosome. Cell Metab *9*, 386-397.
Michaelson, D., Korta, D.Z., Capua, Y., and Hubbard, E.J.A. (2010). Insulin signaling promotes germline proliferation in C. elegans. Development *137*, 671-680.
Miller, M.A., Nguyen, V.Q., Lee, M.-H., Kosinski, M., Schedl, T., Caprioli, R.M., and Greenstein, D. (2001). A Sperm Cytoskeletal Protein That Signals Oocyte Meiotic Maturation and Ovulation. Science *291*, 2144-2147.
Min, K.-J., Lee, C.-K., and Park, H.-N. (2012). The lifespan of Korean eunuchs. Current Biology *22*, R792-R793.
Mishra, P., and Chan, D.C. (2016). Metabolic regulation of mitochondrial dynamics. The Journal of Cell Biology *212*, 379-387.
Morrison, S.J., and Spradling, A.C. (2008). Stem Cells and Niches: Mechanisms That Promote Stem Cell Maintenance throughout Life. Cell *132*, 598-611.
Nadarajan, S., Govindan, J.A., McGovern, M., Hubbard, E.J., and Greenstein, D. (2009). MSP and GLP-1/Notch signaling coordinately regulate actomyosin-dependent cytoplasmic streaming and oocyte growth in C. elegans. Development *136*, 2223-2234.
Neupert, W., and Herrmann, J.M. (2007). Translocation of Proteins into Mitochondria. Annual Review of Biochemistry *76*, 723-749.
Nousch, M., and Eckmann, C.R. (2013). Translational control in the Caenorhabditis elegans germ line. Adv Exp Med Biol *757*, 205-247.
Nunnari, J., and Suomalainen, A. (2012). Mitochondria: In Sickness and in Health. Cell *148*, 1145-1159.
Oka, M., Moriyama, T., Asally, M., Kawakami, K., and Yoneda, Y. (2013). Differential Role for Transcription Factor Oct4 Nucleocytoplasmic Dynamics in Somatic Cell Reprogramming and Self-renewal of Embryonic Stem Cells. The Journal of Biological Chemistry *288*, 15085-15097.
Okimoto, R., Macfarlane, J.L., Clary, D.O., and Wolstenholme, D.R. (1992). The mitochondrial genomes of two nematodes, Caenorhabditis elegans and Ascaris suum. Genetics *130*, 471-498.
Ooi, S.L., Priess, J.R., and Henikoff, S. (2006). Histone H3.3 Variant Dynamics in the Germline of Caenorhabditis elegans. PLoS Genetics *2*, e97.
Pagliarini, D.J., Calvo, S.E., Chang, B., Sheth, S.A., Vafai, S.B., Ong, S.-E., Walford, G.A., Sugiana, C., Boneh, A., Chen, W.K.*, et al.* (2008). A Mitochondrial Protein Compendium Elucidates Complex I Disease Biology. Cell *134*, 112-123.
Pujol, C., Bratic-Hench, I., Sumakovic, M., Hench, J., Mourier, A., Baumann, L., Pavlenko, V., and Trifunovic, A. (2013). Succinate Dehydrogenase Upregulation Destabilize Complex I and Limits the Lifespan of gas-1 Mutant. PLOS ONE *8*, e59493.
Qin, Z., and Hubbard, E.J.A. (2015). Non-autonomous DAF-16/FOXO activity antagonizes age-related loss of C. elegans germline stem/progenitor cells. Nat Commun *6*.
Rea, S.L., Ventura, N., and Johnson, T.E. (2007). Relationship between mitochondrial electron transport chain dysfunction, development, and life extension in Caenorhabditis elegans. PLoS Biol *5*, e259.

Reinders, J., Zahedi, R.P., Pfanner, N., Meisinger, C., and Sickmann, A. (2006). Toward the Complete Yeast Mitochondrial Proteome: Multidimensional Separation Techniques for Mitochondrial Proteomics. Journal of Proteome Research *5*, 1543-1554.
Ringel, R., Sologub, M., Morozov, Y.I., Litonin, D., Cramer, P., and Temiakov, D. (2011). Structure of human mitochondrial RNA polymerase. Nature *478*, 269-273.
Scheckel, C., Gaidatzis, D., Wright, J.E., and Ciosk, R. (2012). Genome-Wide Analysis of GLD-1–Mediated mRNA Regulation Suggests a Role in mRNA Storage. PLOS Genetics *8*, e1002742.
Schmidt, O., Pfanner, N., and Meisinger, C. (2010). Mitochondrial protein import: from proteomics to functional mechanisms. Nature Reviews Molecular Cell Biology *11*, 655.
Sengupta, M.S., Low, W.Y., Patterson, J.R., Kim, H.-M., Traven, A., Beilharz, T.H., Colaiácovo, M.P., Schisa, J.A., and Boag, P.R. (2013). ifet-1 is a broad-scale translational repressor required for normal P granule formation in C. elegans. Journal of Cell Science *126*, 850-859.
Shi, Y., Dierckx, A., Wanrooij, P.H., Wanrooij, S., Larsson, N.-G., Wilhelmsson, L.M., Falkenberg, M., and Gustafsson, C.M. (2012). Mammalian transcription factor A is a core component of the mitochondrial transcription machinery. Proceedings of the National Academy of Sciences of the United States of America *109*, 16510-16515.
Shutt, T.E., and Gray, M.W. (2006). Homologs of Mitochondrial Transcription Factor B, Sparsely Distributed Within the Eukaryotic Radiation, Are Likely Derived from the Dimethyladenosine Methyltransferase of the Mitochondrial Endosymbiont. Molecular Biology and Evolution *23*, 1169-1179.
Sickmann, A., Reinders, J., Wagner, Y., Joppich, C., Zahedi, R., Meyer, H.E., Schönfisch, B., Perschil, I., Chacinska, A., Guiard, B*., et al.* (2003). The proteome of Saccharomyces cerevisiae mitochondria. Proceedings of the National Academy of Sciences *100*, 13207.
Sologub, M., Litonin, D., Anikin, M., Mustaev, A., and Temiakov, D. (2009). TFB2 Is a Transient Component of the Catalytic Site of the Human Mitochondrial RNA Polymerase. Cell *139*, 934-944.
Spike, C.A., Bader, J., Reinke, V., and Strome, S. (2008). DEPS-1 promotes P-granule assembly and RNA interference in C. elegans germ cells. Development *135*, 983-993.
Sumitani, M., Kasashima, K., Matsugi, J., and Endo, H. (2011). Biochemical properties of Caenorhabditis elegans HMG-5, a regulator of mitochondrial DNA. Journal of Biochemistry *149*, 581-589.
Sun, N., Youle, R.J., and Finkel, T. (2016). The Mitochondrial Basis of Aging. Molecular Cell *61*, 654-666.
Surovtseva, Y.V., and Shadel, G.S. (2013). Transcription-independent role for human mitochondrial RNA polymerase in mitochondrial ribosome biogenesis. Nucleic Acids Research *41*, 2479-2488.
Syntichaki, P., Troulinaki, K., and Tavernarakis, N. (2007). eIF4E function in somatic cells modulates ageing in Caenorhabditis elegans. Nature *445*, 922-926.
Taanman, J.-W. (1999). The mitochondrial genome: structure, transcription, translation and replication. Biochimica et Biophysica Acta (BBA) - Bioenergetics *1410*, 103-123.
Teixeira, F.K., Sanchez, C.G., Hurd, T.R., Seifert, J.R.K., Czech, B., Preall, J.B., Hannon, G.J., and Lehmann, R. (2015). ATP synthase promotes germ cell differentiation independent of oxidative phosphorylation. Nat Cell Biol *17*, 689-696.
Trifunovic, A., Wredenberg, A., Falkenberg, M., Spelbrink, J.N., Rovio, A.T., Bruder, C.E., Bohlooly-Y, M., Gidlöf, S., Oldfors, A., Wibom, R*., et al.* (2004). Premature ageing in mice expressing defective mitochondrial DNA polymerase. Nature *429*, 417.

Tuppen, H.A.L., Blakely, E.L., Turnbull, D.M., and Taylor, R.W. (2010). Mitochondrial DNA mutations and human disease. Biochimica et Biophysica Acta (BBA) - Bioenergetics *1797*, 113-128.
Van Hooser, A., Goodrich, D.W., Allis, C.D., Brinkley, B.R., and Mancini, M.A. (1998). Histone H3 phosphorylation is required for the initiation, but not maintenance, of mammalian chromosome condensation. Journal of Cell Science *111*, 3497-3506.
Varum, S., Rodrigues, A.S., Moura, M.B., Momcilovic, O., Easley, C.A.I.V., Ramalho-Santos, J., Van Houten, B., and Schatten, G. (2011). Energy Metabolism in Human Pluripotent Stem Cells and Their Differentiated Counterparts. PLOS ONE *6*, e20914.
Wolke, U., Jezuit, E.A., and Priess, J.R. (2007). Actin-dependent cytoplasmic streaming in C. elegans oogenesis. Development *134*, 2227-2236.
Wright, J.E., Gaidatzis, D., Senften, M., Farley, B.M., Westhof, E., Ryder, S.P., and Ciosk, R. (2011). A quantitative RNA code for mRNA target selection by the germline fate determinant GLD-1. Embo j *30*, 533-545.
Xu, X., Duan, S., Yi, F., Ocampo, A., Liu, G.-H., and Izpisua Belmonte, Juan C. (2013). Mitochondrial Regulation in Pluripotent Stem Cells. Cell Metabolism *18*, 325-332.
Yakubovskaya, E., Guja, K.E., Eng, E.T., Choi, W.S., Mejia, E., Beglov, D., Lukin, M., Kozakov, D., and Garcia-Diaz, M. (2014). Organization of the human mitochondrial transcription initiation complex. Nucleic Acids Research *42*, 4100-4112.
Yang, W., and Hekimi, S. (2010). Two modes of mitochondrial dysfunction lead independently to lifespan extension in Caenorhabditis elegans. Aging Cell *9*, 433-447.
Yee, C., Yang, W., and Hekimi, S. (2014). The intrinsic apoptosis pathway mediates the pro-longevity response to mitochondrial ROS in C. elegans. Cell *157*, 897-909.
Youle, R.J., and van der Bliek, A.M. (2012). Mitochondrial Fission, Fusion, and Stress. Science *337*, 1062-1065.
Zhang, Y., Marsboom, G., Toth, P.T., and Rehman, J. (2013). Mitochondrial Respiration Regulates Adipogenic Differentiation of Human Mesenchymal Stem Cells. PLoS ONE *8*, e77077.
Zhou, Z., Hartwieg, E., and Horvitz, H.R. (2001). CED-1 Is a Transmembrane Receptor that Mediates Cell Corpse Engulfment in C. elegans. Cell *104*, 43-56.

7. Appendix I: The involvement of adiponectin signaling in stress resistance and lipid homeostasis.

In addition to serving fat and energy storage functions, the adipose tissue is a highly active metabolic and endocrine organ which exerts its systemic effects through secretion of adipose derived hormones (adipokines). Adipokines act through an autocrine, paracrine and endocrine fashion and can affect distal tissues, far away from their production site (Fasshauer and Bluher, 2015). The adipokine adiponectin affects organismal homeostasis through binding to its cognate receptors AdipoR1 and AdipoR2 (Yamauchi and Kadowaki, 2013). Impairment of this signaling axis has been associated with human diseases, particularly with type II diabetes and obesity (Nigro et al., 2014). Plasma adiponectin concentration is reduced in obese humans and in type 2 diabetic patients (Weyer et al., 2001). Manipulation of hormonal signaling pathways may influence lifespan by regulating survival under stress conditions, with insulin/IGF signaling being the most prominent example (Kenyon, 2005). We examined the involvement of adiponectin signaling in the ER unfolded protein response (UPR^{ER}) and lipid homeostasis *in vivo*, using *C. elegans* as our model.

A functional adiponectin homologue has not yet been identified in *C. elegans*. We studied the effect of adiponectin signaling attenuation by using *paqr-1(tm3262)* mutants and RNAi-mediated genetic inhibition. PAQR-1 encodes for one of the three adiponectin receptor homologues in *C. elegans*. We found that *paqr-1(tm3262)* mutants are resistant when challenged with the well-established ER stressor tunicamycin, which inhibits the N-glycosylation process taking place in the ER. We assessed UPR^{ER} induction by using hsp-4GFP reporter animals. HSP-4, the grp78/BiP homologue in nematodes, belongs to the hsp-70 family of molecular chaperones and its expression is known to increase when the ER protein environment is challenged (Henis-Korenblit et al., 2010; Taylor and Dillin, 2013). We observed that *paqr-1(tm3262)* mutants exhibit an elevated baseline hsp-4GFP expression and they manage to robustly respond to tunicamycin by increasing hsp-4GFP even more than their wild-type counterparts (app.I, figure 1B and C). Interestingly, we observed a similar trend when we treated animals with *sca-1(RNAi)* to

knockdown the sarco/endoplasmic reticulum $Ca2^{+}$-ATPase (SERCA), without adding tunicamycin (app.I, figure 1C). We hypothesized that the enhanced survival of *paqr-1(tm3262)* mutants can be attributed to a hormetic effect exerted by PAQR-1. Hormesis is a phenomenon where early exposure to a mild stress can prove beneficial when the organisms are later challenged with a more severe stress (Gems and Partridge, 2008; Kourtis et al., 2012; Mattson, 2008). Interestingly, when we combined *sca-1(RNAi)* with tunicamycin treatment, hsp-4GFP could not be induced as in the case of *paqr-1* lesion (app.I, figure 1C). This suggests that the hormetic effect can be specifically attributed to the attenuation of PAQR-1 signaling and not generally to an elevated baseline ER^{UPR} response.

We also asked whether and how adiponectin signaling affects lipid homeostasis. Initial observations of my colleague Manos Kyriakakis suggested that the lipid content is reduced in *paqr-1(tm3262)* mutants compared to their wild-type counterparts. Tunicamycin treatment also affected lipid droplets by reducing their size (data not shown). We reasoned that selective autophagy of lipids (i.e lipophagy) could be activated and affect lipid content. To check this hypothesis we generated a double reporter strain for monitoring lipophagy by combining a GFP-tagged LGG-1/LC-3 (Palmisano and Meléndez, 2016), a widely accepted autophagy marker, with a wmCherry-tagged PLIN/Perilipin, a protein which is highly abundant in lipid droplets (Vrablik et al., 2015). We observed that tunicamycin treatment triggered the increase of overall LGG-1 expression as well as its transition from a diffuse to a more punctuate distribution, indicating an increase in autophagic puncta formation (app.I, figure 2A). Moreover, we found that *paqr-1* downregulation, but not ER stress, causes an increase in the overall levels of ATGL-1 triglyceride lipase (app.I, figure 2B). ATGL-1 has been shown to promote lipolysis in response to fasting in *C. elegans* (Lee et al., 2014). In summary, we believe that the coordinated action of lipophagy and ATGL-1-dependent lipolysis may affect lipid homeostasis downstream of PAQR-1 signaling. Interestingly, a recent publication highlights the interplay between ATGL-1 in lipophagy to promote lipid catabolism in the mouse liver (Sathyanarayan et al., 2017). The results of our study were published a year ago in “Scientific Reports” journal (Kyriakakis et al., 2017).

Materials and Methods (appendix I)

We followed standard procedures for maintaining *C. elegans* strains. Rearing temperature was set at 20^{o}C for all experiments. Tunicamycin resistance assays were performed in the WT (N2) and *paqr-1(tm3262)* mutant genetic backgrounds. Tunicamycin was added on top of NGM plates with UV-killed OP50 bacteria in a final concentration of 50μg/mL for ER stress resistance assays and to assess UPR^{ER} induction in the respective backgrounds. Tunicamycin was supplied at D1 of adulthood and UPR^{ER} induction was measured 24h later using the SJ4005: zcIs4 [hsp-4::GFP] reporter. The *sca-1(RNAi)* construct was generated by N. Kourtis and published in his PhD publication (Kourtis et al., 2012). To generate the lipophagy reporter we crossed the DA2123: adIs2122 [lgg-1p::GFP::lgg-1 + rol-6(su1006)] with the LIU2: ldrIs2 [mdt-28p::mdt-28::mCherry + unc-76(+)] reporter strains.

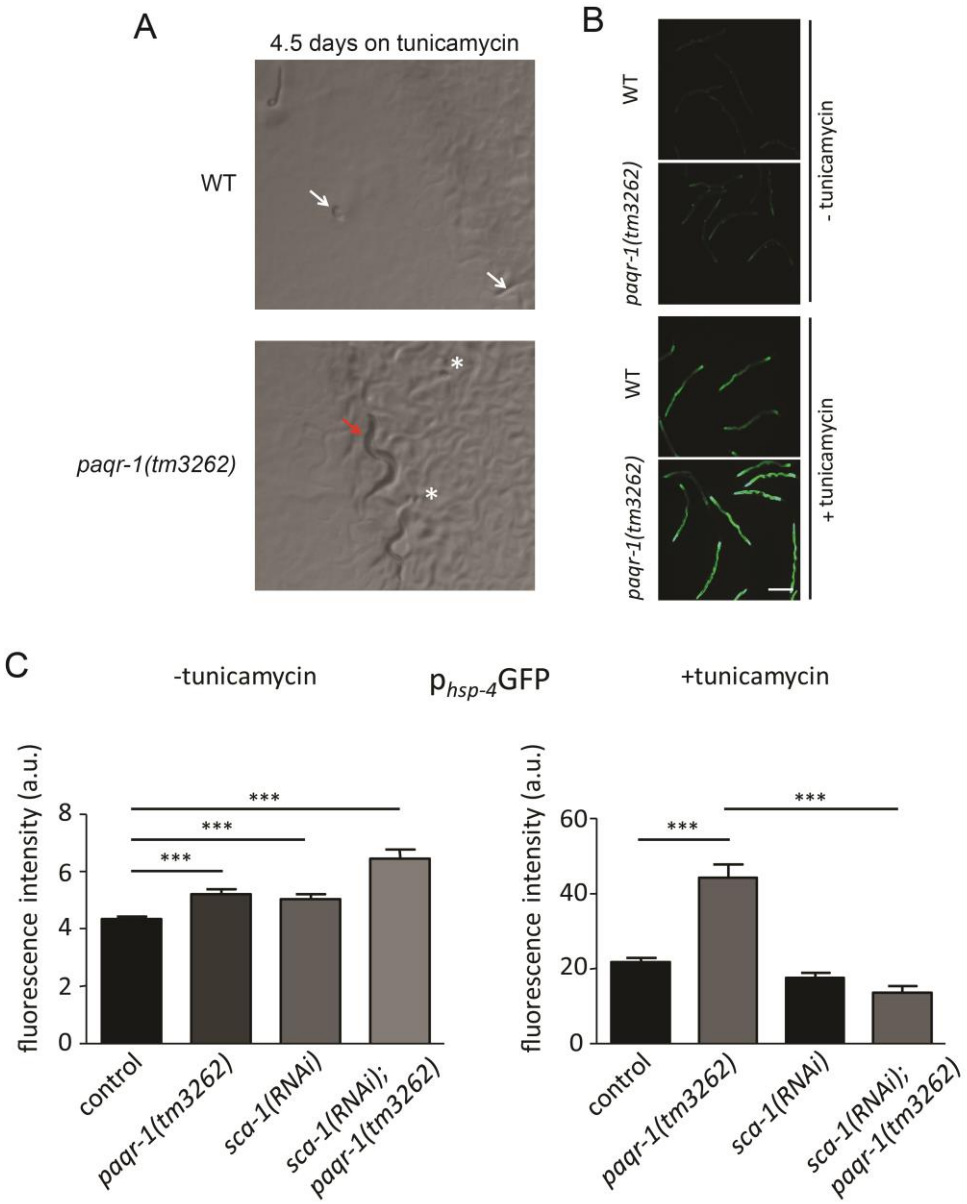

App. I, figure 1. A) *Paqr-1* deficiency renders nematodes resistant to tunicamycin, a well-known ER stressor and ER^{UPR} inducer. White arrows indicate dead WT larvae, the red arrow points to *paqr-1(tm3262)* mutant animals which reached adulthood and white stars denote eggs laid by gravid *paqr-1(tm3262)* mutant adults. B) hsp-4GFP fluorescent reporter animals which are used as a measure for ER^{UPR} induction. *paqr-1(tm3262)* mutants display increased baseline levels of hsp-4GFP and higher induction of hsp-4GFP upon tunicamycin treatment. C) Specificity of the hormetic response exerted by *paqr-1* lesion. Treatment with *sca-1(RNAi)* induces baseline hsp-4GFP expression, nevertheless cannot further increase hsp-4GFP expression upon treatment with tunicamycin.

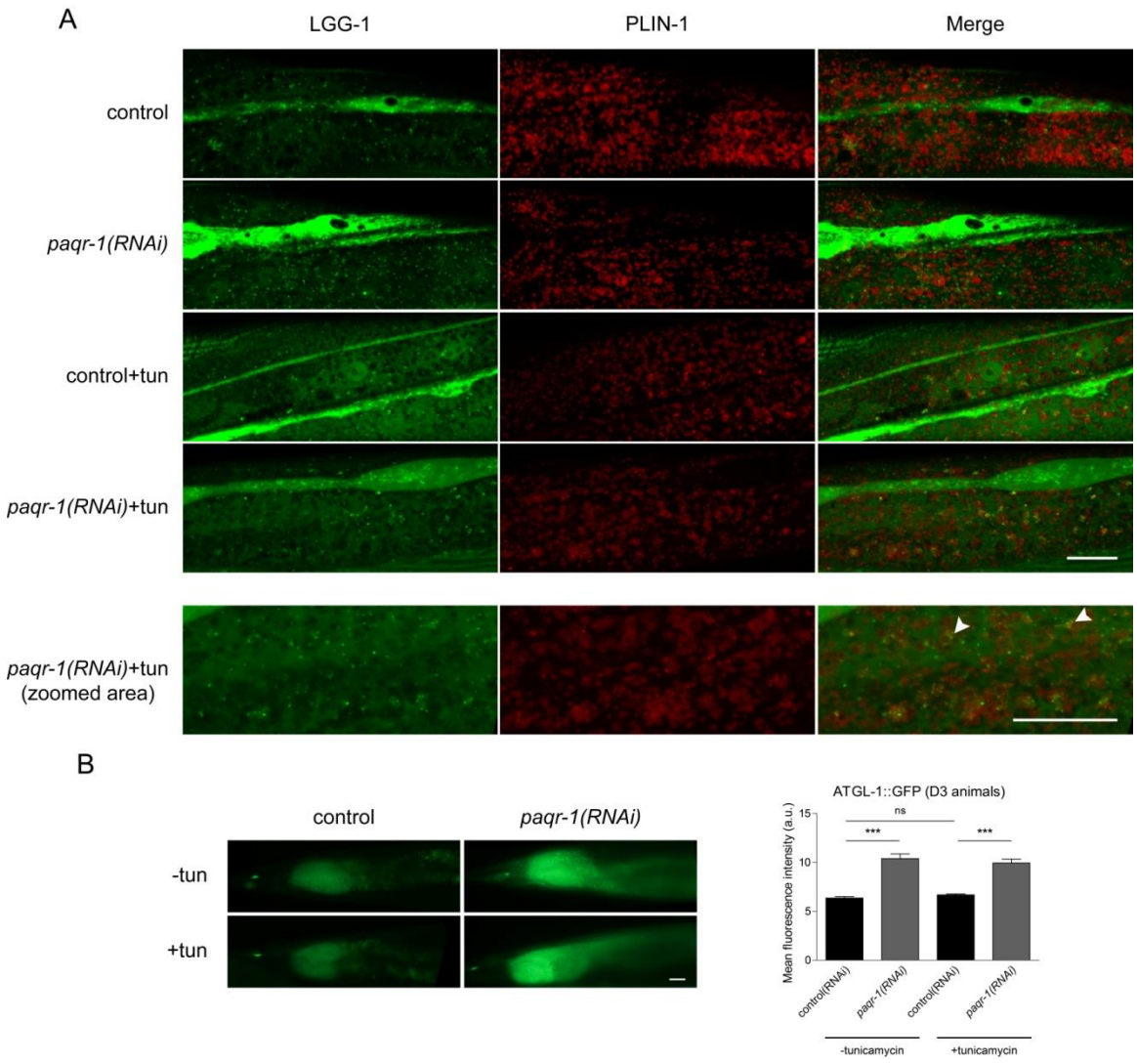

App. I figure 2: A) A reporter for assessing lipophagy *in vivo*. Increased localization of LGG-1/LC-3 GFP positive autophagic puncta (shown in green) in the proximity of PLIN-1::wmCherry lipid droplets (shown in red) is observed when tunicamycin treatment is combined with *paqr-1* knockdown. This can be a consequence of the activation of lipid-specific macroautophagy (i.e lipophagy). B) PAQR-1 signaling negatively regulates ATGL-1 lipase expression. ER stress itself does not affect ATGL-1 levels.

References (appendix I)

Fasshauer, M., and Bluher, M. (2015). Adipokines in health and disease. Trends Pharmacol Sci *36*, 461-470.

Gems, D., and Partridge, L. (2008). Stress-Response Hormesis and Aging: "That which Does Not Kill Us Makes Us Stronger". Cell Metabolism *7*, 200-203.

Henis-Korenblit, S., Zhang, P., Hansen, M., McCormick, M., Lee, S.-J., Cary, M., and Kenyon, C. (2010). Insulin/IGF-1 signaling mutants reprogram ER stress response regulators to promote longevity. Proceedings of the National Academy of Sciences *107*, 9730.

Kenyon, C. (2005). The Plasticity of Aging: Insights from Long-Lived Mutants. Cell *120*, 449-460.

Kourtis, N., Nikoletopoulou, V., and Tavernarakis, N. (2012). Small heat-shock proteins protect from heat-stroke-associated neurodegeneration. Nature *490*, 213-218.

Kyriakakis, E., Charmpilas, N., and Tavernarakis, N. (2017). Differential adiponectin signalling couples ER stress with lipid metabolism to modulate ageing in C. elegans. Scientific Reports *7*, 5115.

Lee, J.H., Kong, J., Jang, J.Y., Han, J.S., Ji, Y., Lee, J., and Kim, J.B. (2014). Lipid droplet protein LID-1 mediates ATGL-1-dependent lipolysis during fasting in Caenorhabditis elegans. Mol Cell Biol *34*, 4165-4176.

Mattson, M.P. (2008). Hormesis Defined. Ageing research reviews *7*, 1-7.

Nigro, E., Scudiero, O., Monaco, M.L., Palmieri, A., Mazzarella, G., Costagliola, C., Bianco, A., and Daniele, A. (2014). New Insight into Adiponectin Role in Obesity and Obesity-Related Diseases. BioMed Research International *2014*, 658913.

Palmisano, N.J., and Meléndez, A. (2016). Detection of Autophagy in Caenorhabditis elegans Using GFP::LGG-1 as an Autophagy Marker. Cold Spring Harbor protocols *2016*, pdb.prot086496.

Sathyanarayan, A., Mashek, M.T., and Mashek, D.G. (2017). ATGL Promotes Autophagy/Lipophagy via SIRT1 to Control Hepatic Lipid Droplet Catabolism. Cell Rep *19*, 1-9.

Taylor, Rebecca C., and Dillin, A. (2013). XBP-1 Is a Cell-Nonautonomous Regulator of Stress Resistance and Longevity. Cell *153*, 1435-1447.

Vrablik, T.L., Petyuk, V.A., Larson, E.M., Smith, R.D., and Watts, J.L. (2015). Lipidomic and proteomic analysis of C. elegans lipid droplets and identification of ACS-4 as a lipid droplet-associated protein. Biochimica et biophysica acta *1851*, 1337-1345.

Weyer, C., Funahashi, T., Tanaka, S., Hotta, K., Matsuzawa, Y., Pratley, R.E., and Tataranni, P.A. (2001). Hypoadiponectinemia in obesity and type 2 diabetes: close association with insulin resistance and hyperinsulinemia. J Clin Endocrinol Metab *86*, 1930-1935.

Yamauchi, T., and Kadowaki, T. (2013). Adiponectin receptor as a key player in healthy longevity and obesity-related diseases. Cell Metab *17*, 185-196.

8. Appendix II: ACBP proteins bridge autophagy with appetite control in *C. elegans*

Acetyl-coenzyme A (acetyl-coA) is a central cellular metabolite and second messenger lying at the crossroad between anabolism and catabolism. It is the molecule through which pyruvate from glycolysis enters the Krebs cycle, a key precursor of lipid biosynthesis and a unique donor of acetyl groups for intracellular acetylation (Pietrocola et al., 2015). Acetylation is a very common post-translational protein modification which can alter the stability and function of the acceptor proteins (Hollebeke et al., 2012). Due to the pleiad of intracellular acetylation acceptors, acetyl-coA directly regulates diverse cellular processes, ranging from cell cycle progression and mitosis, to autophagy, and programmed cell death (Choudhary et al., 2014). Macroautophagy, a self-catabolic process which entails the formation of autophagosomes to deliver the enclosed material to lysosomes for degradation (Feng et al., 2013), is also affected by acetyl-coA abundance. Specifically, acetyl-coA deprivation in the cytoplasm is sufficient to activate AMPK and TORC1, thereby stimulating autophagy (Marino et al., 2014). Moreover, several autophagy proteins, such as ATG-5, ATG-7 and ATG-12, can be acetylated and this modification renders them less active (Madeo et al., 2014).

Acyl-coA-binding (ACBP)/ diazepam binding protein (DBI) proteins bind acyl-coA fatty acids inside the cell but can also be secreted in an autophagy dependent manner (Duran et al., 2010). *C. elegans* encodes four basic ACBP homologues (ACBP-1, ACBP-3, ACBP-4, ACBP-6) which harbor a conserved ACBP domain, as well as three proteins with additional domains (ACBP-2, ACBP-5, MAA-1) (Elle et al., 2011). Our collaborators in Dr. Guido Kroemer's laboratory have established ACBP/DBI as a linker between autophagy induction and appetite control in mice. We checked whether we could establish a conserved role of ACBP protein family in the control of these processes, using the nematode *C. elegans* as our model.

We first wondered whether ACBP proteins regulate autophagy. We used a single mutant strain for *acbp-1* (*acbp-1(sv62)*) as well as a quadruple mutant for all four basic ACBP family members (*acbp-1(sv62); acbp-6(tm2995); acbp-4(tm2896); acbp-3(sv73)*). We crossed these strains with an autophagy reporter strain which expresses GFP::LGG-1. LGG-1 encodes for an

LC-3 homologue in nematodes which shows diffuse distribution under baseline conditions, nevertheless acquires a more punctuate expression pattern, indicative of autophagic puncta formation, when autophagy is induced (Palmisano and Meléndez, 2016). We noticed that autophagic puncta increased in both the single and the quadruple mutant genetic backgrounds (App. II, figure 1A). The quadruple mutant showed the most pronounced increased, indicating basic ACBP proteins act redundantly to inhibit autophagy. The increase of autophagic puncta can be either attributed to an increase in autophagic flux (i.e enhanced formation of autophagosomes which end up in lysosomes for degradation) or to defective autophagy, where the autophagic process is arrested and autophagosomes cannot reach lysosomes. To distinguish between these two possibilities we used an SQST-1::GFP reporter. SQST-1 is a substrate of autophagy, thus its expression is expected to decline upon autophagy induction (Tian et al., 2010). Indeed, SQST-1::GFP puncta in the head region of animals are reduced upon genetic inhibition of *acbp* family members (App. II, figure 1B), indicating that ACBP protein family members repress the autophagic flux.

We generated a translational reporter strain by fusing *acbp-1* genomic sequence with wmCherry under the control of its endogenous promoter. ACBP-1 is expressed mainly in the intestine of adult animals. We also noticed that ACBP-1::wmCherry also localized at the six coelomocytes, which are scavenger cells which endocytose extracellular material. This indicates that ACBP-1 may also be secreted similarly to DBI, its mammalian homologue. Interestingly upon a 24 hour starvation, the expression of ACBP increased profoundly (App. II, figure 2). We wondered whether ACBP-1 can regulate appetite, similar to DBI. We measured food intake by assessing pharyngeal pumping (data not shown) as well as by feeding with RFP fluorescent bacteria for a short period and measuring total intestinal fluorescence. We found that depletion of ACBP-1, as well as all four basic ACBP proteins, resulted in a reduction of fluorescent bacteria intake (App. II, figure 3). Overall, ACBP proteins negatively regulate autophagy and promote appetite in nematodes, suggesting a conserved function during evolution.

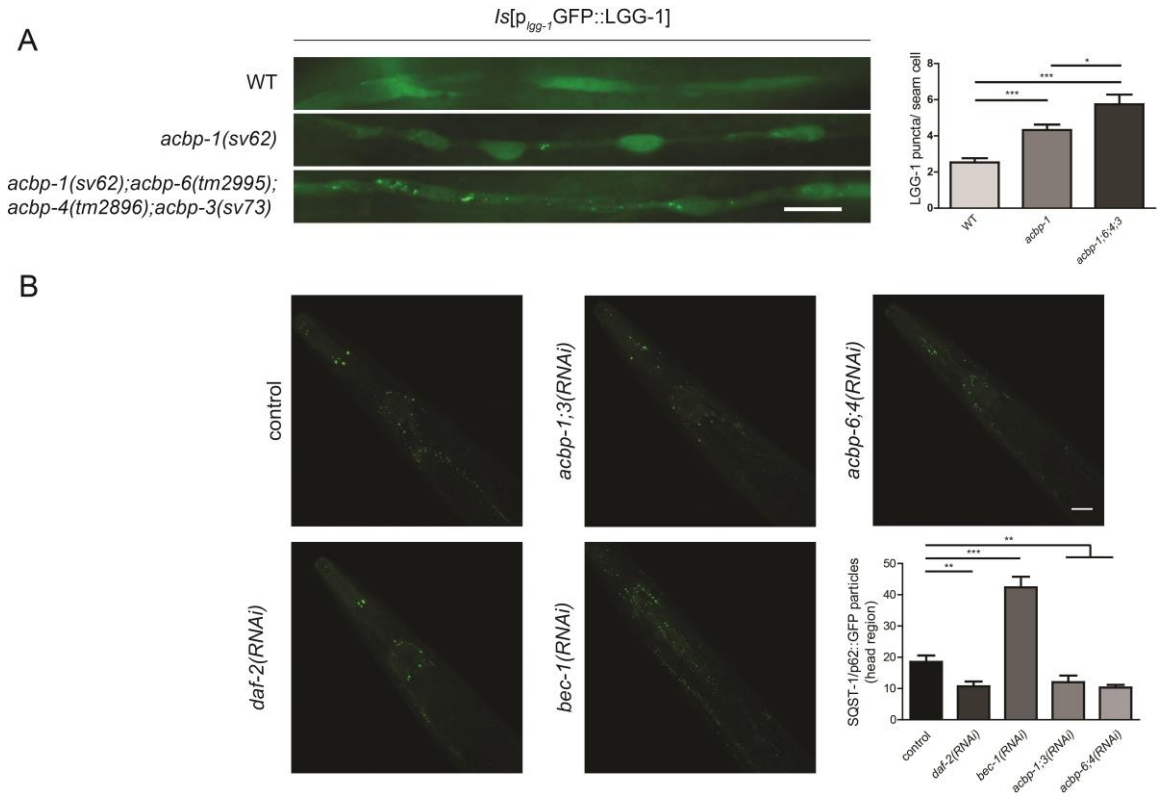

App. II, figure 1. ACBP protein family members repress autophagy in *C. elegans*. A) High magnification images (63x) of hypodermal seam cells of WT, *acbp-1* single and *acbp-1,6,4,3* quadruple mutant animals. A transition from a diffuse to a punctuate LGG-1/LC3 distribution associated with the formation of autophagic puncta is evident in both *acbp* mutant genetic backgrounds. Quantification is provided in the upper right panel. B) Confocal images of SQST-1/p62::GFP worms treated with known regulators of autophagy as well as *acbp* RNAis. A quantification of the puncta in the head region is provided in the lower right panel. *daf-2(RNAi)* is a treatment which increases the autophagic flux, whereas *bec-1(RNAi)* blocks autophagy. Scale bars, 20μm.

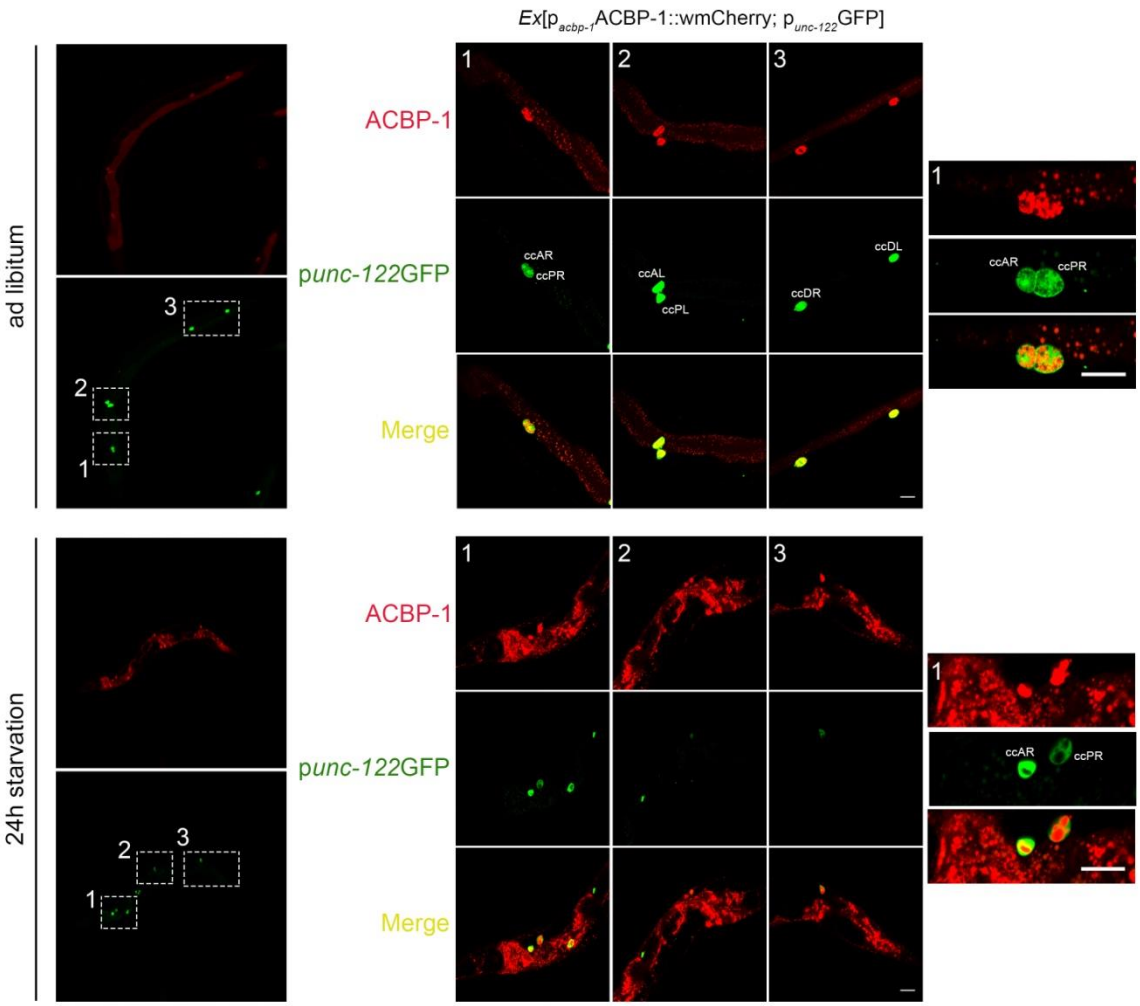

App. II, figure 2. ACBP-1 expression pattern. Fluorescent images of D2 adult ACBP-1::wmCherry animals fed ad libitum or upon 24 hour starvation. Strong expression is observed in coelomocytes, marked with the punc-122GFP marker. The intracellular levels of ACBP-1 increase profoundly upon starvation. Scale bar, 20μm.

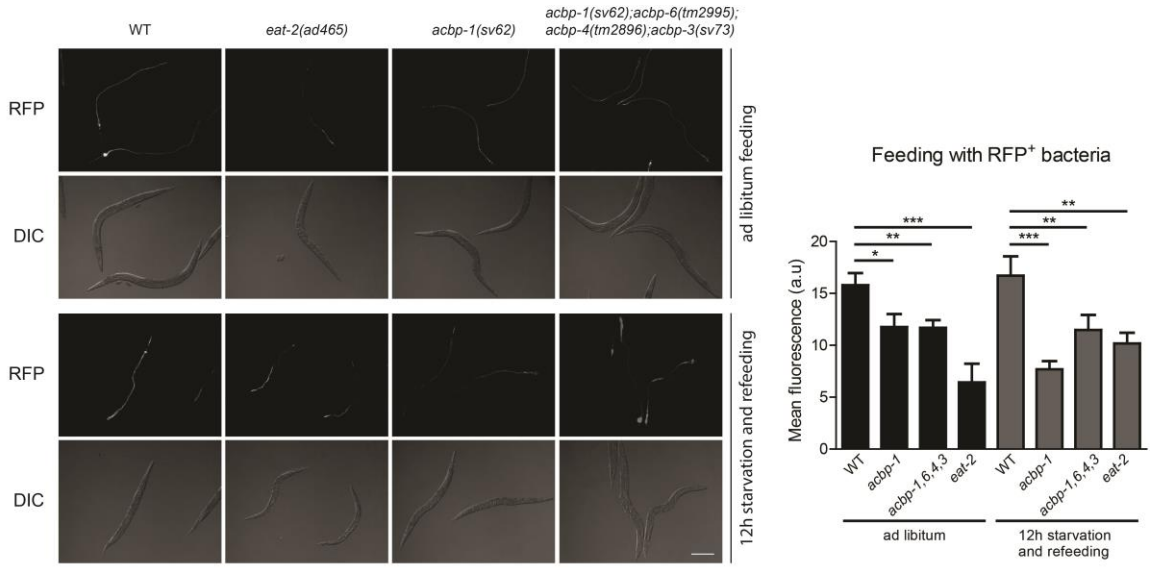

App. II, figure 3. ACBP family members regulate appetite in *C. elegans*. Fluorescent images of D1 adult animals of the respective genotypes fed with RFP fluorescent bacteria for five minutes. ACBP deficient animals exhibit a decrease in the food intake compared to their control counterparts. *eat-2(ad465)* mutants are used as a positive control for reduced food uptake due of reduced pharyngeal muscle contractions. Scale bar, 200μm.

Materials and Methods (appendix II)

We followed standard procedures for maintaining *C. elegans* strains. Rearing temperature was set at 20ºC for all experiments. We used the DA2123: adIs2122 [lgg-1p::GFP::lgg-1 + rol-6(su1006)] to measure LGG-1/LC-3 autophagic puncta and the HZ589: *him-5(e1490)V*;bpIs151 [sqst-1p::sqst-1::GFP + unc-76(+)] to measure SQST-1/p62 puncta (Egan et al., 2011; Kang et al., 2007). The DA2123 strain was crossed with the SV62:*acbp-1(sv62)I* and the quadruple FE0017:*acbp-1(sv62)I*;*acbp-6(tm2995)II*;*acbp-4(tm2896)III*;*acbp-3(sv73)X* strains (Elle et al., 2011) to monitor autophagy upon depletion of the *acbp* family genes. For pharyngeal pumping measurements, the SV62 and FE0017 strains were used in together with DA465: *eat-2(ad465)II*, a genetic model for reduced pharyngeal pumping. Autophagy was measured as described in the literature (Palmisano and Meléndez, 2016). For measuring LGG-1/LC-3 puncta, 10 well-fed adult worms of the respective genetic backgrounds were allowed to lay eggs on nematode growth medium or RNAi plates. Four hours later, parents were removed and plates were placed at 20ºC. 2.5 days later, synchronized animals were collected, anaesthetized with 10 mM levamisole and mounted on slides for microscopic examination. The number of GFP::LGG-1 positive autophagic puncta was counted in hypodermal seam cells at the L3-L4 larval stages (Meléndez et al., 2003). Starvation was performed by placing the animals in NGM plates devoid of bacteria for 24 h. For assessing food intake using fluorescent bacteria, we fed synchronized day one adult animals for five minutes with RFP-expressing HT115 bacteria transformed with a IPTG-inducible His-RFP expressing plasmid (modification of the protocol published by (You et al., 2008). Upon this short feeding period, the animals were immediately immobilized with levamisole and mounted on coverslips for microscopic observation in a Zeiss AxioImager Z2 epifluorescence microscope. Image J software was used for the quantification of mean RFP fluorescence. The following sets of primers were used both for the construction of acbp RNAi constructs and the detection of acbp gene deletions:

acbp-1 FW: 5'-TTGCAGAATTTTGCGAGTTTC-3'

acbp-1 REV: 5'-AGAATTTATTTAGGCTCCGTACTTG-3'

acbp-3 FW: 5'-TTAGGTCAACAGCAGCAGCC-3'

acbp-3 REV: 5’-ACACACATAACTCACGCAATTCTGA-3’

acbp-4 FW: 5’-CGATTATTCTGTTTTAGAGTGTTTGA-3’

acbp-4 REV: 5’-GAAGTGCTCACGGAGTTGATT-3’

acbp-6 FW: 5’-ACGCCCCATAATAGTAAAAGATGC-3’

acbp-6 REV: 5’-AAACATTCCCCATTTCTCTATCTCTC-3’

The respective genomic fragments were initially cloned in TOPO and then in pL4440 vector backbone in combinations to generate double *acbp* RNAi constructs (*acbp-1* together with *acbp-3* and *acbp-4* together with *acbp-6*). For generating the ACBP-1 translational reporter animals, the following sets of primers were used:

acbp-1 promoter FW: 5’-CTGCAGTTTGAAGACGATGAGAAGAGC-3’

acbp-1 promoter REV: 5’-AAGCTTGGATTTTCTTTTTTCGTCAAC-3’

acbp-1 gene FW: 5’-TCTAGACGTCTTCAAAATGACCCTCTCG-3’

acbp-1 gene REV: 5’-ACCGGTGGCTCCGTACTTGGCGATG-3’

The fragment containing the *acbp-1* gene was cloned in frame with mCherry in the pPD95.77-wmCherry vector using XbaI-AgeI restriction enzymes. The fragment containing the *acbp-1* promoter was cloned in the pPD95.77-GFP vector backbone using HindIII-PstI restriction enzymes. In the final step the full *acbp-1*::wmCherry cassette was removed from the wmCherry backbone and inserted downstream of the *acbp-1* promoter using XbaI-EcoRI restriction enzymes. Microinjection in *C. elegans* germlines was used for generating transgenic animals. All plasmids (p_{acbp-1}acbp-1::wmCherry, $p_{unc-122}$GFP as a marker for coelomocytes and pRF4 as a coinjection marker) were injected at a final concentration of 50ng/µL.

References (appendix II)

Choudhary, C., Weinert, B.T., Nishida, Y., Verdin, E., and Mann, M. (2014). The growing landscape of lysine acetylation links metabolism and cell signalling. Nature reviews Molecular cell biology *15*, 536-550.

Duran, J.M., Anjard, C., Stefan, C., Loomis, W.F., and Malhotra, V. (2010). Unconventional secretion of Acb1 is mediated by autophagosomes. The Journal of Cell Biology *188*, 527.

Egan, D.F., Shackelford, D.B., Mihaylova, M.M., Gelino, S., Kohnz, R.A., Mair, W., Vasquez, D.S., Joshi, A., Gwinn, D.M., Taylor, R.*, et al.* (2011). Phosphorylation of ULK1 (hATG1) by AMP-Activated Protein Kinase Connects Energy Sensing to Mitophagy. Science *331*, 456.

Elle, Ida C., Simonsen, Karina T., Olsen, Louise C.B., Birck, Pernille K., Ehmsen, S., Tuck, S., Le, Thuc T., and Færgeman, Nils J. (2011). Tissue- and paralogue-specific functions of acyl-CoA-binding proteins in lipid metabolism in Caenorhabditis elegans. Biochemical Journal *437*, 231.

Feng, Y., He, D., Yao, Z., and Klionsky, D.J. (2013). The machinery of macroautophagy. Cell Research *24*, 24.

Hollebeke, J., Van Damme, P., and Gevaert, K. (2012). N-terminal acetylation and other functions of Nalpha-acetyltransferases. Biol Chem *393*, 291-298.

Kang, C., You, Y.-j., and Avery, L. (2007). Dual roles of autophagy in the survival of Caenorhabditis elegans during starvation. Genes & Development *21*, 2161-2171.

Madeo, F., Pietrocola, F., Eisenberg, T., and Kroemer, G. (2014). Caloric restriction mimetics: towards a molecular definition. Nat Rev Drug Discov *13*, 727-740.

Marino, G., Pietrocola, F., Eisenberg, T., Kong, Y., Malik, S.A., Andryushkova, A., Schroeder, S., Pendl, T., Harger, A., Niso-Santano, M.*, et al.* (2014). Regulation of autophagy by cytosolic acetyl-coenzyme A. Mol Cell *53*, 710-725.

Meléndez, A., Tallóczy, Z., Seaman, M., Eskelinen, E.-L., Hall, D.H., and Levine, B. (2003). Autophagy Genes Are Essential for Dauer Development and Life-Span Extension in C. elegans. Science *301*, 1387.

Palmisano, N.J., and Meléndez, A. (2016). Detection of Autophagy in Caenorhabditis elegans Using GFP::LGG-1 as an Autophagy Marker. Cold Spring Harbor protocols *2016*, pdb.prot086496.

Pietrocola, F., Galluzzi, L., Bravo-San Pedro, J.M., Madeo, F., and Kroemer, G. (2015). Acetyl coenzyme A: a central metabolite and second messenger. Cell Metab *21*, 805-821.

Tian, Y., Li, Z., Hu, W., Ren, H., Tian, E., Zhao, Y., Lu, Q., Huang, X., Yang, P., Li, X.*, et al.* (2010). C. elegans screen identifies autophagy genes specific to multicellular organisms. Cell *141*, 1042-1055.

You, Y.J., Kim, J., Raizen, D.M., and Avery, L. (2008). Insulin, cGMP, and TGF-beta signals regulate food intake and quiescence in C. elegans: a model for satiety. Cell Metab *7*, 249-257.